McDermott Technology, Inc.
a McDermott company
Research & Development Division

Final Report

Particulate Characterization and Ultra Low-NO_x Burner for the Control of NO_x and $PM_{2.5}$ for Coal Fired Boilers

This report does not contain Trade Secret/Proprietary Information

Project Manager: Jim Warchol
Period of Performance: October 1998 – September 2001

Prepared by

Ralph Bailey
Hamid Sarv
Jim Warchol
Debi Yurchison

McDermott Technology, Inc.
Combustion & Clean Air Systems Section
1562 Beeson Street
Alliance, OH 44601

This project was funded in part by the Ohio Coal Development Office, Department of Development, State of Ohio

September 26, 2001 - Final Version
MTI Report No. RDD:01:43712-242-000:01
DOE Contract No. DE-FC26-98FT40007
OCDO Contract No. CDO D-97-8/9

DISCLAIMER

TABLE OF CONTENTS

Section **Page**

TABLE OF CONTENTS (Con'td)

Section **Page**

LIST OF TABLES

Table **Page**

LIST OF TABLES (Cont'd)

Table **Page**

LIST OF FIGURES

Figure **Page**

LIST OF FIGURES (Cont'd)

1.0 ABSTRACT

In response to the serious challenge facing coal-fired electric utilities with regards to curbing their NO_x and fine particulate emissions, Babcock & Wilcox and McDermott Technology, Inc. conducted a project entitled, "Particulate Characterization and Ultra Low-NO_x Burner for the Control of NO_x and $PM_{2.5}$ for Coal Fired Boilers." The project included pilot-scale demonstration and characterization of technologies for removal of NO_x and primary $PM_{2.5}$ emissions. Burner development and $PM_{2.5}$ characterization efforts were based on utilizing innovative concepts in combination with sound scientific and fundamental engineering principles and a state-of-the-art test facility. Approximately 1540 metric tonnes (1700 tons) of high-volatile Ohio bituminous coal were fired. Particulate sampling for $PM_{2.5}$ emissions characterization was conducted in conjunction with burner testing.

Based on modeling recommendations, a prototype ultra low-NO_x burner was fabricated and tested at 100 million Btu/hr in the Babcock & Wilcox Clean Environment Development Facility. Firing the unstaged burner with a high-volatile bituminous Pittsburgh 8 coal at 100 million Btu/hr and 17% excess air achieved a NO_x goal of 0.20 lb NO_2/million Btu with a fly ash loss on ignition (LOI) of 3.19% and burner pressure drop of 4.7 in H_2O for staged combustion. With the burner stoichiometry set at 0.88 and the overall combustion stoichiometry at 1.17, average NO_x and LOI values were 0.14 lb NO_2/million Btu and 4.64% respectively. The burner was also tested with a high-volatile Mahoning 7 coal. Based on the results of this work, commercial demonstration is being pursued.

Size classified fly ash samples representative of commercial low-NO_x and ultra low-NO_x combustion of Pittsburgh 8 coal were collected at the inlet and outlet of an ESP. The mass of size classified fly ash at the ESP outlet was sufficient to evaluate the particle size distribution, but was of insufficient size to permit reliable chemical analysis. The size classified fly ash from the inlet of the ESP was used for detailed chemical analyses. Chemical analyses of the fly ash samples from the ESP outlet using a high volume sampler were performed for comparison to the size classified results at the inlet.

For all test conditions the particulate removal efficiency of the ESP exceeded 99.3% and emissions were less than the NSPS limits of ~48 mg/dscm. With constant combustion conditions, the removal efficiency of the ESP increased as the ESP voltage and Specific Collection Area (SCA) increased. The associated decrease in particle emissions occurred in size fractions both larger and smaller than 2.5 microns. For constant ESP voltage and SCA, the removal efficiency for the ultra low-NO_x combustion ash (99.4 – 99.6%) was only slightly less than for the low-NO_x combustion ash (99.7%). The decrease in removal efficiency was accompanied by a decrease in ESP current. The emission of $PM_{2.5}$ from the ESP did not change significantly as a result of the change in combustion conditions. Most of the increase in emissions was in the size fraction greater than 2.5 microns, indicating particle re-entrainment. These results may be specific to the coal tested in this program.

In general, the concentration of inorganic elements and trace species in the fly ash at the ESP inlet was dependent on the particle size fraction. The smallest particles tended to have higher concentrations of inorganic elements/trace species than larger particles. The concentration of most elements by particle size range was independent of combustion condition and the concentration of soluble ions in the fly ash showed little change with combustion condition when evaluated on a carbon free basis.

2.0 EXECUTIVE SUMMARY

Coal-burning utilities are facing a major NO_X ($NO + NO_2$) control compliance challenge due to various emissions regulations with regard to acid rain, ground level ozone, and particulate matter formation. In response to this challenge, Babcock & Wilcox and McDermott Technology, Inc. have developed and tested a high-velocity, ultra low-NO_X pulverized coal (PC) burner for retrofitting wall-fired units. Numerical modeling and prototype testing in the Clean Environment Development Facility played key roles in the successful development and evaluation of the burner. The new burner is a plug-in version of the Babcock & Wilcox's DRB-4Z™ ultra low-NO_X PC burner with new features for pressure drop and unburned carbon reductions.

In addition to, and concurrent with, the development and performance testing of the burner, a comprehensive, high-quality database characterizing primary $PM_{2.5}$ emissions from utility plants firing Ohio coals was developed. The database includes 1) the characteristics and quantities of current particulate emissions under a range of operating conditions, and 2) the effectiveness of available control devices such as electrostatic precipitators in capturing particulate in this size range. These efforts were conducted as part of a project titled "Particulate Characterization and Ultra Low-NO_x Burner for the Control of NO_X and $PM_{2.5}$ for Coal Fired Boilers." The U.S. Department of Energy, the Ohio Coal Development Office within the Ohio Department of Development, and the Babcock & Wilcox Company jointly sponsored the program.

Non-reactive flow simulations were performed to evaluate the effects of burner flow entrance and turning vane designs on pressure drop and swirl generation efficiency. Based on the modeling results, flow entrance modifications, and installations of curved-shaped fixed and adjustable vanes in the inner secondary air zone were recommended for proper swirl generation and pressure drop minimization. Combustion modeling confirmed that the aerodynamically optimized burner design produces a well-attached and stable flame with low-NO_X emissions and high combustion efficiency.

Following the modeling recommendations, a prototype burner was fabricated and tested at 100 million Btu/hr in the Babcock & Wilcox Clean Environmental Development Facility. Firing the unstaged burner with a high-volatile bituminous Pittsburgh 8 coal at 100 million Btu/hr and 17% excess air (1.17 burner air/fuel stoichiometry) achieved a NO_X performance goal of 145 PPMV (0.20 lb NO_2/million Btu). Corresponding loss on ignition (a measure of fly ash unburned carbon) and burner pressure drop were 3.19%, and 4.7 in H_2O, respectively. These superb results represent 47% lower NO_X and only 28% higher LOI than what was achieved with the commercial prototype of the low-NO_X XCL® PC burner at 100 million Btu/hr in our test facility. Simultaneous and significant reductions in NO_x (24%) and LOI (32%) for one of the plug-in DRB-4Z™ configurations were also demonstrated relative to the DRB-XCL® burner results. With the burner stoichiometry set at 0.88 and the overall combustion stoichiometry at 1.17, average NO_X and LOI values were 104 PPMV (0.14 lb NO_2/million Btu) and 4.64%, respectively. Consequently, we also met our staged combustion NO_X goal of 0.15 lb NO_2/million Btu in the test facility. These performance results are presented graphically in Figure 2-1.

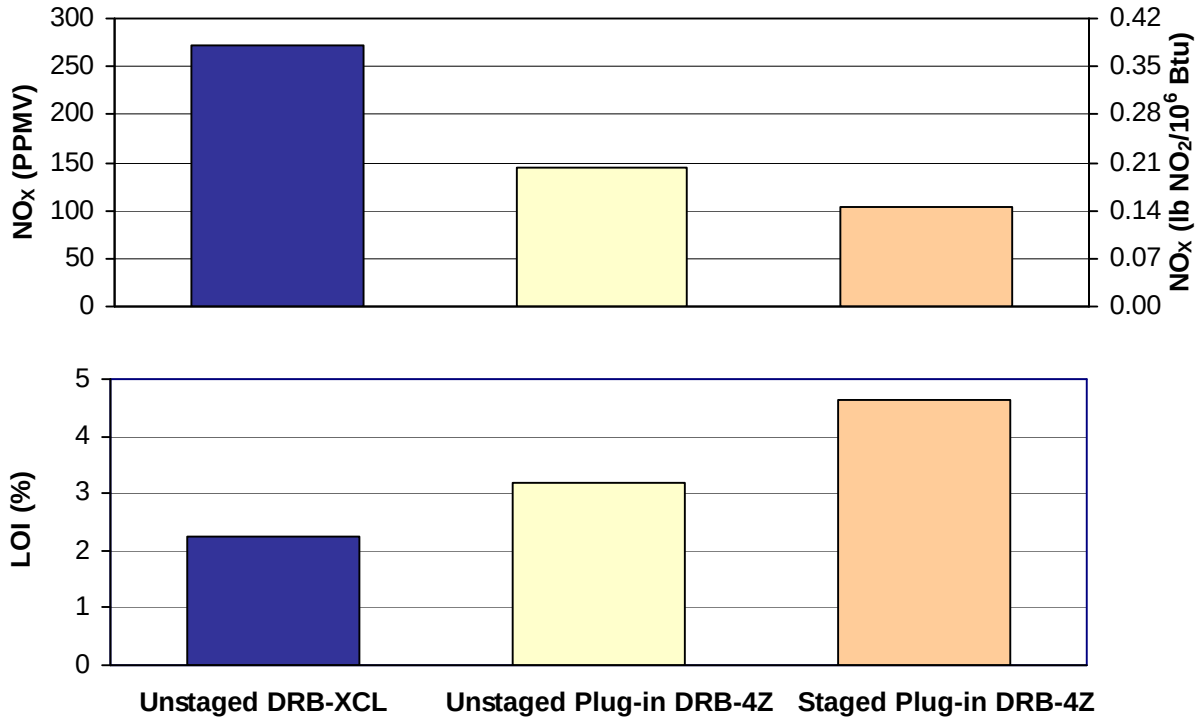

Figure 2-1. Performance summary of the DRB-4Z™ ultra low-NO_X PC burner firing Pittsburgh seam #8 coal

The burner was also test fired with a high-volatile Mahoning 7 coal having a slightly higher fixed carbon-to-volatile matter ratio and fuel-nitrogen content. At 17% excess air and 70% through a 200-mesh screen PC fineness, NO_X emissions and LOI values from firing the Mahoning 7 coal averaged 165 PPMV (0.23 lb/million Btu) and 6.40%. Increasing the coal fineness did not have an appreciable effect on NO_X but lowered the LOI levels. When a multi-blade swirler was installed in the coal nozzle, NO_X increased to 177 PPMV (0.24 lb/million Btu) and LOI levels dropped to 5.43% due to better mixing between the fuel and oxidizer. Use of the swirler could be considered as an option in situations requiring very low unburned carbon levels. Another configuration that reduced the coal nozzle diameter by 39% with the installation of two sleeve inserts achieved 154 PPMV NO_X (0.22 lb/million Btu) and 6.27% LOI under normal operating conditions.

Based on the results of the work, commercial demonstration is being pursued. In situations where the compliance limits cannot be met by burners alone, partial-scale post-combustion NO_X control systems (i.e., SCR or SNCR) can be added in combination with ultra low-NO_X burners to achieve the desired NO_X levels.

Size classified fly ash samples representative of commercial low-NO_x and ultra low-NO_x combustion of Pittsburgh 8 coal were collected at the inlet and outlet of an ESP. The mass of size classified fly ash at the ESP outlet was sufficient to evaluate the

particle size distribution, but was of insufficient size to permit reliable chemical analysis. The size classified fly ash from the inlet of the ESP was used for detailed chemical analyses. Chemical analyses of the fly ash samples from the ESP outlet collected using a high volume sampler were performed for comparison to the size classified results at the inlet.

For the specific combustion conditions tested, ultra low-NO_x combustion resulted in higher unburned carbon than conventional low-NO_x combustion (4.3% vs 1.3%). The greater carbon-in-ash for the ultra low-NO_x combustion was not unexpected since the burner was not optimized for unburned carbon. For all test conditions the particulate removal efficiency of the ESP exceeded 99.3% and emissions were less than the NSPS limits of ~48 mg/dscm.

With constant combustion conditions, the removal efficiency of the ESP increased as the ESP voltage and Specific Collection Area (SCA) was increased. The associated decrease in particle emissions occurred in size fractions both larger and smaller than 2.5 microns. For constant ESP voltage and SCA, the removal efficiency for the ultra low-NO_x combustion ash (99.4 – 99.6%) was less than for the low-NO_x combustion ash (99.7%). The decrease in removal efficiency was accompanied by a decrease in ESP current. The emission of $PM_{2.5}$ from the ESP increased only slightly as a result of the change in combustion conditions. Most of the increase in emissions was in the size fraction greater than 2.5 microns, indicating particle re-entrainment. These results may be specific to the coal tested in this program.

Although the increase in unburned carbon on an average basis was quite small, the increase in carbon content was strongly dependent on particle size. While the carbon content of PM greater than 10 microns increased from about 1% to 4%, the carbon content of the $PM_{2.5}$ size fraction increased from about 7% to 45%.

In general, the concentration of elements and species in the fly ash was dependent on the particle size fraction. The smallest particles tended to have higher concentrations of elements/species than larger particles. This trend was strongly dependent on the volatility of the element or species. The concentration of the least volatile elements tended to be depleted in the smallest particles while the concentration of the most volatile elements/species tended to be enriched.

The concentration of most elements by particle size range was independent of combustion condition when evaluated on a carbon free basis. The exceptions to this generality were Se, As, and Hg. The concentration of these elements in the $PM_{2.5}$ size fraction remained relatively constant as the carbon content increased.

The concentration of soluble ions in the fly ash showed little change with combustion condition when evaluated on a carbon free basis. For the high sulfur Pittsburgh 8 coal that was burned in these tests, the predominate ionic species in the fly ash was sulfate. As with the volatile elements, soluble ions were enriched in the $PM_{2.5}$ size fraction.

3.0 INTRODUCTION

3.1 Background

3.1.1 NO_X Emissions

Coal-fired electric utilities in the United States are facing a serious challenge with regard to curbing their NO_x emissions. Emissions of oxides of nitrogen (NO_X = NO + NO_2) have been associated with acid rain, ozone formation in the lower troposphere, photochemical smog, ozone depletion in the stratosphere, and potential damage to ecosystems and human health. Studies have also linked NO_x to the formation of aerosol nitrates, a secondary source of fine particulate matter known as $PM_{2.5}$ (smaller than 2.5 microns). Under Title IV (acid rain control), Phase II of the Clean Air Act Amendments (CAAA), wall-fired coal burning utilities must comply with annual NO_X emission limits of 0.46 lb/million Btu. Meanwhile, power importing states within the Northeastern Ozone Transport Region (as defined under Title I of the CAAA) are demanding further NO_X emission reductions from the coal-fired Midwestern electric utilities. In addition, the proposed Ozone Transport Rule, National Ambient Air Quality Standards (NAAQS), and New Source Performance Standards (NSPS) could impose substantial NO_X control requirements beyond the year 2002. It is anticipated by the year 2003, the stipulated NO_X emission levels will be 0.15 lb NO_2/million Btu, and affect most of the 115,000 MW wall-fired PC boilers within 22 eastern states, including those already retrofitted with first- and second-generation low-NO_x burners.

3.1.2 B&W Low-NO_X Burners

Between 1976 and 1986, B&W installed 40,000 MW of low-NO_X dual register pulverized coal burners (DRB's) in the U.S. Roughly thirty percent of these units generate more than 0.5 lb NO_X/million Btu. In addition, there is approximately 26,000 MW capacity of wall-fired PC boilers that use high-NO_X generating circular-type burners. Some of these units may require significant downtime and expenses associated with boiler modifications to retrofit the existing smaller diameter burners with the larger throat, low-NO_X burners. Development of a high-velocity low-NO_X burner that easily plugs in and replaces existing equipment would provide the most cost-effective means of meeting the emissions regulations. Successful development of such a burner will enable utilities with wall-fired boilers to continue burning coals by significantly reducing their NO_X emissions. Reduction of NO_X will decrease the formation of acid rain, ground level ozone, and secondary $PM_{2.5}$.

One of the best candidates for plug-in (small throat) adaptation is the ultra low-NO_X DRB-4Z™ burner. A full-diameter (large throat) version of this burner [1 through 4] was designed for application in new boilers and evaluated successfully in a pilot-scale facility as part of a U.S. Department of Energy-sponsored Combustion 2000 program titled "Engineering Development of Advanced Coal-Fired Low Emission Boiler Systems". In the present work the full-diameter DRB-4Z™ PC burner was adapted for plug-in, ultra low-NO_X application in wall-fired utility boilers. This report discusses the development and performance evaluation of the ultra low-NO_X, plug-in version of the DRB-4Z™ PC burner by McDermott Technology, Inc. (MTI) and Babcock & Wilcox (B&W).

3.1.3 Primary $PM_{2.5}$ Emissions

The original NAAQS for particulate matter (PM) were promulgated in 1971 by the Environmental Protection Agency (EPA) under the Clean Air Act. These standards were for "total suspended particulate" (TSP) quantified by sampling with a "high-volume" sampler, which collects PM as large as 25-45 microns. On the basis of evidence that smaller particulates pose a greater health hazard, these rules were revised in 1987 in such a manner that TSP was replaced with a new indicator that only included particles with an aerodynamic equivalent diameter less than or equal to 10 microns (PM_{10}).

More recently, research has indicated that health effects occur at ambient levels below the current PM_{10} NAAQS. Other research suggests that particles *smaller* than PM_{10} may contribute significantly to the most serious health effects, because the finer PM can penetrate deeper into the lungs. According to the EPA, fine particles have several properties that affect health risk. These include high surface area and number, a more uniform (than larger particles) distribution at a regional scale, long atmospheric lifetimes, and increased ability to infiltrate indoors. Based on the health effects of PM identified in EPA's review, agency staff has recommended the addition of new 24-hour and annual $PM_{2.5}$ standards, as well as retention of the current annual PM_{10} standard, either alone or in combination with a 24-hour PM_{10} standard.

Reduction of $PM_{2.5}$ emissions by utilities, if mandated by environmental regulations, requires information on 1) the characteristics and quantities of current particulate emissions under a range of typical operating conditions, and 2) the effectiveness of available control devices such as electrostatic precipitators in reducing particulate in this ultrafine size range. The parametric testing required to generate this database provides the first step toward the development of cost-effective primary $PM_{2.5}$ emission control strategies.

In addition to, and concurrent with, the development and performance testing of the plug-in ultra low-NO_x burner in this project, a comprehensive, high-quality database characterizing primary $PM_{2.5}$ emissions from utility plants firing Ohio coals was developed. Primary $PM_{2.5}$ refers to particulate matter which leaves the stack in the form of fine solid particles or liquid droplets whose aerodynamic diameter is less than 2.5 microns (a micron is 10^{-6} meter). This is in contrast to secondary $PM_{2.5}$, which forms downstream of the stack from gaseous precursor emissions such as SO_2 and NO_x. As a point of reference, 2.5 microns is about $1/30^{th}$ the diameter of a human hair. The primary $PM_{2.5}$ emissions were quantified and characterized, or "fingerprinted", as functions of boiler/combustion conditions and emissions control equipment operation. Representative samples of primary $PM_{2.5}$ obtained during combustion testing in the Clean Environment Development Facility (CEDF) were sent to the EPA to be used directly in their health studies. The detailed analysis and characterization of $PM_{2.5}$ samples generated in this project can be used in source apportionment studies and can serve to augment and verify the representative nature of other samples used by EPA in its various health impact studies.

3.2 Overview of the Project

3.2.1 Project Goal and Description

In response to the serious challenge facing coal-fired electric utilities with regards to curbing their NO_X and fine particulate emissions, MTI conducted a project that included pilot-scale demonstration and characterization of technologies for removal of NO_x and primary $PM_{2.5}$ emissions. The overall goal of the project is to keep coal both economically and environmentally competitive as an electric utility boiler fuel, thereby supporting the continued use of our country's abundant coal reserves. This goal was addressed through the following efforts:

(a) Development and testing of an ultra low-NO_X pulverized coal (PC) burner for plug-in retrofit applications without boiler wall tube modifications

(b) Assessing the impact of low-NO_X PC burner operation on NO_X and $PM_{2.5}$ control

(c) Providing high-quality data to ensure that the potential $PM_{2.5}$ regulations are based on good scientific information.

Burner development and $PM_{2.5}$ characterization efforts were based on utilizing innovative concepts in combination with sound scientific and fundamental engineering principles and a state-of-the-art test facility. Approximately 1540 metric tonnes (1700 tons) of high-volatile Ohio bituminous coal were fired. Particulate sampling for $PM_{2.5}$ emissions characterization was conducted in conjunction with burner testing at conditions representative of commercial utilities. Primary $PM_{2.5}$ emissions were quantified and characterized as functions of boiler/combustion conditions and ESP operation.

These efforts were conducted in B&W's 29.3 MW_t (100 million Btu/hr), CEDF located at MTI in Alliance, OH. An isometric diagram of the CEDF is shown in Figure 3-1. The CEDF was configured to simulate a boiler followed by an ESP -- the most common configuration at utility sites. To ensure that the burner could be deployed readily and cost-effectively in coal-fired utility boilers, the design considered the following specifications.

Throat Velocity and Diameter:	• Equivalent to pre-retrofit design
NO_x Emissions:	• Less than 86 g/GJ (0.20 lb/million Btu) without air staging
	• Less than 64 g/GJ (0.15 lb/million Btu) with staging and overfire air
Unburned Carbon:	• Less than or equal to other commercial low-NO_x burners
$PM_{2.5}$ Emissions:	• Less than or equal to other commercial low-NO_x burners
Commercial Readiness:	• January 2000

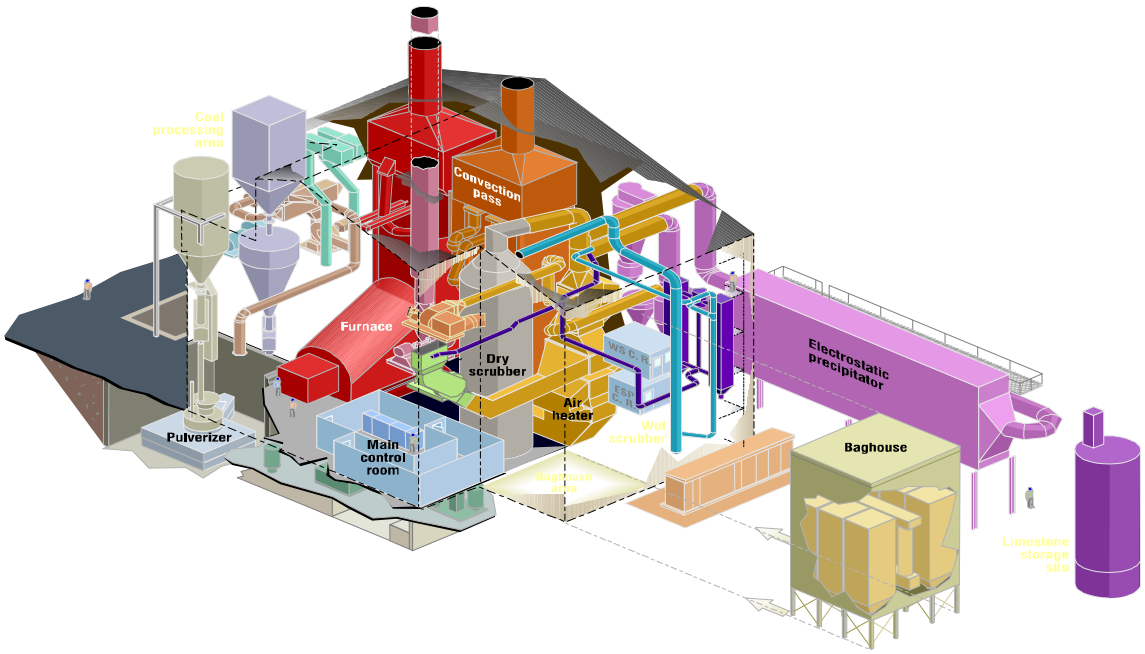

Figure 3-1. Clean Environment Development Facility

3.2.2 Project Sponsors

MTI entered into a Cooperative Agreement with the United States Department of Energy (DOE) and the Ohio Coal Development Office (OCDO) in October 1998 to study "Fine Particulate Characterization and Ultra Low-NO_X Burner for the Control of NO_X and $PM_{2.5}$ for Coal-Fired Boilers". The project was supported by the United States Department of Energy, The Ohio Coal Development Office within the Ohio Department of Development, and Babcock and Wilcox (B&W) – a McDermott International Company. The guidance and support of the project managers from the sponsoring organizations, Thomas J. Feeley III and William Aljoe of DOE-NETL, Howard Johnson of the OCDO, and Al LaRue of Babcock & Wilcox is gratefully acknowledged.

4.0 DESCRIPTION OF CLEAN ENVIRONMENT DEVELOPMENT FACILITY

4.1 CEDF General Description

The CEDF is a state-of-the-art facility for integrated evaluation of combustion and post-combustion emissions control options. Key components of the overall facility are illustrated in Figure 4-1.

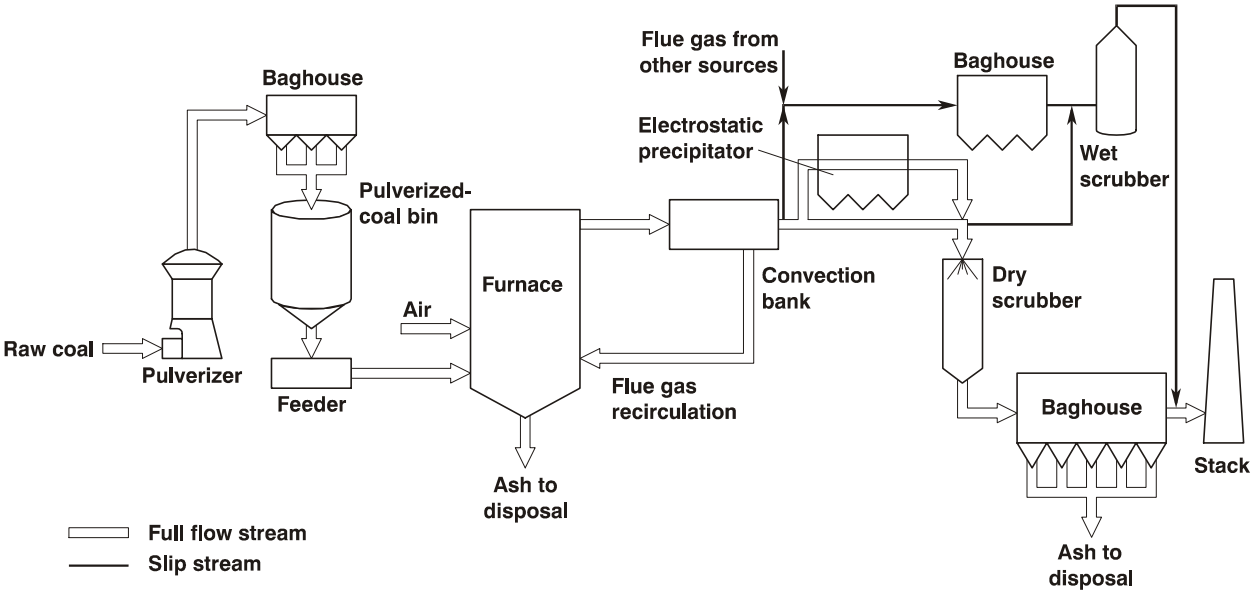

Figure 4-1. Schematic of the CEDF

Pre-crushed and partially dried raw coal is supplied by a gravimetric feeder to a B&W EL-56 pulverizer. The pulverizer is equipped with a dynamically staged, variable speed (DSVS^{TM}) classifier to control PC fineness. Preheated air carries the pulverized coal to a small filterhouse that vents the air and drops the PC into a storage bin. Pulverized coal flow from the bottom of the storage bin is controlled by a weigh feeder. The coal is then transported to the burner by heated primary air at the desired air-to-fuel ratio. Typical primary air temperatures are around 66^{o}C (150^{o}F) at the burner inlet. Secondary air is preheated by the flue gas and a gas-fired heater to 316^{o}C (600^{o}F). For staged combustion, part of the secondary air is directed to two opposed overfire air (OFA) windboxes located above the furnace tunnel section. Each windbox houses two OFA registers equipped with outer spin vanes and a central core air damper control. Damper control and pressure drop indications across in-duct orifice plates are used to balance the OFA flow equally to each side of the furnace.

After leaving the convection bank, the flue gas enters an air preheater. Exit flue gas temperature is controlled further by a heat exchanger to values suitable for dry scrubber operation and sulfur dioxide emissions control. Coal fly ash can be removed by an electrostatic precipitator (ESP) prior to entering the dry scrubber system. A finely atomized slurry of hydrated lime is sprayed in the dry scrubber. As the gas and liquid flow co-currently through the tower, the hydrated lime reacts with sulfur dioxide and the

slurry water evaporates, leaving calcium sulfite and fly ash as a suspended dry powder. The dry powder is filtered from the gas by a multi-chambered baghouse. The dust is dislodged from the bags by a pulse jet cleaning cycle and then transferred via a pneumatic conveyor system to an ash silo for disposal. A slipstream of the flue gas may also be directed to a small pulse-jet fabric filter and wet scrubber. The emission control equipment can be combined in a variety of arrangements to represent a wide range of commercial installations.

4.2 CEDF Boiler/Furnace Description

Figure 4-2 shows the construction of the CEDF furnace and convection pass. The inside surface of the furnace is refractory lined to replicate the thermal environment and flow characteristics of a typical utility boiler. The CEDF furnace accommodates a single 29.3 MW_t (100 million Btu/hr burner) for firing natural gas, fuel oil, or coal. Testing burners at 29.3 MW_t (100 million Btu/hr) minimizes the potential uncertainties with scale-up to full-scale commercial design 44 MW_t to 59 MW_t (typically 150-200 million Btu/hr).

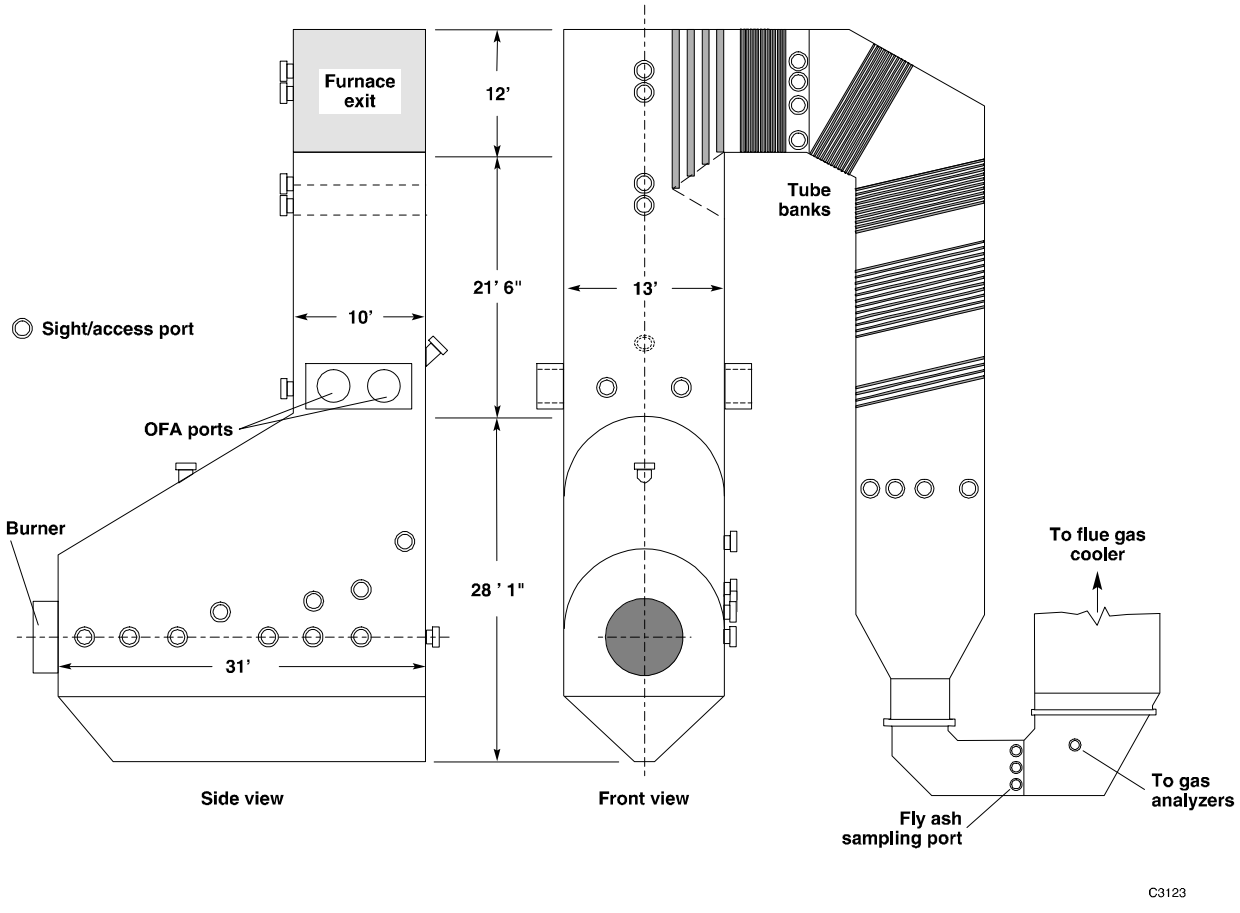

Figure 4-2. Furnace and convective pass section schematic of the CEDF

4.3 CEDF Instrumentation

Flow rate measurements of the primary combustion air, total secondary air to the windbox, etc., rely on calibrated pressure transducers, thermocouples, and flow metering and control devices. Commercially available LABVIEW™ software is used for data acquisition, real time computations, and averaging the engineering calculations. Live flame imaging and non-intrusive flame temperature mapping are done with an optical pyrometry system called FLAMEVIEW™. The unit is mounted just above the furnace tunnel exit on the rear wall.

Gaseous species are sampled continuously from a location at the convection pass section outlet through a heated sample line. After filtering and drying, CO, CO_2, O_2, SO_2, and NO_X concentrations are measured and recorded. All analyzers are calibrated daily with certified gas standards. A complete list of the gas analysis instrumentation and their measurement principles is given in Table 4-1.

Table 4-1. Gas Analysis Instrumentation

Gas Species	Analyzer	Model Number	Measurement Principle
O_2	Rosemount	NGA-PND	Paramagnetic
CO_2	Rosemount	NGA-NDIR	NDIR
CO	Rosemount	NGA-NDIR	NDIR
NO_X	Rosemount	NGA-CLD	Chemiluminescense
SO_2	Rosemount	NGA-NDIR	NDIR

Fly ash is sampled across the duct via a multi-point probe with equally-spaced holes. Representative samples at each test condition are collected on a glass fiber filter and analyzed for loss-on-ignition (LOI). Previous work has shown that LOI measurements closely approximate the fly ash unburned carbon levels for Eastern bituminous coals. Flue gas and fly ash sampling locations are shown in Figure 4-2.

A continuous emissions monitoring (CEM) system measures the flue gas opacity and concentrations of O_2, SO_2, and NO_X leaving the stack. Table 4-2 lists the analyzers that comprise the CEM system.

Table 4-2. CEM System			
Emissions	**Analyzer**	**Model Number**	**Measurement Principle**
O_2	Rosemount	NGA-PND	Paramagnetic
NO_X	Rosemount	NGA-CLD	Chemiluminescense
SO_2	Rosemount	NGA-NDIR	NDIR
Opacity	Rosemount	OPM2000	Light transmission

4.4 Post-Combustion Emissions Control

For the test program the post-combustion emissions control equipment was configured as follows:

- Electrostatic precipitator (ESP): Particulate control device used for test data
- Dry Scrubber/Full-flow baghouse: Used for facility SO_2 compliance, no test data
- Slip-stream wet scrubber/baghouse: Not used

The ESP description is provided below. Since the dry scrubber/full-flow baghouse and the slip-stream wet scrubber/baghouse were not used for data, detailed descriptions are not provided.

4.4.1 Electrostatic Precipitator

The design of the B&W/Rothemuhle ESP reflects recent advances in mechanical engineering and control systems for commercial units. The ESP contains discharge electrodes which impart an electric charge to particles in the flue gas as the gas passes through the ESP. The charged particles are attracted to collector plates and are removed from the gas. The plates and electrodes are rapped periodically to remove the collected particles. The ash falls into hoppers below the plates and is removed from the ESP through rotary air locks at the bottom of each hopper.

The ESP is sufficiently flexible to treat flue gas from a range of coals with variable ash, sulfur and moisture contents. Sufficient collection area and operating voltage are available to reduce particulate emissions to less than the NSPS of 13 g/GJ (0.03 lb/million Btu). The primary design characteristics for the ESP are summarized in Table 4-3. The ESP incorporates wire discharge frames in field 1 and rigid discharge electrodes (RDE) in fields 2 through 4. Both discharge systems are used in commercial ESPs. A three-point support arrangement is used to support the discharge frame carriers and maintain alignment in each field. Each field is powered by a separate transformer/rectifier (T-R) set. The T-R sets step up the 480 Vac line voltage to a maximum of 75 kVdc.

Table 4-3. ESP Design Summary	
Characteristic	**Description**
Electric Field (4)	6m high x 4m deep x 2.4m wide
Specific Collection Area (SCA)	1085-1216 m^2/1000 m^3/min (330-370 ft^2/1000 acfm)
Plate Spacing	400 mm (16 in.)
Gas Passages	6
Full Load Gas Flow	1060 cmm at 177^oC (37,365 acfm @ 350^oF)
Flue Gas Velocity	1.1 to 1.2 m/sec (3.6 to 4.0 ft/sec)
Migration Velocity	7.5 to 9.8 cm/sec
Residence Time	13 to 14 sec
Design particulate Loading	855 kg/hr (1885 lb/hr)
Transformer Rectifier Sets (4)	75 kV, 125mA dc

The ESP operates at maximum efficiency when power input to the discharge electrodes is maintained within a prescribed range to account for small fluctuations in flue gas composition. The high voltage (60,000 to 75,000 Vdc) between the discharge frames and the collector plates must be maintained at or near the spark-over voltage for optimal performance. Continuous sparking, referred to as arcing, draws high current flow reducing the secondary voltage resulting in reduced precipitator performance. The microprocessor T-R set controls are set in automatic mode which monitors the secondary current relative to the selected control limit value to maintain a specified power level for operation. The protection circuit includes alarm indication devices and control trips due to over current, overvoltage, or undervoltage.

The ESP is illustrated in Figure 4-3. Flue gas flow through the ESP is from left to right. Figure 4-3 does not include the ash handling equipment which consists of a rotary airlock at the bottom of each ash hopper and a screw conveyor which traverses the length of the ESP to transport the ash from each hopper to a common pick-up box for pneumatic transfer to the ash storage silo. Hopper level detectors are provided in each ash hopper to alert operating personnel of high ash build up. The elevation has been set to ensure that the hopper ash level will remain below the detector when the ash removal system is operated at normal frequencies.

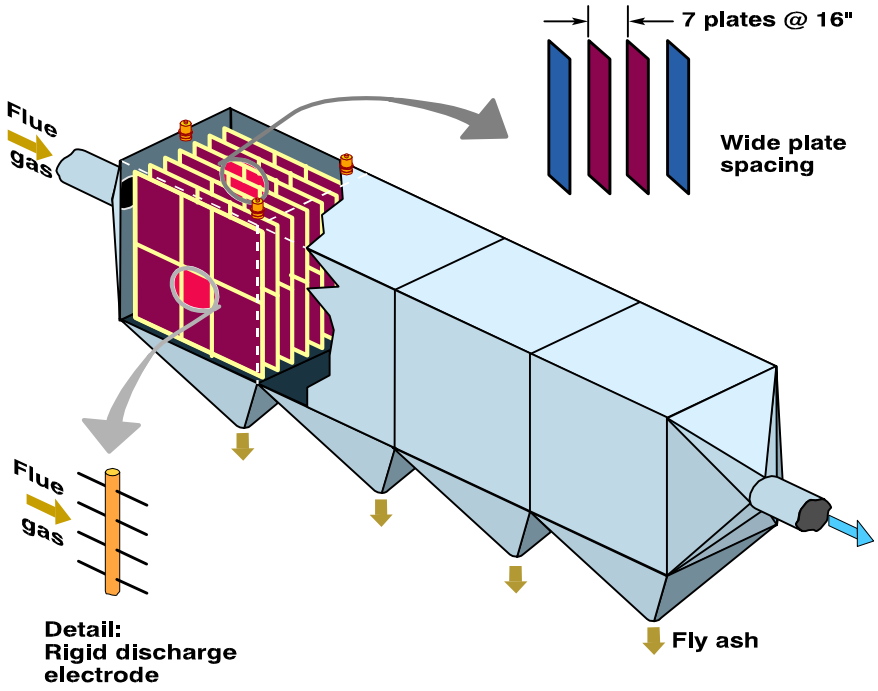

Figure 4-3. Electrostatic precipitator

5.0 ULTRA LOW-NO_X BURNER DEVELOPMENT

5.1 Burner Design

Burner development efforts began by adapting the highly successful full-diameter DRB-4Z™ low-NO_X PC burner design for plug-in application. Figure 5-1 shows a schematic of the initial plug-in design. Relative to the previously developed full-diameter DRB-4Z™ burner, the smaller barrel diameter of the plug-in design resulted in approximately 36% higher combustion air velocity for the same fuel mass throughput. Since, higher air velocities could alter the flow mixing patterns and would tend to increase the windbox-to-furnace pressure drop, innovative concepts for reducing the pressure drop and optimizing the airflow distribution were considered for further evaluation. These concepts included modifying sharp entries and flow obstacles along with the use of aerodynamic vanes. Computational fluid dynamics (CFD) modeling and prototype testing were used methodically to refine the plug-in ultra low-NO_X PC burner design.

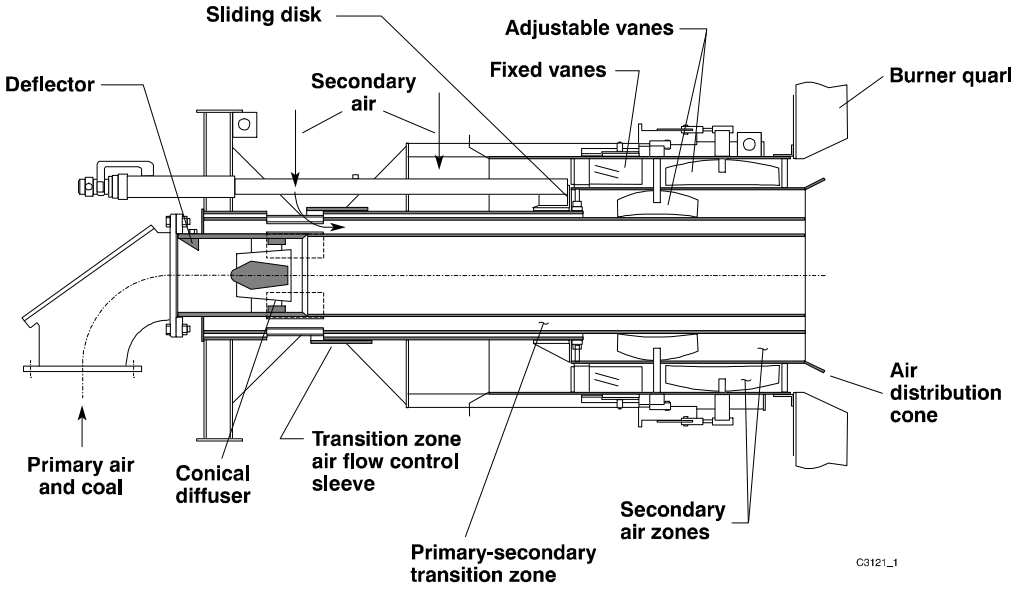

Figure 5-1. Initial plug-in DRB-4ZÔ PC burner design

5.2 Model Description

Modeling evaluations of various design options were conducted prior to burner construction and testing. MTI's in-house numerical combustion model COMO was used to support the design work. COMO is a numerical model for predicting turbulent, reacting or non-reacting flow characteristics in complex geometries [5-7]. The algorithm is built around a cell-centered, finite-volume formulation of the steady, incompressible Navier-Stokes equations and the solution of radiative heat transfer by the discrete ordinates method [7]. Mass and momentum equations are solved on a non-staggered

grid using a projection method; pressure-velocity coupling is achieved using Rhie and Chow [8] interpolation. Turbulence is considered using the k-ε turbulence model [9]. Advection terms are treated using a bounded, high-resolution scheme to insure bounded, non-oscillatory solutions in regions of high gradients. For reacting flows, additional transport equations are solved for energy and constituent species. Chemical reactions may be modeled using two-step (global) or multi-step (detailed) mechanisms. The model is applicable to unstructured discretizations in either two or three dimensions.

In this work, COMO simulated the entire burner windbox, including internal burner components and flow passages, as well as the furnace. Burner and CEDF furnace models were constructed with sufficient control volumes to provide proper numerical resolution for minimal grid dependence. Local grid refinement was designed to resolve the large gradients in flow, temperature, and species concentration in the burner near-field regions. Recognizing the model's limitation in accurate prediction of combustion and emissions performance, the application of modeling in this work was mainly intended for trend indication and as a design-screening tool.

5.3 Non-Reactive Flow Modeling

Previous modeling studies of another dual-register burner indicated that the adjustable inner vanes are responsible for a significant portion of the pressure loss. Other components that could contribute to pressure drop included the boilermaker's bell-mouth (entrance region) and the air separation vane (exit region). Since burner ΔP is influenced mainly by the air velocity, temperature, and the design and orientation of the flow turning vanes, non-reactive flow simulations provided the most efficient way to predict the pressure drop as well as air velocity and temperature distributions.

The effect of velocity on burner pressure drop was examined by comparing loss coefficients for a model of a single vane over a range of flow velocities at different orientations. The loss coefficient for unrecoverable pressure drop (K-factor or inertial resistance coefficient) is defined as:

$$K_x = \frac{\Delta p}{\frac{1}{2} \cdot r \cdot V_x^2} \qquad (1)$$

In order to compare the swirl generating efficiency of various vane geometries both standard swirl numbers, S_1 and S_2, were calculated [10]. The swirl numbers, S_1 and S_2, were calculated from the ratio of tangential momentum to the axial momentum and thrust, respectively defined with the following definitions.

Axial Momentum [N]:

$$M_x \equiv 2p \int_{R_{\min}}^{R_{\max}} r \cdot \overline{U}^2 \cdot r \cdot dr \qquad (2)$$

where :

R_{max} is the zone outer radius

R_{min} is the zone outer radius

$\overline{U}$ is the time-averaged axial velocity

Thrust [N]:

$$G_x \equiv 2p\left(\int_{R_{\min}}^{R_{\max}}\left(r\cdot\overline{U}^2+\left(p-p_o\right)\right)\cdot r\cdot dr\right) \tag{3}$$

where :

p_o is the pressure at the inner zone radius

Tangential Momentum $[N\cdot m]$:

$$G_j \equiv 2p\int_{R_{\min}}^{R_{\max}} r\cdot\overline{U}\cdot\overline{W}\cdot r^2\cdot dr \tag{4}$$

The Swirl Number, S_1, is defined as follows:

$$S_1 \equiv \frac{G_j}{R_{\min}\cdot G_x} \tag{5}$$

The Alternative Swirl Number, S_2, is defined as follows:

$$S_2 \equiv \frac{G_j}{R_{\min}\cdot M_x} \tag{6}$$

Due to experimental difficulties in accurately measuring the pressure gradient, swirl numbers are almost exclusively reported as S_2. In most of the current analyses S_1 and S_2 were usually within a couple of percent of each other. The swirl numbers at the model outlets were obtained as follows:

$$S_1 \approx \frac{\sum_{i=1}^{n} r_i\cdot A_i\cdot\overline{U_i}\cdot\overline{W_i}\cdot r_i}{R_o\cdot\sum_{i=1}^{n} A_i\cdot\left(r_i\cdot\overline{U_i}^2+\left(p_i-p_o\right)\right)} \tag{7}$$

and

$$S_2 \approx \frac{\sum_{i=1}^{n} r_i\cdot A_i\cdot\overline{U_i}\cdot\overline{W_i}\cdot r_i}{R_{\min}\cdot\sum_{i=1}^{n} r_i\cdot A_i\cdot\overline{U_i}^2} \tag{8}$$

The mass-averaged values of static and total pressure are obtained through the relationship:

$$\overline{p} \approx \frac{\sum_{i=1}^{n} r_i \cdot A_i \cdot \overline{U_i} \cdot p_i}{\sum_{i=1}^{n} r_i \cdot A_i \cdot \overline{U_i}} \qquad (9)$$

5.3.1 Flow Entrance Modification

Modeling was used to investigate the effect of burner flow entrance area on pressure drop. For this purpose, the boilermaker's bell-mouth (BMB) was moved forward equivalent to 3.8 times the original gap as shown in Figure 5-2. The green surface represents the secondary air damper, the blue represents the exit surface of the inner secondary air zone, and the red the exit surface of the outer secondary air zone. With this change, the burner pressure decreased by 0.091 kPa (0.37 inch of water).

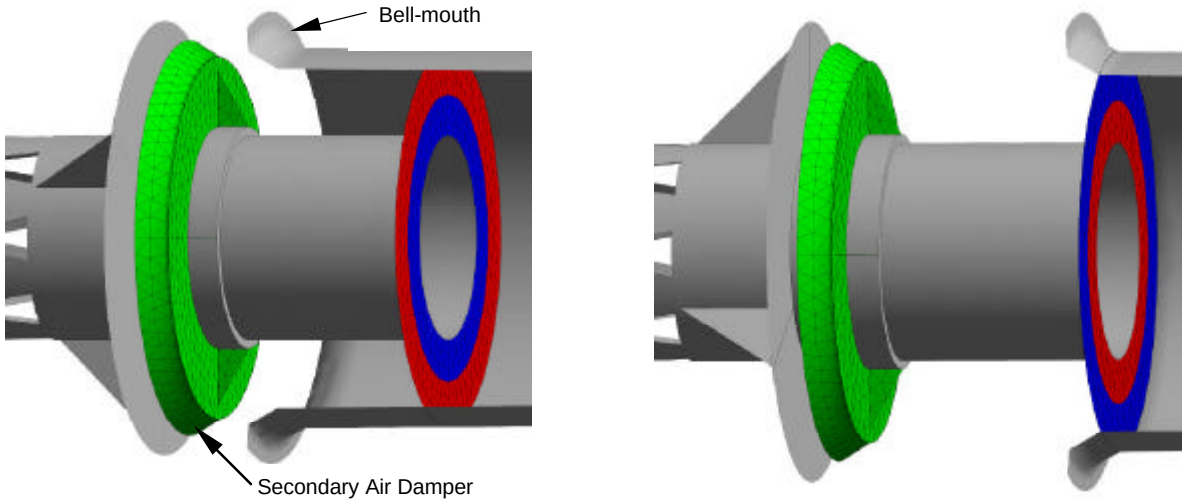

Figure 5-2. Boilermaker's bell-mouth position for the baseline (left) and modified (right) configurations

Another hardware simulation included a boilermaker's bell-mouth at the inner secondary air zone entrance and a matching airflow control disk to replace the larger disk shown in Figure 5-2. With this change, the pressure drop increased 0.603 kPa relative to the baseline burner. However, this feature was retained in the final design in order to provide a way for independent control of secondary airflow through the inner zone.

5.3.2 Swirl Vane Design Optimization

Rotationally periodic models of the standard inner vane design were evaluated at secondary air velocity intervals of 10 m/s from 10 m/s to 50 m/s. Vane angle orientations were varied by intervals of 5° from 30° to 80° (0° ≡ aligned with burner centerline). Figures 5-3 and 5-4 show that the inertial resistance coefficient and swirl numbers are constant at each vane setting and differentially continuous with respect to vane angle. Plots showing the variation of inertial resistance coefficient with swirl number are used to characterize the swirl generation efficiency in this work. In Figure 5-4, points that lie above the curves' inflection generate less swirl at higher pressure drops. The collapse of the data at different velocities onto a single curve reduces the number of modeling cases required to describe the system by allowing a single inlet velocity to be modeled at each vane orientation.

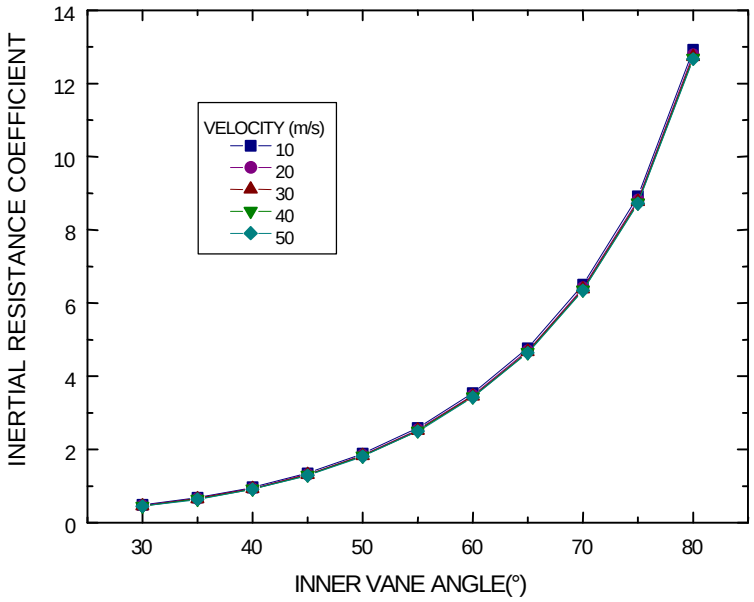

Figure 5-3. Inertial resistance coefficient versus standard adjustable inner vane angle

Following the baseline flat vane profile modeling, the effect of blade perforation on reducing flow separation and pressure drop was investigated by adding porosity to the leading and trailing edges of the standard blade design. Although the predicted pressure drops in both cases are slightly lower than the standard design values at a given vane orientation, the swirl generation efficiency is somewhat diminished as shown in Figure 5-5.

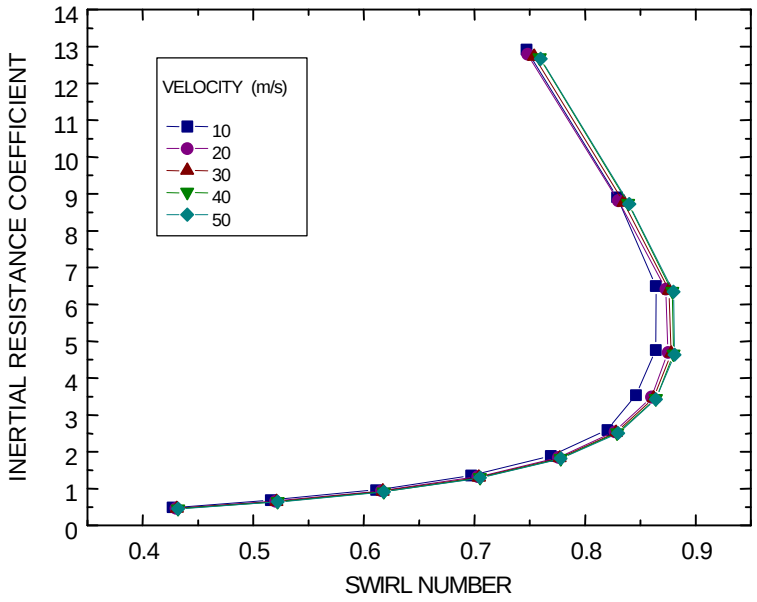

Figure 5-4. Inertial resistance coefficient versus swirl number (S_2) for standard adjustable inner vanes

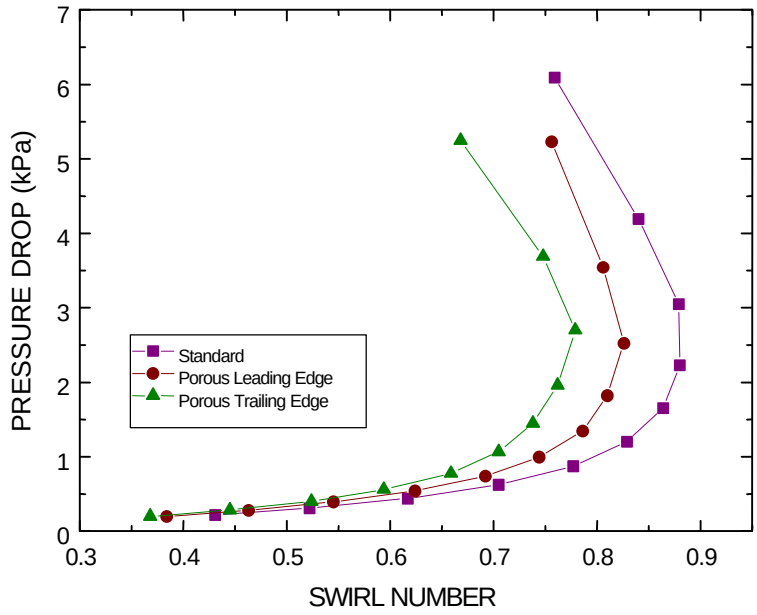

Figure 5-5. Pressure drop versus swirl number (S_2) for standard adjustable inner vanes with and without blade porosity

Two more alternative adjustable swirl blade designs for the inner secondary zone were evaluated. Respective results are compared in Figures 5-6 through 5-8. For a given (desired) swirl number, the curved vanes have the least pressure drop.

Modeling application was further extended to predict the pressure drop variation by placing fixed turning vanes upstream of the adjustable vanes in the inner secondary air zone. Figures 5-9 through 5-11 compare the results for three different vane profiles. For applications requiring moderate swirl (0.4-0.8), such as utility burners, the curved shape vanes are as efficient as the airfoils and are easier to fabricate.

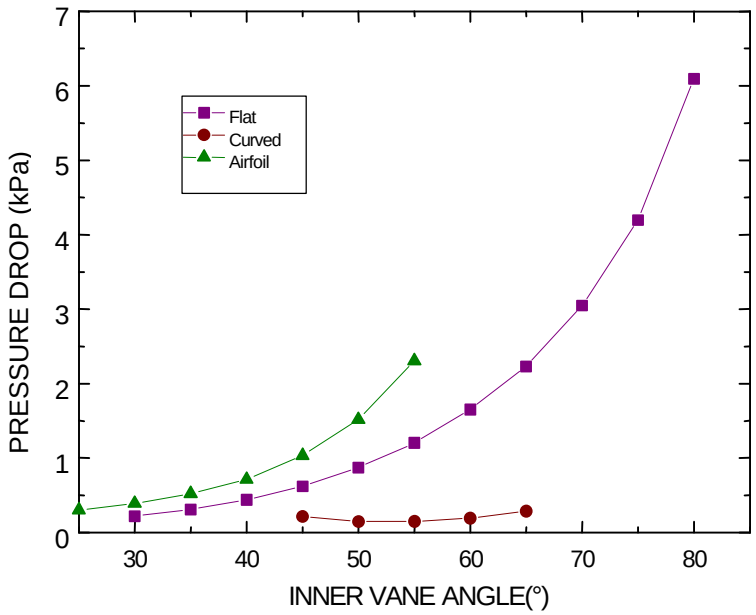

Figure 5-6. Pressure drop versus vane angle for three different adjustable vane profiles

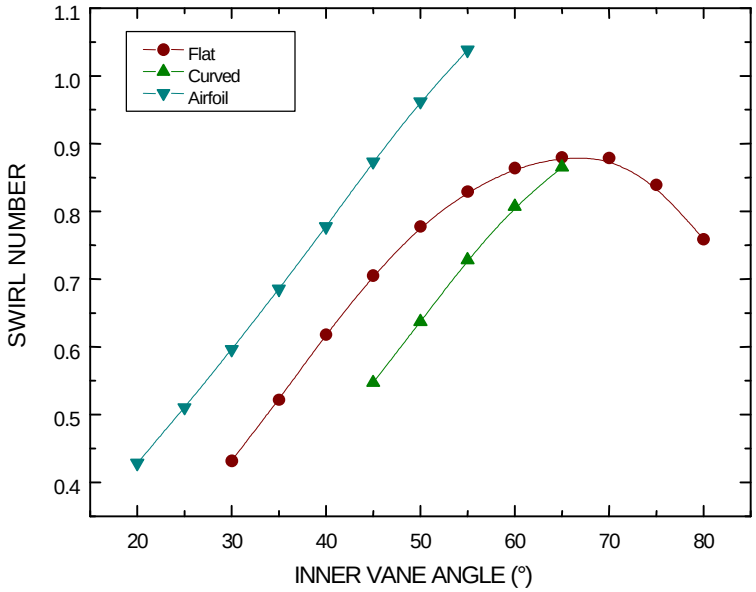

Figure 5-7. Swirl number (S_2) versus inner vane angle for three different adjustable vane profiles

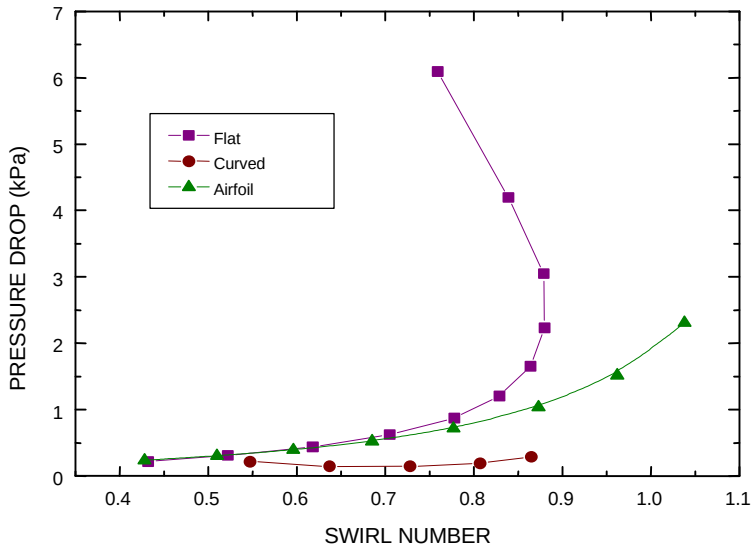

Figure 5-8. Pressure drop versus swirl number (S_2) for three different adjustable vane profiles

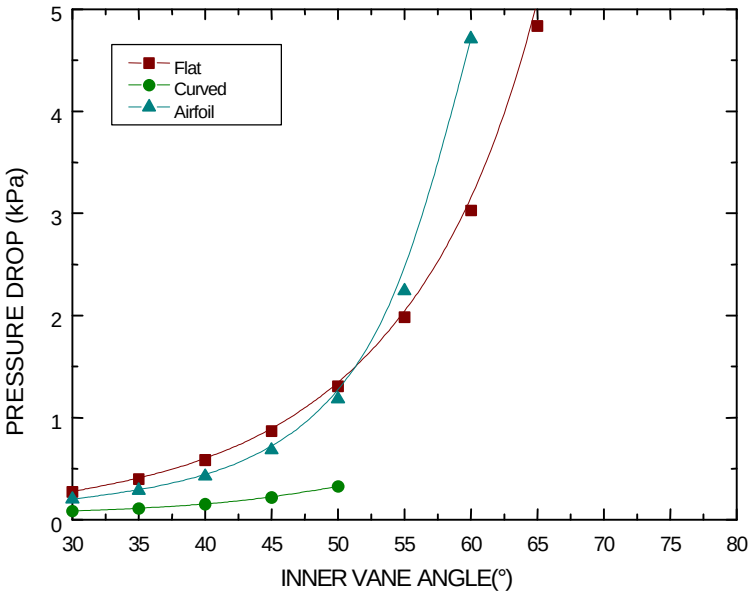

Figure 5-9. Total pressure drop versus vane angle for three different fixed vane profiles

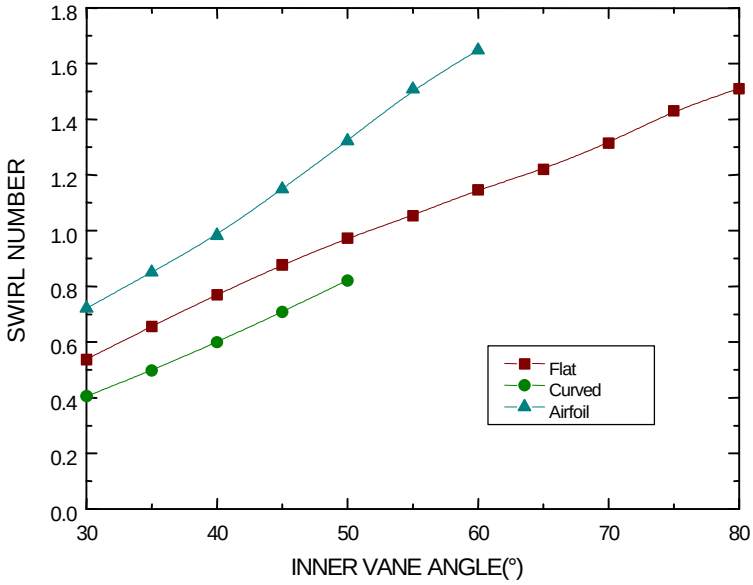

Figure 5-10. Swirl number versus vane angle for three different fixed vane profiles

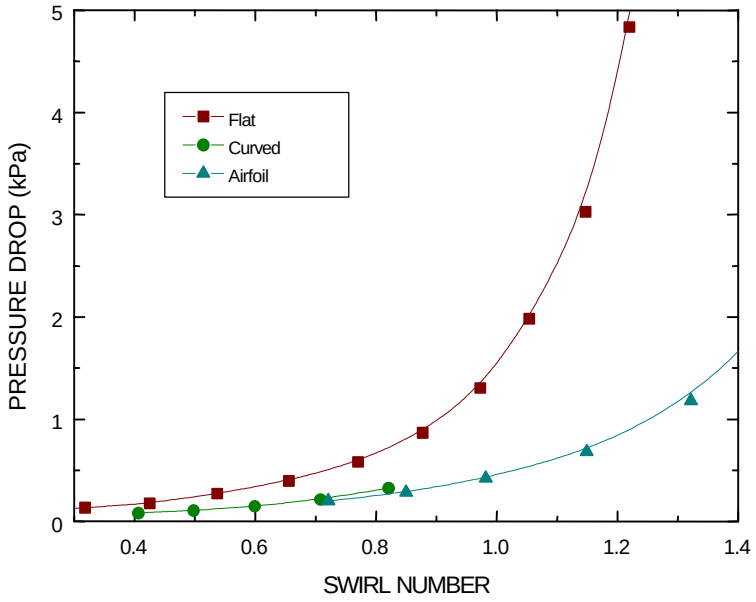

Figure 5-11. Pressure drop versus swirl number for three different fixed vane profiles

Finally, the total burner pressure drop was predicted by simulating the full geometry from the windbox entrance to exit at a reference inner/outer zone adjustable vane angles of 30°/45° (90° ≡ aligned with burner centerline). Figure 5-12 shows a detailed model of the plug-in 4Z™ PC burner inside the windbox. Secondary air pressure distribution is also superimposed on the burner model in Figure 5-12 showing pressure variations from the windbox zone (darker shading) to burner exit (lighter shadings). Total pressure drop for the full geometry was 1.5 kPa (6.0 inches water compared with the measured value of about 5.4). Removing the air separation vane from the baseline burner reduced the pressure drop by 0.1 kPa (0.4 inch of water).

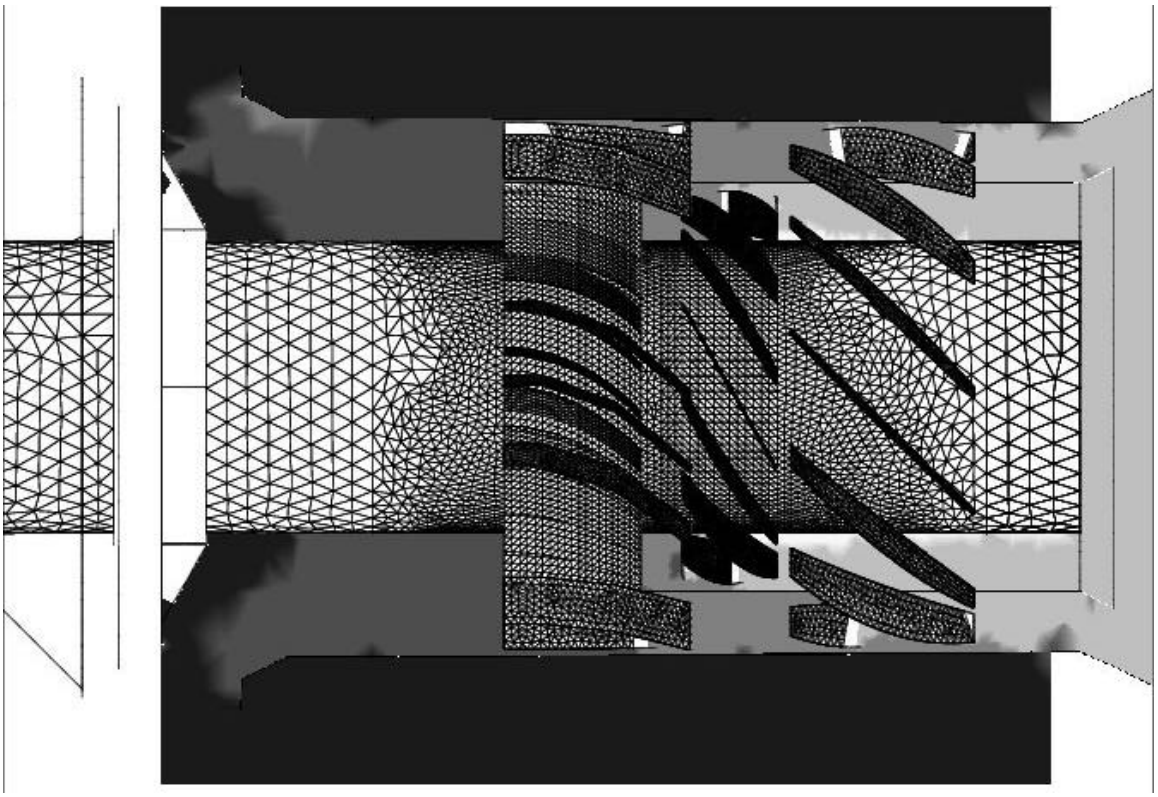

Figure 5-12. Windbox model of the baseline burner

5.4 Reactive Flow (Combustion) Modeling

Once the most promising burner design was selected, the chemically reactive (combustion) model was then applied to predict the flame structure, combustion efficiency, and NO_X emissions. Fuel-specific kinetics information for a high volatile bituminous coal was incorporated in the model. A Lagrangian particle model tracked the coal particle trajectories, fuel devolatilization, and char oxidation. NO_X concentrations were determined with a NO_X post-processor model.

5.4.1 Model Inputs

The single-burner CEDF furnace and convection pass were modeled with COMO, Version 8.10.57. The model is based on as-built furnace dimensions and refractory specifications. The facility geometry was modeled from the burner outlet to the exit of the convection pass, including the tube banks, with 80504 elements using an unstructured mesh generated in Fluent Inc.'s grid generation software GAMBIT version 1.2.4.

Table 5-1 specifies the furnace thermal boundary conditions and refractory conductances. The bottom of the furnace hopper was modeled with a zero heat flux boundary condition and an emissivity of 0.7. Table 5-2 lists the tube bank conductance

parameters. A uniform surface emissivity of 0.7 was used to account for aging and ash deposition on tube surfaces. Table 5-3 lists the inertial resistance coefficients estimated using tube bank correlations [11].

Table 5-1. CEDF Refractory Specification

Surface	Conductance (W/m^2-K)	External Temperature (K)	Emissivity
Hopper	19.9	394	0.7
Burner Tunnel	19.9	394	0.7
Tunnel/Shaft Transition	26.7	394	0.7
Vertical Furnace Shaft	42.6	383	0.7
Furnace Exit	28.4	373	0.7
Convection Pass Mid-region	7.4	373	0.7
Convection Pass Exit	1.7	373	0.7

Table 5-2. CEDF Tube Bank Conductances

Surface	Conductance (W/m^2-K)	External Temperature (K)	Emissivity
Bank 1	8971.7	377.6	0.7
Bank 2A/2B	41.9	377.6	0.7
Bank 4A/4B	36.1	377.6	0.7
Bank 5A	22.1	377.6	0.7
Bank 5B	19.0	377.6	0.7
Bank 5C	17.3	377.6	0.7

Table 5-3. CEDF Tube Bank Resistance Coefficients

Surface	X1 (Pa/m)	X2 (Pa/m)	X3 (Pa/m)
Bank 1	0.8779	0.0	4.4535
Bank 2A/2B	1.9690	0.0	8.7002
Bank 4A/4B	4.1858	0.0964	2.6361
Bank 5A	3.5359	1.9741	0.3254
Bank 5B	3.5666	1.9823	0.3268
Bank 5C	3.5872	2.0874	0.3441

Table 5-4 lists a representative as-fired coal analysis.* Air and coal flow rates are tabulated in Table 5-5. The pulverized coal size distribution was obtained through an average of five sieved size distributions (C-23326 thru C-23330) and plotted in Figure 5-13. A continuous distribution was obtained by fitting a Rosin-Rammler distribution to the average size distribution.

Table 5-4. Representative Mahoning Coal Properties

Ultimate Analysis	As-fired (%)
Carbon	71.52
Hydrogen	4.96
Sulfur	1.96
Oxygen	6.38
Nitrogen	1.45
Ash	11.73
Moisture	2.00
HHV (MJ/kg)	29.7761

Table 5-5. CEDF Model Input Conditions

Zone	Flow Rate (kg/s)	Temperature (K)
Pulverized Coal	0.98367	338.71
Primary Air	1.72138	338.71
Secondary Air	9.47857	588.70

*The Mahoning coal composition used in the modeling was based on historic data and is slightly different from the analysis of the coal used during testing (see Table 6-1).

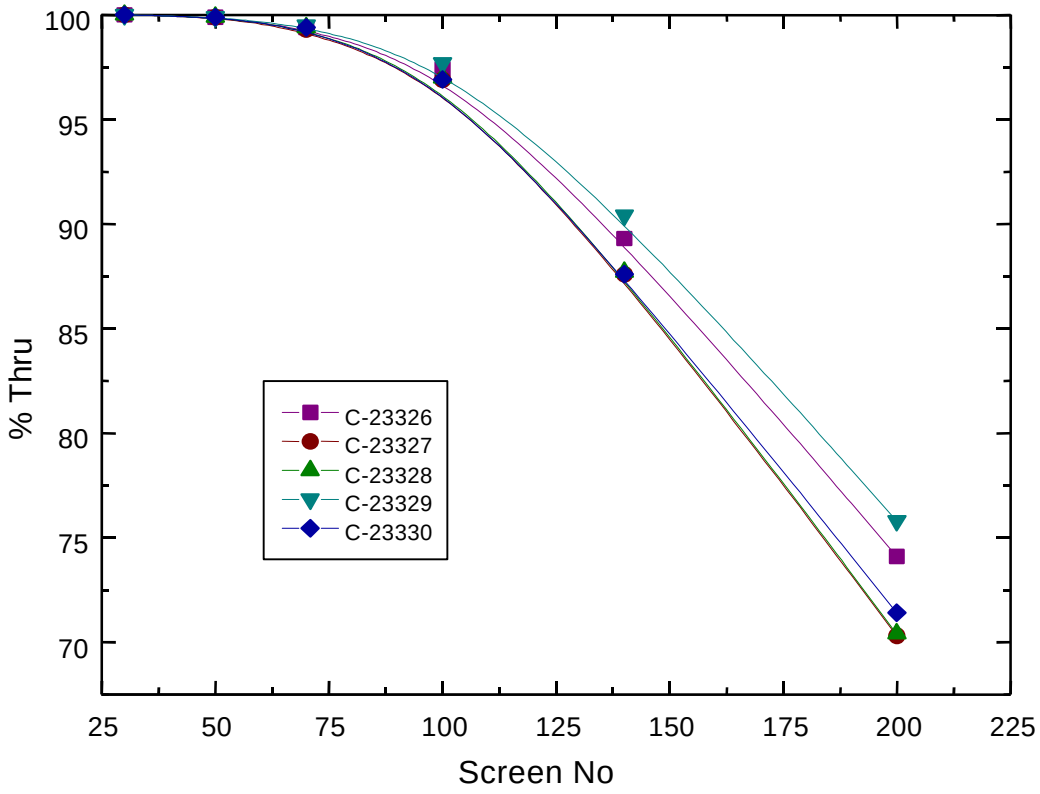

Figure 5-13. Measured screen size distributions

Coal particle trajectories were modeled with a combination of Eulerian and Lagrangian transport models. Small particles (70% <74 microns) have negligible slip and their trajectories are well approximated by Eulerian transport model while larger particles (30% >74 microns) are better tracked by the Lagrangian model. Large particles are the major contributors to the unburned carbon loss. The probability density function for the pulverized coal is shown in Figure 5-14. Coal devolatilization and char oxidation rate parameters were approximated by values for the high volatile bituminous Pittsburgh #8 coal [12].

Initial velocities assignments were based on the 3D non-reactive flow model of the plug-in DRB-4Z™ burner in a 30/45° adjustable swirl vane orientation for inner/outer secondary air zones. Presence of the fixed vanes upstream of the adjustable inner and outer vanes was also simulated. The primary and transition air zones were modeled as uniform non-swirling flows.

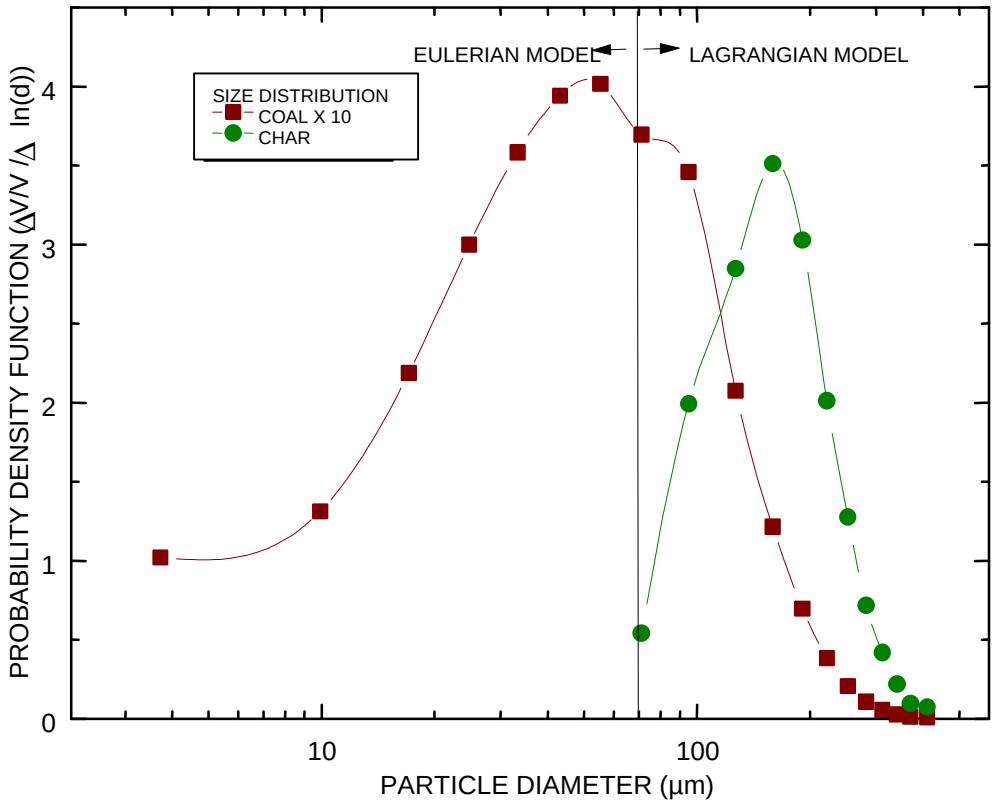

Figure 5-14. Probability density function for the as-fired coal and char at the model exit.

Nitric oxide concentrations were determined by post-processing the flow, temperature, and species concentration fields. Coal-N was assumed to evolve as 80% HCN/20% N_2 and transform to NO_X according to the following global NO_X model:

Fuel –N → HCN
HCN + O_2 → NO
HCN + NO → N_2
NO + CH_i → HCN

5.4.2 Combustion Model Predictions

Mid-plane predictions of velocity, temperature, and species concentrations for 100 million Btu/hr firing of high volatile bituminous Ohio Mahoning coal with 17% excess air are shown in Figures 5-15 through 5-17. Figure 5-15 shows the velocity vectors in the tunnel section and the temperature contours in the furnace and convective pass sections of the CEDF. The flame appears attached with a peak temperature of 1750°C (3182°F) in the near-burner zone. Figures 5-16 and 5-17 show the predicted O_2, CO, HCN, and NO profiles. Predicted NO_X at the convection pass exit was 206 PPMV on a dry basis compared with a measured value of 174 PPMV at an oxygen concentration of 3% in the CEDF.

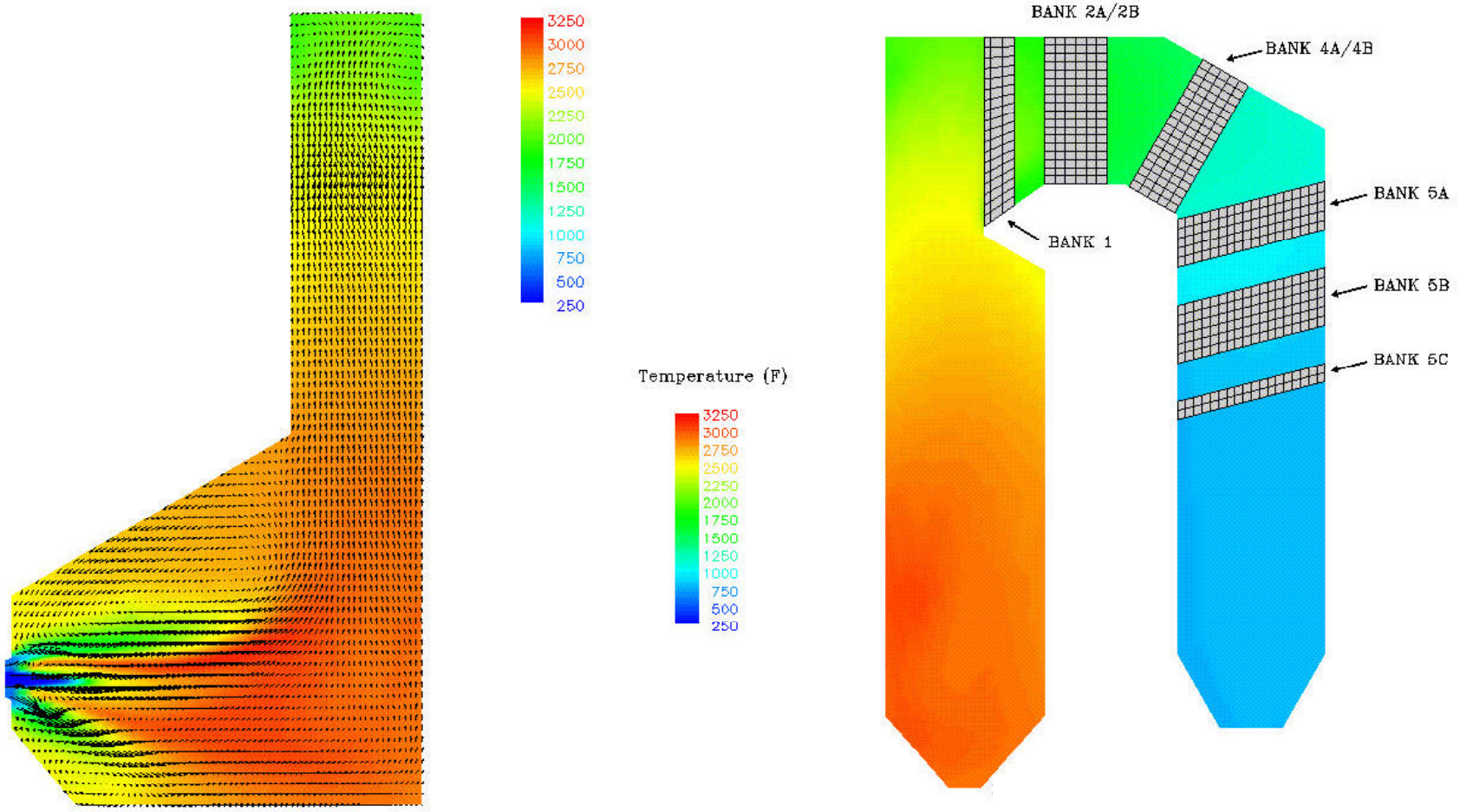

Figure 5-15. Predicted velocity vectors and temperature for 100 million Btu/hr firing of Ohio Mahoning coal at 17% excess air in the CEDF

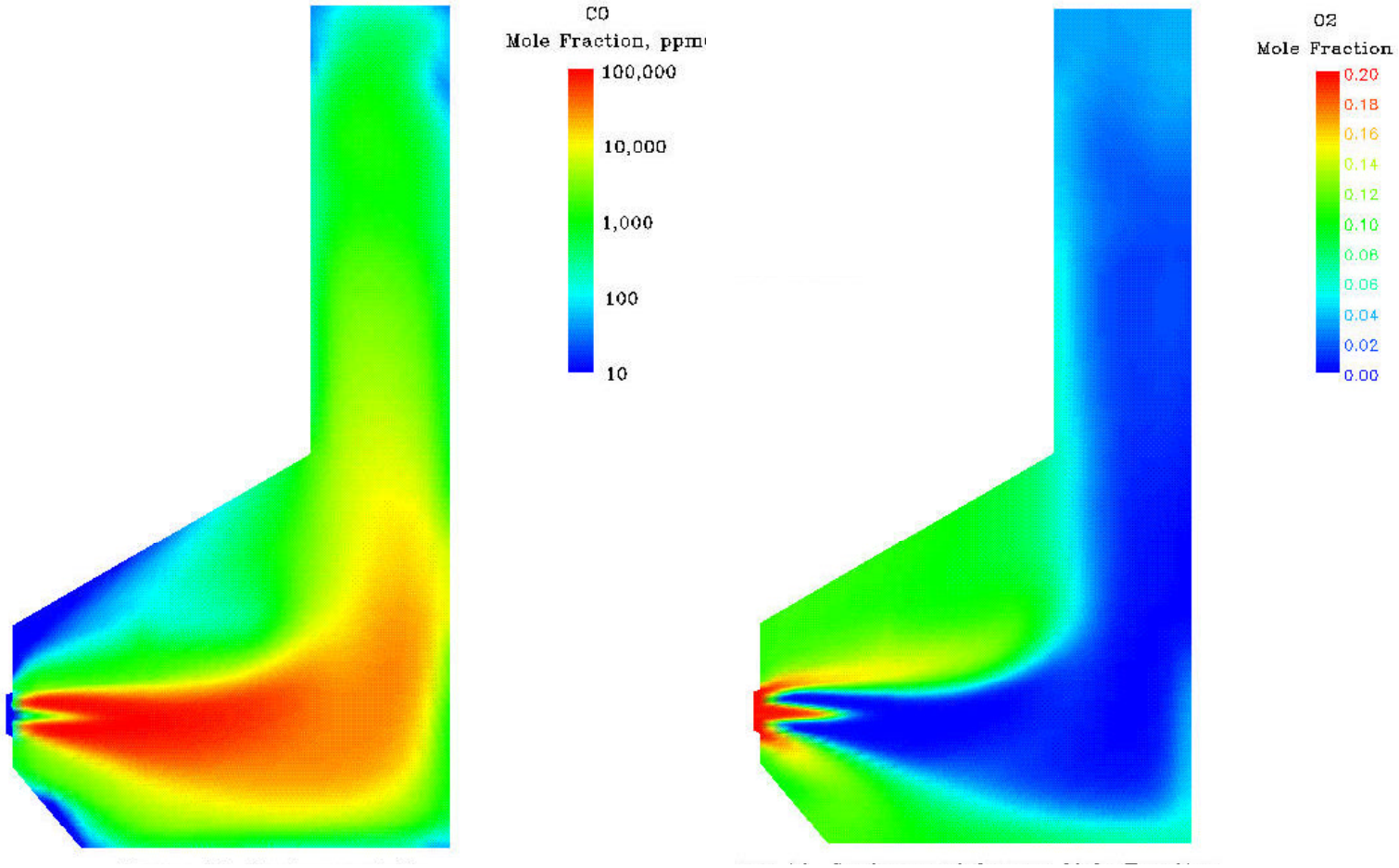

Figure 5-16. Predicted CO and O_2 concentrations for 100 million Btu/hr firing of Ohio Mahoning coal at 17% excess air in the CEDF

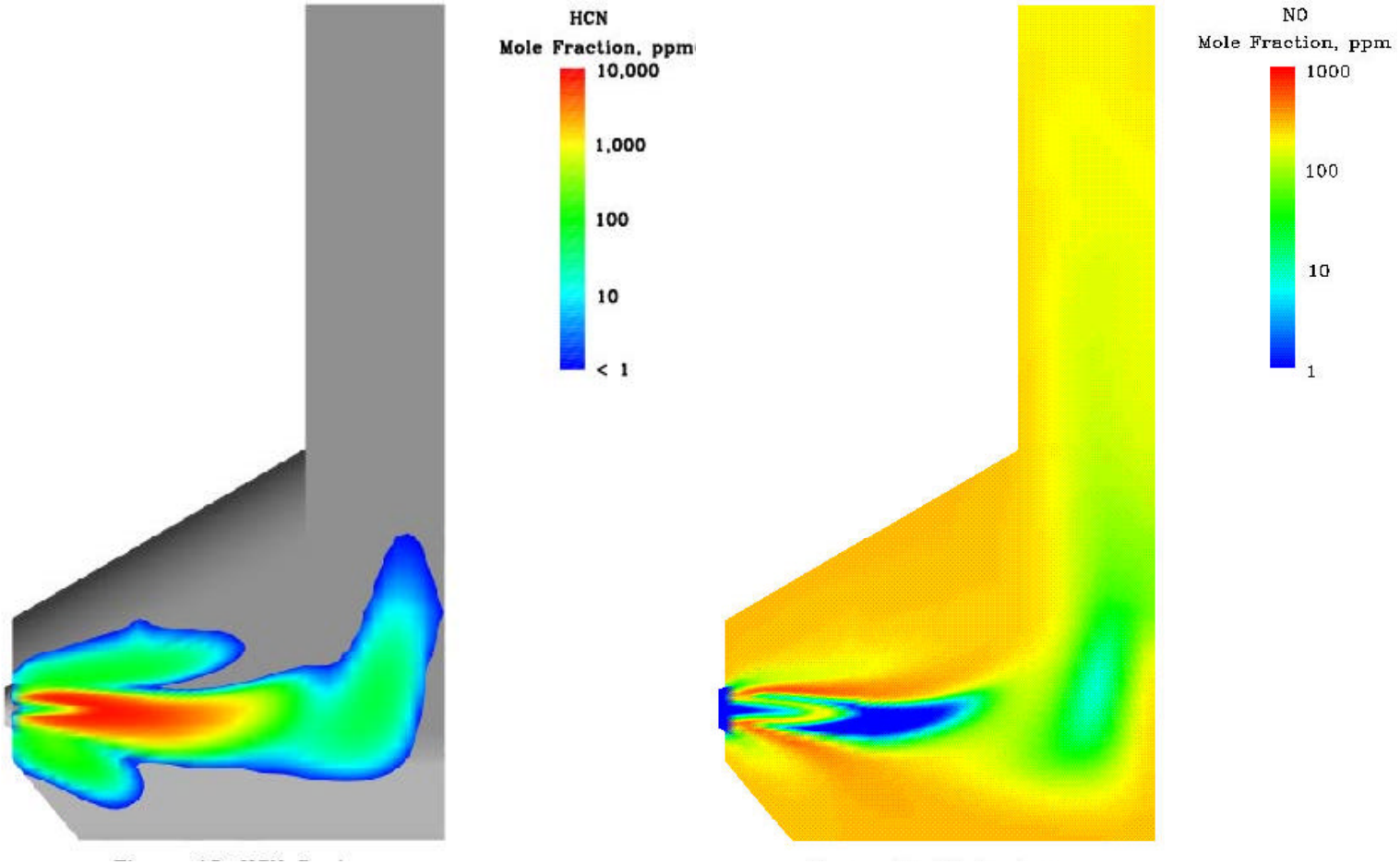

Figure 5-17. Predicted HCN and NO concentrations for 100 million Btu/hr firing of Ohio Mahoning coal at 17% excess air in the CEDF

5.5 Prototype Design

Guided by the numerical modeling simulations and engineering experience, a 100 million Btu/hr plug-in adaptation of the ultra low-NO_X DRB-4Z™ burner was designed and fabricated for prototype testing. The burner operates on the principle of controlled separation, distribution, and mixing of the combustion air and fuel to minimize NO_X and unburned carbon emissions. As such, the design has many commonalties with Babcock & Wilcox's commercially offered low-NO_X DRB-XCL® PC burner.

What sets the DRB-4Z™ burner apart from its predecessor DRB-XCL® design is the incorporation of special features that provide greater NO_X reduction. For instance, the implementation of a "transition zone" allows a small fraction of the secondary air to flow around the coal nozzle. The transition zone promotes coal devolatilization and NO_X reduction by acting as a buffer between the non-swirling primary air and swirling secondary air flows, thereby, eliminating the need for a flame stabilizer.

Two full-size, 29.3 MW_t (100 million Btu/hr), unstaged, low-NO_X DRB-4Z™ and DRB-XCL® PC burners and their preformed refractory quarls (throats) were installed separately in the CEDF for testing. Photographs of the burner hardware are shown in Figure 5-18. In addition to the initial DRB-4Z™ burner, other configurations featuring curved adjustable and fixed vanes for the inner secondary air zone, air distribution devices for the transition zone, and a coal nozzle sleeve insert were also installed and tested for performance improvement.

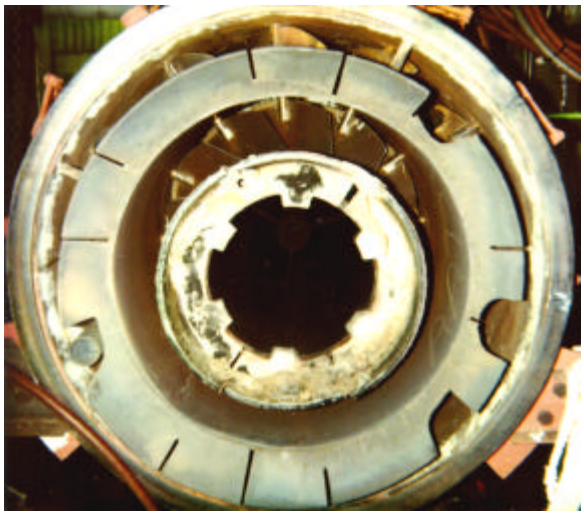

Full-Diameter DRB-XCL®

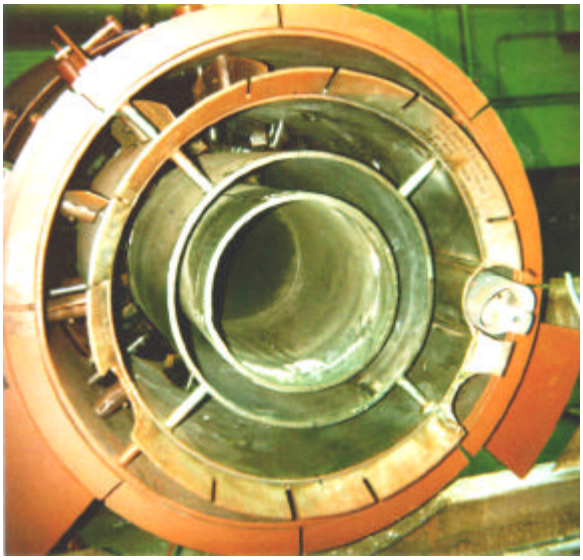

Initial Plug-in DRB-4Z™

Figure 5-18. Photographs of the DRB-XCL® and DRB-4Z™ PC burners

6.0 TEST DESCRIPTION

6.1 Coal Procurement and Analysis

Two high-volatile bituminous Ohio coals, namely Pittsburgh 8 and Mahoning 7 were procured for testing. Table 6-1 shows representative as-received analyses of the coals. Pittsburgh 8 is one of the most mined coals in Ohio and therefore it was chosen as the reference fuel. Over the past five years, MTI and B&W have compiled a large, CEDF burner performance database on the Mahoning 7 coal. For this reason, the evaluation of various design permutations of the plug-in, ultra low-NO_X burner was conducted with the Mahoning 7 coal for comparison with previous burner data.

Table 6-1. Mahoning 7 and Pittsburgh 8 Coal Analyses

	Pittsburgh 8	Mahoning 7
Proximate		
Fixed Carbon (%)	46.42	49.92
Volatile Matter (%)	41.37	39.16
Moisture (%)	3.84	3.47
Ash (%)	8.37	7.45
Fixed Carbon/Volatile Matter	1.12	1.27
Ultimate		
Carbon (%)	71.21	74.10
Hydrogen (%)	4.95	5.16
Nitrogen (%)	1.27	1.44
Sulfur (%)	4.28	1.82
Oxygen (%)	6.08	6.56
Heating Value (kJ/kg)	30,080 (12,930 Btu/lb)	31,020 (13,337 Btu/lb)
Hardgrove Grindability Index	53	49

For each coal, pulverizer settings were adjusted to produce the desired fineness. Pulverized coal samples were extracted from the PC-laden stream after the mill (before the filterhouse) according to the ASME PTC 4.2 procedure. Mass percentage of as-fired PC particles passing through stacked sieves of 200 to 30 mesh screens (74 to 595 micron) were checked each day that coal was pulverized. Table 6-2 shows representative size distributions.

Table 6-2. Pulverized Coal Size Distributions

Mesh Designation and Size (micron)	Percent Smaller		
	Coarse	Standard	Fine
30 (595)	100.0	100.0	100.0
50 (297)	99.6	99.9	100.0
70 (210)	98.2	99.3	99.9
100 (149)	91.9	96.9	99.5
140 (105)	78.0	87.6	97.3
200 (74)	61.9	70.3	88.9

6.2 Burner Performance Tests

Two full-size, 100 million Btu/hr, unstaged, low-NO_X PC burners and their preformed refractory quarls were installed separately in the CEDF for testing. They were evaluated in four series of tests as shown in Table 6-3. In Test Series I, baseline information on gaseous and particulate emissions for a prototype of B&W's commercial DRB-XCL® low-NO_X PC burner were obtained using the reference Pittsburgh 8 coal. The data from this test were compared with the plug-in, ultra low-NO_X, PC burner performance data (Test Series II, III, and IV). Time was also devoted to sampling and collecting particulate matter (PM_{10} and primary $PM_{2.5}$) at fixed operating conditions and burner settings.

Three test campaigns (Test Series II, III, and IV) as outlined in the burner test matrix, Table 6-3, were conducted to evaluate and optimize the plug-in, ultra low-NO_X PC burner performance. The first campaign (Test Series II) utilized the prototype plug-in burner that was designed and selected with the aid of computer modeling. Various devices that potentially enhanced fuel/air mixing and reduced carbon burnout without appreciably changing the NO_X emissions were installed in the burner for Test Series III. Since the burner was rack-mounted inside the CEDF windbox, it could be retracted from the hot furnace environment for modification immediately after shutdown. By minimizing furnace heat loss during burner modifications, testing resumed within four hours after restart, thus maximizing the number of hardware arrangements that were evaluated. High combustion efficiency, short flame length, low-NO_X emissions, low burner ΔP, and flame stability at minimum load were among the factors that were evaluated to determine the best plug-in design for further evaluation. As stated earlier, initial evaluation of the plug-in, ultra low-NO_X burner and various hardware permutations including mixing devices was conducted with the Mahoning #7 coal.

Air staging effects on NO_X and $PM_{2.5}$ emissions were characterized using the Pittsburgh #8 coal in the final test campaign of the plug-in burner at a fixed overall excess air level of 17%. Both the burner and OFA register settings were re-optimized at a nominal burner stoichiometry of 0.85. Burner stoichiometry was then varied from 0.85 to 1.10 by splitting the total secondary air flow between the burner and the OFA ports. These tests were used to assess the impact of staged combustion on NO_X control and primary $PM_{2.5}$ emissions relative to unstaged operation.

Table 6-3. Combustion Test Parameters

Burner Hardware and Nominal Operating Conditions										Sampling and Measurements	
Burner Design & Configuration	Heat Input (Million Btu/hr)	Coal	Burner Settings			OFA Settings		Stoichiometry		CO, CO_2, SO_2, O_2, NO_X, and LOI	PM_{10} And $PM_{2.5}$
			Spin Vane Angle (° open)		Mixing Device Position	Damper (% open)	Vane Angle (° open)	Burner	Overall		
			Inner	Outer							
Test Series I Commercial DRB-XCL® Prototype	100	Pittsburgh 8	20 to 45	40 to 60	NA	NA	NA	1.17	1.17	All	--
	100	Pittsburgh 8	Optimum	Optimum	NA	NA	NA	1.10 to 1.28	1.10 to 1.28	All	Yes
	Minimum	Pittsburgh 8	Optimum	Optimum	NA	NA	NA	1.28 to 1.35	1.28 to 1.35	All	--
Test Series II Initial Plug-in Prototype	100	Mahoning 7	20 to 45	40 to 60	NA	NA	NA	1.17	1.17	All	--
	100	Mahoning 7	Optimum	Optimum	NA	NA	NA	1.10 to 1.28	1.10 to 1.28	All	--
	Minimum	Mahoning 7	Optimum	Optimum	NA	NA	NA	1.28 to 1.35	1.28 to 1.35	All	--
Test Series III Plug-in Prototype + Mixing Devices	100	Mahoning 7	20 to 45	40 to 60	Fore/Aft	NA	NA	1.17	1.17	All	--
	100	Mahoning 7	Optimum	Optimum	Optimum	NA	NA	1.10 to 1.28	1.10 to 1.28	All	--
	Minimum	Mahoning 7	Optimum	Optimum	Optimum	NA	NA	1.28 to 1.35	1.28 to 1.35	All	--
Test Series IV Final Plug-in Prototype	100	Pittsburgh 8	20 to 45	40 to 60	Optimum	NA	NA	1.17	1.17	All	--
	100	Pittsburgh 8	Optimum	Optimum	Optimum	NA	NA	1.10 to 1.28	1.10 to 1.28	All	Yes
	Minimum	Pittsburgh 8	Optimum	Optimum	Optimum	NA	NA	1.28 to 1.35	1.28 to 1.35	All	--
	100	Pittsburgh 8	20 to 45	40 to 60	Optimum	30 to 100	30 to 60	0.85	1.17	All	--
	100	Pittsburgh 8	Optimum	Optimum	Optimum	Optimum	Optimum	0.85 to 1.10	1.17	All	Yes

6.2.1 Burner Test Procedures

Each burner hardware test series began with a three-hour warm-up period that involved heating the combustion air and firing natural gas through the ignitor and an auxiliary spud. Instrument calibration and general system checks were done during this period and re-examined periodically throughout the day. Once suitable furnace conditions for coal firing were reached, pulverized coal and air were introduced gradually into the burner and ignited by the natural gas pilot flame. Shortly after, the pilot flame was shut off and the pulverized coal feed rate was increased progressively over two hours, until the desired load was established. The furnace was then allowed to warm-up for at least two more hours until the convection pass exit temperature and gas species concentrations reached steady state levels.

Optimum burner settings for each burner hardware configuration were then established at full load 29.3 MW_t (100 million Btu/hr) and 17% excess air (1.17 stoichiometric ratio). Table 6-4 lists the nominal CEDF operating conditions for an Ohio coal. Swirl vane angles of the burner were adjusted systematically between 20 and 60° (0° is fully closed and 90° is wide open) to determine their optimum orientation. Where applicable, the position of air distribution and/or coal nozzle mixing devices were varied. Other major experimental variables included overall excess air, burner stoichiometry, and thermal load. Gas species concentrations were measured for each test. Unburned carbon loss (UBCL) values were calculated from the LOI measurements and fuel analysis. UBCL is a measure of the unutilized fuel and combustion efficiency. Approximate flame lengths were determined from the available furnace sight ports shown in Figure 4-2. Key measurements and operating conditions including NO_X, CO, LOI, burner ΔP, air flow rates, heat input, combustion stoichiometry, burner settings, etc. were tabulated and in some cases represented graphically. Visual observations and other pertinent test information were recorded in a logbook.

6.2.2 Burner Performance Test Matrix

Table 6-3 summarizes the test parameters and measurements. In all cases, computerized data acquisition was used for monitoring and recording gas species concentrations, flow rates, temperatures, pressures, and other relevant information. CO, CO_2, SO_2, O_2, and NO_X concentrations were measured continuously at the convective pass section exit. SO_2 and O_2 levels were measured at the ESP inlet. NO_X, SO_2, and O_2 emissions were also monitored at the CEDF stack. Reproducibility of the data was checked at optimum burner settings by repeating the test conditions. Typical intervals from adjusting the burner settings and/or operating conditions to reaching steady state conditions for data collection is about 10 to 20 minutes. Burner performance data representing a new test condition (i.e., different settings and/or operation) were scanned every 15 seconds and saved electronically for 10 to 30 minutes.

Table 6-4. Nominal CEDF Operating Conditions	
Heat input rate (MW_t)	29.3 (100 million Btu/hr)
Coal feed rate (kg/hr)	3,570 (7880 lb/hr)
Coal fineness (% through 200 mesh screen)	70
Primary air flow rate (kg/hr)	6440 (14200 lb/hr)
Primary air temperature (°C)	66 (150°F)
Secondary air flow rate (kg/hr)	33,700 (74300 lb/hr)
Secondary air temperature (°C)	316 (600°F)
Excess combustion air (%)	17
Stack SO_2 compliance limit (g/GJ)	513 (< 1.2 lb/million Btu)
Stack NO_X compliance limit (g/GJ)	300 (< 0.7 lb/million Btu)
Opacity compliance limit (%)	< 6
Dry scrubber lime slurry solids (%)	24
Dry scrubber slurry flow rate (m^3/min)	.0367 (9.7 gal/min)
Dry scrubber dilution water flow rate (m^3/min)	.002 (0.5 gal/min)
Dry scrubber inlet temperature (°C)	107-163 (225 to 325°F)
Dry scrubber outlet temperature (°C)	63-77 (145 to 170°F)
ESP inlet temperature (°C)	121-177 (250 to 350°F)

Sampling and measurement of primary $PM_{2.5}$ emissions as described in Section 6.3 was done at various locations on a selective basis when firing the baseline DRB-XCL® and the refined prototype of the plug-in ultra low-NO_X PC burners. In most instances particulate matter sampling was simultaneously conducted at the ESP inlet and ESP outlet.

6.3 $PM_{2.5}$ Sampling and Analysis

The objective of the $PM_{2.5}$ tests was to collect and chemically characterize the primary $PM_{2.5}$ emissions representative of coal fired power plants. Primary $PM_{2.5}$ emissions were collected and analyzed for different boiler/burner operation and varied ESP operation. $PM_{2.5}$ sampling and characterization was divided into two series of CEDF tests representing a baseline "conventional low-NO_x" combustion, and "ultra low-NO_x" combustion. In the baseline tests, primary $PM_{2.5}$ emissions were characterized for a commercial version of the B&W DRB-XCL® low-NO_x PC burner (expected emissions of 0.40 lb NO_x/million Btu), and particulate control using an ESP. The ESP was operated at three different conditions (voltage and number of fields) to vary the particle removal efficiency. The emission levels for these tests were all below the NSPS of 0.03 lb/million Btu.

In the "ultra low-NO_x" series of tests, primary $PM_{2.5}$ emissions were characterized using the plug-in ultra low-NO_x DRB-4Z™ burner that was developed in this program. NO_x emissions for this burner are about 0.20 lb NO_x /million Btu with unstaged combustion. NO_x is reduced to about 0.15 lb NO_x /million Btu using secondary air staging. The burner is an adaptation of a full-diameter (large throat) version of the DRB-4Z™ burner developed by B&W and MTI as part of the U.S. Department of Energy-sponsored Combustion 2000 Program. For the ultra low-NO_x tests the ESP was operated the same as earlier tests of the DRB-XCL burner, so that the effect of combustion conditions on the fly ash and ESP removal efficiency could be evaluated. The particulate emission levels for the ultra low-NO_x tests were also below the NSPS limit of 0.03 lb/million Btu.

The $PM_{2.5}$ testing was conducted using Pittsburgh 8 coal. After collection, the PM samples were analyzed to determine the carbon content, soluble ion concentration and elemental composition. Additionally, the mass of condensable organic and inorganic compounds were determined from flue gas sampling.

6.3.1 Operating Conditions for $PM_{2.5}$ Sampling

The operating conditions of the CEDF equipment and the ESP for $PM_{2.5}$ tests are presented in Table 6-5. Burner settings were established before the start of sampling, and the burner/furnace operation was maintained constant within the limitations of the equipment and the variability of the coal. The total excess oxygen for all tests was held constant at about 3.2%, which is equivalent to a combustion stoichiometry ratio (S.R.) of 1.17. In Test D secondary air to the furnace was staged, with a S.R. of 0.85 at the burner and the balance supplied to the OFA ports. In Test D and E, the excess oxygen and CO concentrations were the same, while the staged combustion provided lower NO_x concentrations. $PM_{2.5}$ sampling was not conducted during upset conditions such as soot blowing.

The conventional low-NO_x burner was adjusted to represent field operation, which provided low-NO_x as well as low CO and low unburned carbon in the fly ash. The ultra low-NO_x plug-in burner was adjusted to achieve the lowest possible NO_x in order to examine the effect of minimum NO_x and higher unburned carbon levels on $PM_{2.5}$.

Likewise, the ESP was operated to determine the effect of ESP operating parameters on PM emissions (Tests A, B and C), and the effect of combustion conditions on PM emissions for constant ESP operation (Tests A, D and E). The ESP was not adjusted to achieve specific values of particulate emissions.

Table 6-5. Summary of Combustion Conditions and ESP Operation for the Low NO_x and Ultra Low-NO_x $PM_{2.5}$ Sampling

Burner	Test A DRB-XCL®	Test B DRB-XCL®	Test C DRB-XCL®	Test D DRB-4Z™	Test E DRB-4Z™
Firing Mode	Low-NO_x Unstaged	Low-NO_x Unstaged	Low-NO_x Unstaged	Ultra Low-NO_x Staged	Ultra Low-NO_x Unstaged
Oxygen (dry, %)	3.18	3.18	3.14	3.14	3.17
NO_x (ppm dry at 3% O_2)	286	276	262	105	142
CO (ppm dry at 3% O_2)	34	41	46	270	264
SO_2 (ppm dry at 3% O_2)	3460	3349	3195	3345	3194
Flue Gas Flow, kg/hr (acfm)	44,200 (33480)	43,876 (32650)	43,957 (33140)	43,751 (32782)	44,043 (33341)
ESP Inlet Temperature, °C (°F)	175 (348)	169 (335)	173 (343)	165 (329)	168 (335)
Number of ESP Fields	2	3	3	2	2
Specific Collection Area (ft^2 per 1000 acfm)	185	285	281	189	186
Field Voltages (kV)	No. 1 – 54 No. 2 – 54 No. 3 – off	No. 1 – 54 No. 2 – 54 No. 3 – 34	No. 1 – 54 No. 2 – 54 No. 3 – 54	No. 1 – 52 No. 2 – 52	No. 1 – 52 No. 2 – 52

6.3.2 Sampling Locations

Flue gas sampling was conducted in the 1.2 meter (48 inch) diameter flues leading to and from the ESP. The geometry and cross-section of these flues and the location of the sample ports are shown in Figure 6-1. The sampling ports are located in the flues in accordance with EPA Method 1.

In addition to the flue gas sampling for primary particulate, solid samples of the as-fired coal and the ESP hopper ash were collected. Samples of the as-fired pulverized coal were collected at regular intervals as part of the normal CEDF operation. Ash samples from the hopper of each of the operating ESP fields were collected for each test.

6.3.3 Sampling Methods

Particulate sampling was conducted using established and draft EPA Methods for stationary source sampling. A high volume sampling method was used to collect relatively large quantities of particulate at the ESP outlet. These methods are listed in Table 6-6. As indicated, the particulate sampling methods provide gravimetric representations of primary particulate in different size fractions. EPA Method 202 is an impinger based method for quantifying organic and inorganic condensable particulate.

The particulate samples collected using these procedures were used for chemical analyses of the fly ash constituents. The matrices which specify the methods used at the ESP inlet and outlet are given in Appendix A.

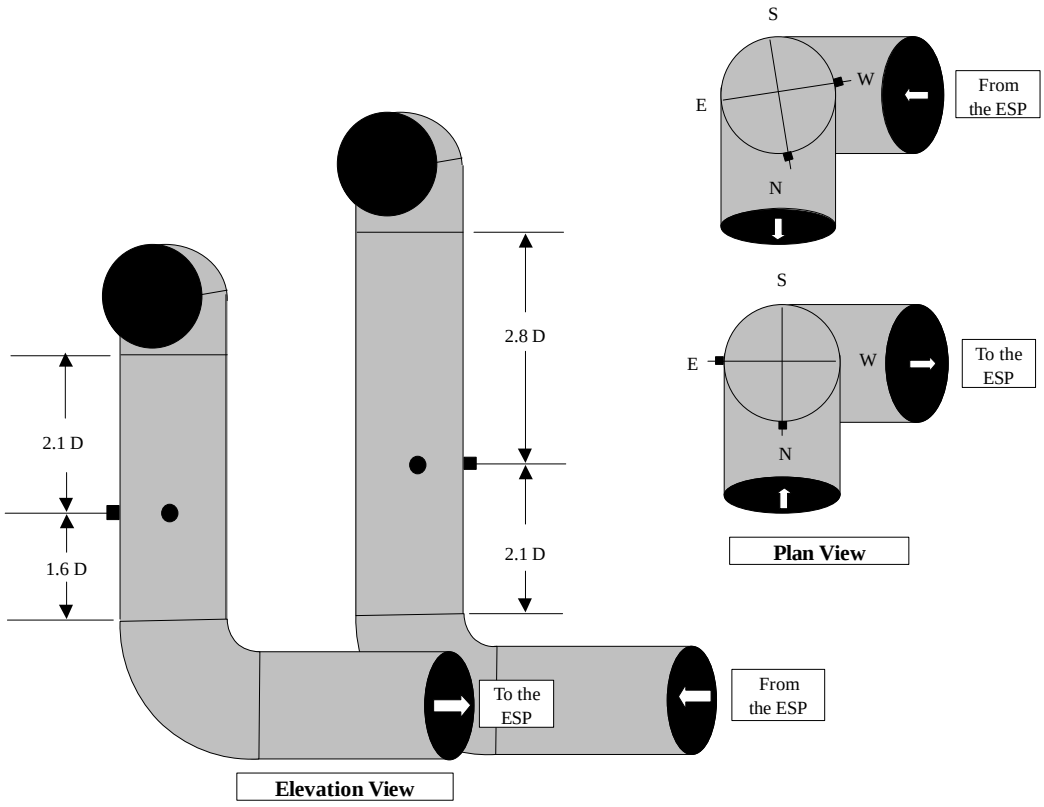

Figure 6-1. Particulate sampling locations at the ESP inlet and exit

Table 6-6. Sampling Procedures for Collection of Particulate Matter		
Measurement	Method	Back-Up Filter Media
Particle Size Distribution (Cascade Impactor)	EPA 201A	Quartz
Mass Loading PM >10, 10 > PM > 2.5, PM < 2.5	$PM_{10}/PM_{2.5}$ Draft EPA[1]	Quartz/Teflon
Condensable Organic and Inorganic Mass	EPA 202	N/A
Sulfuric Acid Mist	Controlled Condensation	N/A
PM at ESP Outlet (High Volume)	---[2]	Quartz/Teflon

1. Draft Method for Determination of PM_{10} and $PM_{2.5}$ Emissions (Constant Sampling Rate Procedure), EPA Method PRE 4.
2. Approximately 10 ACFM sample flow with 8”X10” filter substrate.

A description of the different sampling methods is provided below.

Cascade Impactor (EPA Method 201A)

An Anderson Mk III eight stage cascade impactor was used to measure the fly ash aerodynamic particle size distribution. At the ESP inlet the impactor was equipped with a cyclonic pre-separator. The pre-separator collects particulate greater than about 10 microns in diameter, which prevents overloading of the first impactor stage and carryover to subsequent stages. The eight impactor stages span an aerodynamic size range of about 0.5 to 10 microns. Material smaller than 0.5 microns was collected on a back-up filter. The cascade impactor was positioned in the stack during sampling. The back-up filter was located either "in-stack" or in a heated sample box attached to the end of the sampling probe.

At the ESP outlet, sampling was conducted at a total of 12 points in the duct (six points in each of the two traverse directions) as specified in Method 201A. The sample flow rate through the cascade impactor was maintained constant so that the particle cut-sizes of the impactor stages remain the same for all sample points. The sample time at each point was adjusted according to the local velocity so that a representative sample volume was collected at each point.

At the ESP inlet the total sample time was necessarily short because of the high particle loading. The number of sample points was reduced to prevent overloading of the impactor stages. Quartz fiber filter material was used to collect particulate for each impactor stage.

$PM_{10}/PM_{2.5}$ Particulate

The Draft EPA Method for PM_{10} and $PM_{2.5}$ emissions was used to obtain particulate samples with aerodynamic diameters greater than 10 microns, between 2.5 and 10 microns, and smaller than 2.5 microns. Quartz filters and Teflon membranes were used as backup filters to collect the $PM_{2.5}$ size fraction. The different filter substrates were used to accommodate different analytical techniques.

The sampling procedure for this method was the same as for the cascade impactor (Method 201A). The sample flow rate was maintained constant to maintain a constant aerodynamic size separation of the fly ash. The sampling time at a point in the flue gas was inversely proportional to the gas velocity.

To accommodate the different mass loading at the inlet and outlet of the ESP, different sampling times and/or back-up filters of different sizes were used. The cyclones used for size separation of particulate were located "in-stack". The backup filters that collect the smallest particulate (i.e. PM

< 2.5 microns) were located either “in-stack” or in a heated sample box, depending on the specific requirements of the test. Out of stack filters were contained in a heated filter box and maintained at the flue gas temperature. All of the flue gas sampling was conducted using heated, glass lined sample probes. The out of stack filters were either connected directly to the glass lined sample probe, or connected to the sample probe by way of a trace heated Teflon sample line maintained at the flue gas temperature.

The recovered particulate sample consisted of loose particulate collected in the cups of the cyclones, the $PM_{2.5}$ collected on the backup filter, and particulate collected as rinses of the hardware. The particulate collected in rinses was dried and weighed, but was not chemically analyzed.

Condensable Particulate (EPA Method 202 and Controlled Condensation)

EPA Method 202 used for measuring condensable organic and inorganic mass is an impinger based measurement that is independent of the particulate sampling technique. Condensable particulate is primarily acid gases and organic compounds that are in the vapor state at typical ESP temperatures, but condense as the temperature is reduced to ambient temperatures. This method was used on some, but not all of the particulate sampling measurements. The condensable inorganic fraction of the condensable material was analyzed for ion concentration (sulfates, nitrates, chlorides, fluorides, etc.).

In addition, for Test Series I, the fraction of condensable particulate represented by sulfuric acid was independently measured using the controlled condensation method. This method is described in EPA Publication EPA-600/3-84-056 (NTIS PB84-182823), “Miniature Acid Condensation System Design and Operation”.

High Volume Sampler

In addition to the EPA (and draft EPA) sampling Methods, a high volume sampler was used to collect particulate at the outlet of the ESP. The purpose of this sampler was to collect a larger mass of particulate in a shorter period of time than is possible with the Draft EPA Method. The sample probe for the high volume sampler was constructed of stainless steel with a tapered inlet nozzle. The sample probe and filter box was insulated and trace heated as needed to maintain the flue gas temperature. The sample flow rate was measured using an orifice plate. The particulate sample was collected on 8 inch x 10 inch quartz and Teflon filter substrates. Traverses of the duct during the high volume sampling were performed using the same 12 point sampling positions as the other sampling procedures.

Other Sampling

Solid samples of coal and fly ash were collected at regular intervals during each test. These samples included as-fired pulverized coal and ash samples from each of the three ESP fields.

Pulverized coal was sampled between the pulverizer and the PC hopper once during each pulverizing cycle. A composite of these individual samples was submitted for chemical analyses.

For the initial test, the ESP collection plates and ash hoppers were in a "clean" condition. The plates were rapped and the hoppers were emptied of all loose fly ash. The CEDF and ESP were operated for approximately 24 hours on the test coal before the first test began. The ESP hoppers were again emptied before the start of the first test.

6.3.4 Sample Analyses Methods

Table 6-7 lists the analysis methods that were conducted on the different samples collected during CEDF testing. An example flue gas sampling and analysis matrix is in Appendix A.

Table 6-7. Analysis and Analysis Methods for Collected Samples

Sample	Analysis	Method
Flue Gas Particulate Matter	Mass	Gravimetric
	Total Carbon	Loss on Ignition (LOI) Carbon Dioxide Absorption
	Organic & Elemental Carbon	Thermal Optical Analyzer (TOA)
	Elements	ICP and AA
	Soluble Ions	IC, FES and ISE
ESP Hopper Ash	Particle Size Distribution	Microtrac
Flue Gas Condensable Inorganic Matter	Mass	Gravimetric
	Ions	IC, FES, and ISE
Controlled Condensation	Sulfuric Acid	IC
Flue Gas Condensable Organic Matter	Mass	Gravimetric
Coal	Standard Coal Analysis	Ultimate and Proximate Analysis
	Trace Elements	ICP and AA
	Particle Size	Sieving, Microtrac

ICP = Inductively Coupled Plasma
IC = Ion Chromotography
ISE = Ion Selective Electrode
AA = Atomic Absorption
FES = Flame Emission Spectroscopy

The following is a general discussion of the analyses and techniques that were performed on the collected samples.

Mass

Electronic balances with resolutions 0.1 mg, 0.01 mg, and 0.001 mg were used for particle catch mass determinations and the preparation of standards. The most appropriate balance was selected for each weighing based on the required accuracy and the mass to be determined. In general, the uncertainty in the mass of collected particulate was less than 2%.

Carbon

The carbon content of the different size fractions was determined by LOI, Thermal Optical Analyzer (TOA, NIOSH Method 5040), and carbon dioxide absorption (ASTM Method D-3178). LOI is a conservative measure of total carbon through a loss in weight measurement. The TOA is a direct measure of the carbon content of the ash using a FID (Flame Ionization Detector). By virtue of the method of operation associated with the TOA, portions of the total carbon are identified as organic, carbonate and elemental. Carbon dioxide absorption is the determination of carbon by burning a weighed quantity of sample in a closed system and fixing the products of combustion in an absorption train after complete oxidation and purification from interfering substances. The method gives the total percentage of carbon in the coal as analyzed, and includes the carbon in carbonates.

Since LOI is fundamentally a mass measurement, larger samples provide greater resolution. The TOA has an upper limit of about 100 μg of carbon per 1.5cm^2 filter sample, and smaller particulate masses are usually required. Both analyses were performed on quartz fiber filter substrates.

Elements

Fly ash major constituents and trace elements were measured with ICP, or AA depending on the required sensitivity for specific elements. The trace element concentrations that were determined using ICP and AA and the expected detection limits in the particulate, assuming a 40 mg particulate sample are provided in Appendix B.

Coal major constituents and trace elements were also determined using ICP and AA. A list of the sample preparation and analysis procedures for these measurements is provided in Appendix B.

Ions

Ions were analyzed by a combination of Ion Chromatography (IC), Flame Emission Spectroscopy (FES) and Ion Selective Electrode (ISE). For specific ions, all three techniques provide similar detection limits. IC was used to determine anions (sulfates, nitrates and phosphates, chlorides and fluorides). FES was used for cations (sodium and potassium), while ISE was used for ammonia. The use of two techniques for anions and cations eliminated the need to change ion columns and the associated calibration. Ion concentrations were determined for the inorganic fraction of condensable particulate. De-ionized water extracts of the particulate were analyzed for ion concentration. The soluble ions that were determined using IC, FES and ISE and the detection limits in the solid phase based on a 40 mg particulate sample is provided in Appendix B. Appendix B also provides a listing of the sample preparation and analysis procedures for these measurements.

Ultimate/Proximate Analysis

Coal analyses were conducted on a composite of samples taken during the pulverizing process over the duration of the test. The ultimate and proximate analysis of the coal were conducted in accordance with ASTM procedures. The chlorine and fluorine content of the coal was also determined. The test procedures for these analyses are provided in Appendix B.

Scanning Electron Microscope

Selected samples of $PM_{2.5}$ were analyzed using SEM. Although SEM can provide detailed information on the form and constituents of a fly ash sample, the technique is strongly dependent on the form of the sample and the size of the particulate. SEM was primarily used to provide a visual representation of collected particulate.

Particle Size Distribution Microtrac

The fly ash samples from the hoppers of the ESP fields were analyzed with a Microtrac particle analyzer to determine the relative particle sizes associated with the three ESP hoppers. The Microtrac provides an optical particle size, which does not necessarily correspond to the aerodynamic particle size classification provided by the cascade impactors and cyclones. The fly ash obtained from hopper samples can be significantly agglomerated and may not completely re-disperse for this measurement. Microtrac analyses were also conducted on a composite pulverized coal sample.

6.4 Quality Assurance

Work performed under this project was performed in accordance with the MTI Research and Development Division (R&DD) STANDARD PRACTICE Quality Program. This program is the baseline operating level designation for normal business practices within R&DD. The program is specified in the Quality Management Manual and implemented by the Standard Practice Manual.

The project workscope was defined by way of project planning with the result being an agreement with the customer at the outset of the project. Changes to the workscope were also agreed upon with the customer. Accordingly, project records are maintained throughout the testing program to provide a historical account of all significant activities. The calibration of all measurement standards and measuring and test equipment used within the R&DD is controlled in order to ensure that measurements made are quantifiable and reproducible in terms of nationally recognized standards.

The quality of work in a given project is in evidence within the final report which was prepared upon completion of the project. If there are specific customer requirements such as material certification, inspections, special tests or calibration, they are specified in the work authorizing document. The individual project leader and the R&DD management ensures these requirements are met and appropriate documentation is on file.

The Quality Assurance organization exercises general surveillance over projects conducted according to STANDARD PRACTICE. Internal audits are planned and conducted to verify the implementation and effectiveness of the internal quality system.

Project records are available for customer review at the R&DD. The retention of these records is in accordance with MTI policy (minimum five years) or as specified by customer requirements, applicable codes, standards or specifications.

7.0 ULTRA LOW-NO_X BURNER RESULTS

7.1 Prototype Plug-in DRB-4ZÔ Burner Testing

Initial evaluation of the plug-in, ultra low-NO_X burner and various hardware permutations was conducted with the Ohio Mahoning 7 coal. Optimum burner settings for each hardware arrangement was established at full load 29.3 MW_t (100 million Btu/hr) and 17% excess air by systematic adjustments of spin vane angles, and/or coal nozzle mixing device position. Secondary air swirl vane angles were varied between 20 and 70° (0° is fully closed and 90° is wide open) to determine their optimum orientation. Other major variables included primary air-to-pulverized coal ratio (PA/PC), thermal load, and excess air level.

7.2 PA/PC Effects

Investigation of the effect of PA/PC mass ratio on the combustion and emissions performance of the plug-in DRB-4Z™ burner led to an important finding that was later implemented in the design. We discovered that the NO_X emissions for the PPVANE configuration decreased and LOI levels remained relatively unchanged as shown in Figure 7-1, when PA/PC was increased above the normal value of 1.8.

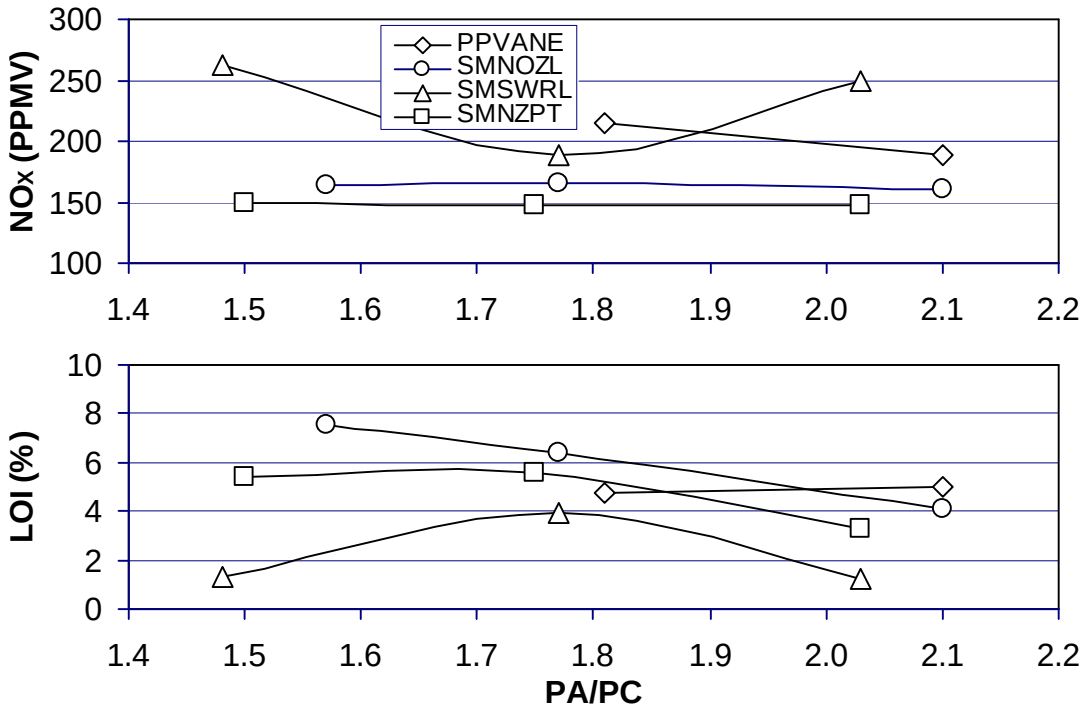

Figure 7-1. Primary air-to-pulverized coal ratio effect on NO_X and LOI for four configurations of the ultra low-NO_X plug-in DRB-4ZÔ PC burner firing 70% through 200 mesh fineness pulverized coal at 100 million Btu/hr and 17% excess air

Within limits, raising the primary airflow rate or the primary combustion zone stoichiometry increases the flame temperature and enhances the early release of NO_X reducing precursors. It also helps to preserve the pulverized coal jet from rapid dispersion and mixing with the swirling secondary air streams. Therefore, a thick-walled sleeve was installed inside the coal nozzle to increase the primary air velocity incrementally. With a multi-bladed swirler positioned inside the reduced diameter coal nozzle (SMSWRL case), the axial momentum of the PC transport jet was no longer preserved and after an initial drop in the NO_X emissions, further increase in PA/PC resulted in higher NO_X generation. The SMNOZL and SMNZPT series also retained the sleeve insert but had no swirler and represented identical burner hardware for firing Mahoning 7 and Pittsburgh 8, respectively. Both sets of data indicate that increasing the PA/PC further reduces the LOI levels and has nearly no effect in NO_X concentrations.

7.3 Coal Nozzle Swirler Position Effects

Changes in NO_X and LOI due to the retraction of a swirler inside the plug-in DRB-4Z™ PC burner at a constant burner register settings and fixed thermal load and excess air levels are shown in Figure 7-2. A key difference between the SMSWRL and SMSWRLCON configurations is a diverging cone in the latter case that spreads out the swirling PC-laden primary air. And because of this device, the NO_X emissions are higher and tend to increase (opposite to LOI) as the swirler is positioned close to the nozzle exit (swirler position ≡ 0).

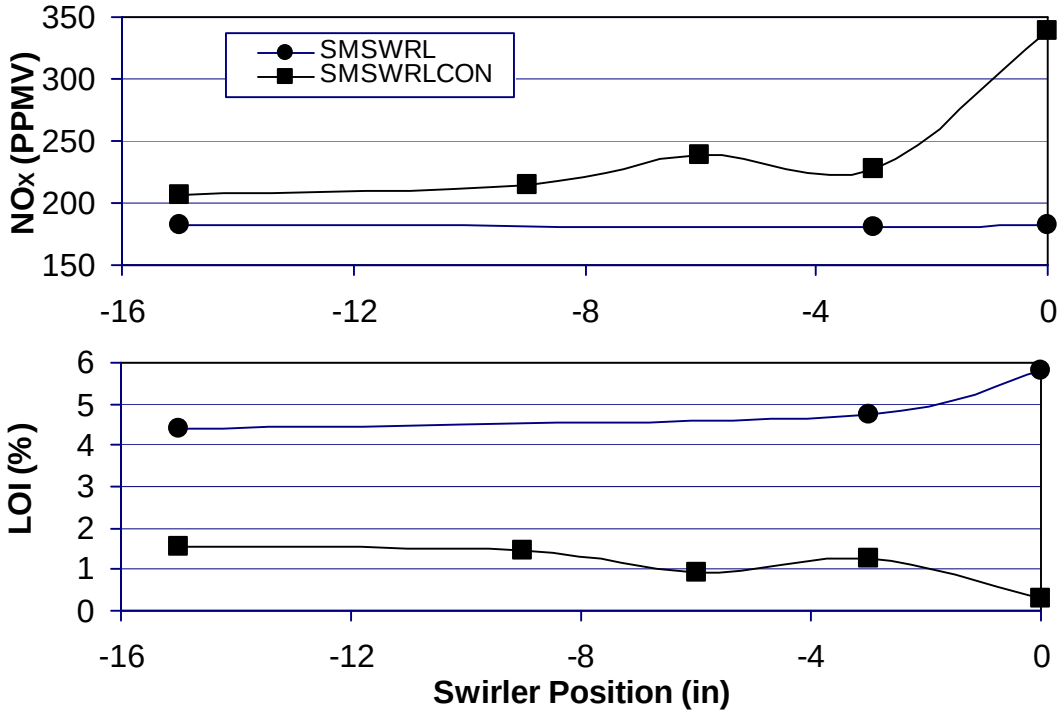

Figure 7-2. Swirler position effect on NO_X and LOI for two configurations of the ultra low-NO_X plug-in DRB-4Z™ PC burner firing 70% through 200 mesh fineness pulverized Mahoning 7 coal at 29.3 MW_t (100 million Btu/hr) and 17% excess air

7.4 Transition Zone Air Flow Damper Position Effects

Another hardware parameter that was optimized was the position of the sleeve damper that controls the secondary airflow into the transition zone. As with other burner settings, the optimum position of the transition zone damper was not the same for all configurations and varied depending on the hardware arrangement as shown in Figure 7-3. Based on the windbox ΔP variation with the damper positioning, the estimated maximum flow into the transition zone was about 11% of the total combustion air at normal operation. At high damper openings, mixing of the transition zone air with the primary air/pulverized coal stream was particularly enhanced for swirler-equipped coal nozzle configurations (SMSWRL series), resulting in higher NO_X and lower LOI values while firing Mahoning 7 coal. In the absence of the coal nozzle swirler, NO_X and LOI levels did not change significantly with the damper position and were influenced mainly by coal variations (SMNOZL designates Mahoning 7 and SMNZPT denotes Pittsburgh 8 data).

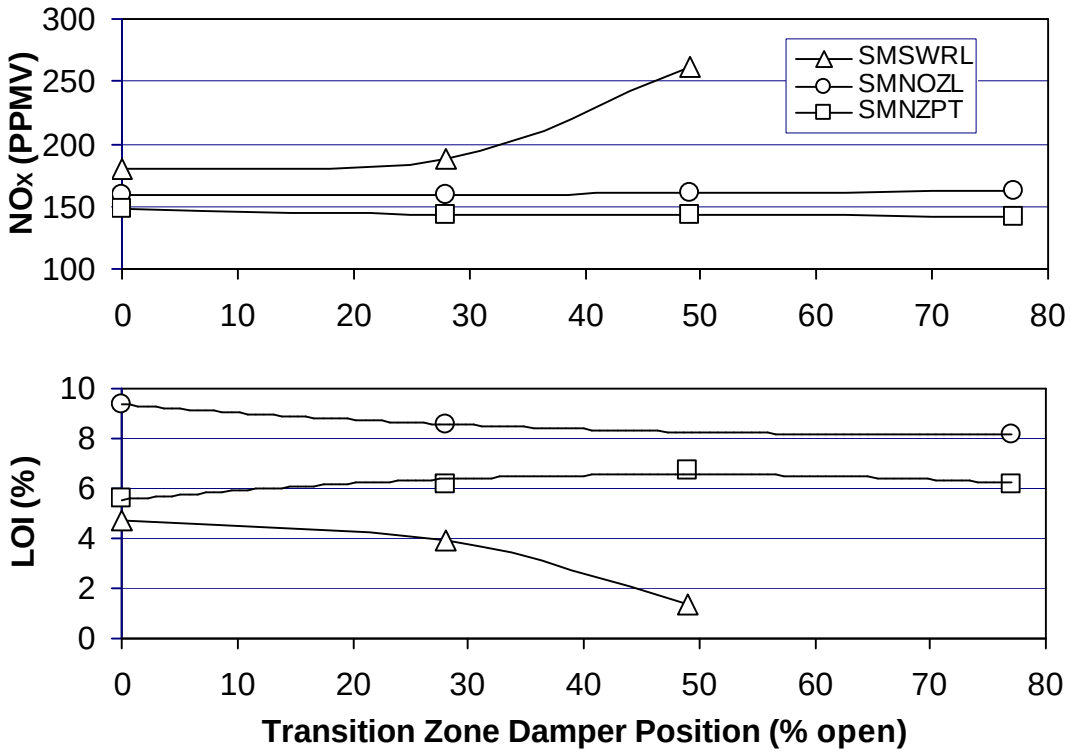

Figure 7-3. Transition zone damper position effect on NO_X and LOI for three configurations of the ultra low-NO_X plug-in DRB-4Z$\hat{O}$ PC burner firing 70% through 200 mesh fineness pulverized coal at 100 million Btu/hr and 17% excess air

7.5 Selection of the Best Hardware Configuration

Figure 7-4 summarizes the performance of various configurations tested in this program by firing 70% through a 200-mesh screen pulverized Mahoning 7 coal at the normal operating conditions of 29.3 MW_t (100 million Btu/hr), 17% excess air, and optimum burner settings. High combustion efficiency, short flame length, low NO_X and CO emissions, low burner ΔP, flame stability at minimum load, and the suitability of fly ash for recycling were among the factors that determined the best plug-in design.

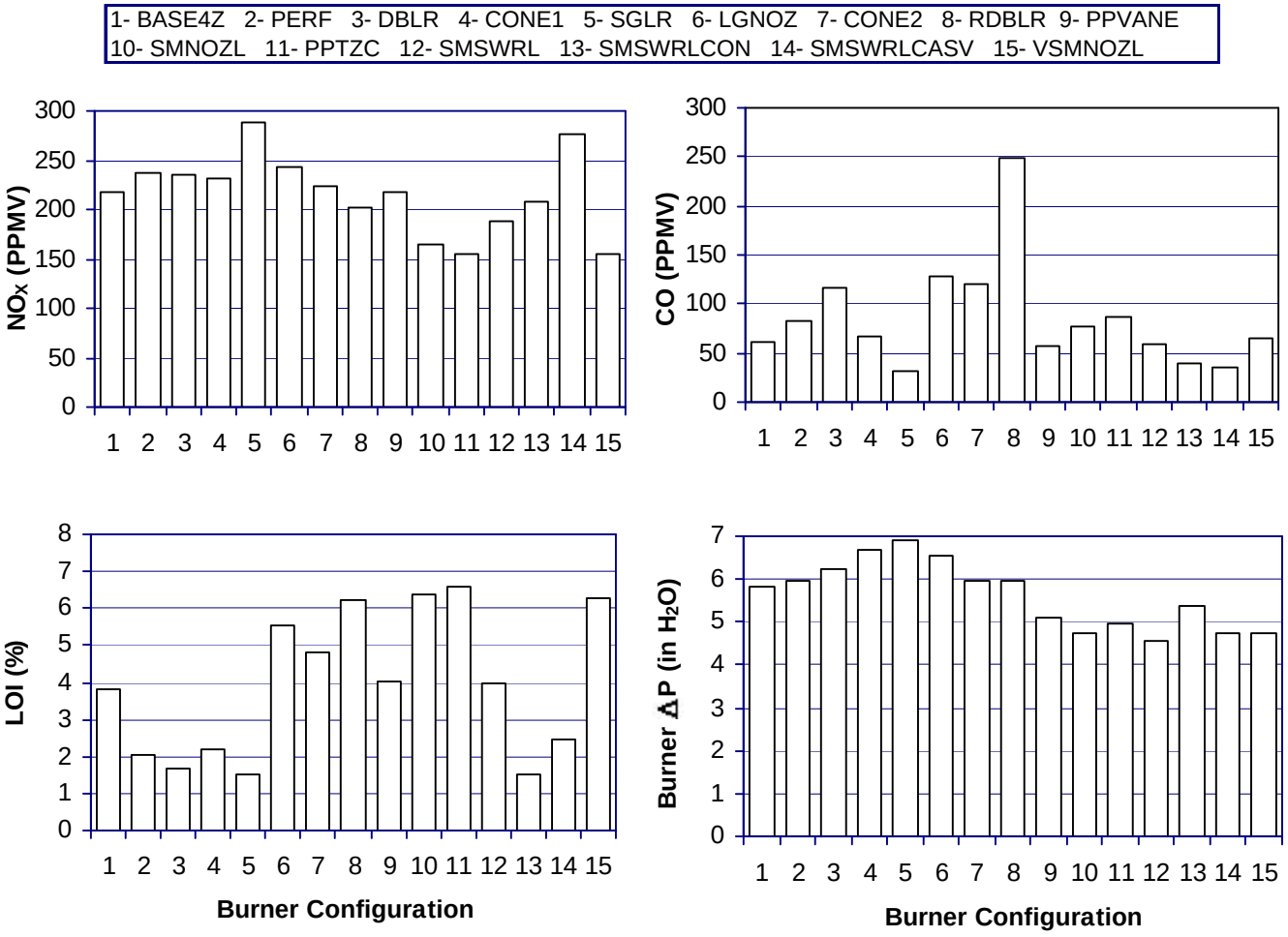

Figure 7-4. Key performance data at optimum settings for various configurations of the plug-in DRB-4ZÔ PC burner when firing 70% through 200 mesh pulverized Mahoning 7 coal at 29.3 MW_t (100 million Btu/hr) and 17% excess air

After testing configurations 1 through 8, the burner ΔP was reduced by modifying the inner secondary air zone aerodynamics. The modifications included replacing the flat-bladed adjustable spin vanes with curved blades and installing a fixed vane assembly with curved vanes upstream of the adjustable vanes. As a result of these changes, the burner ΔP for configurations 9 through 15 dropped by at least 0.2 kPa (0.7 inch) of water. Configurations 10, 11, 12, 13, and 15 exhibited low-NO_X and low to moderate LOI levels. Based on these performance data, configuration 10 was chosen to represent the lowest NO_x with acceptable CO and LOI levels. Configuration 13 demonstrated simultaneous and significant reductions in NO_x and LOI relative to the DRB-XCL® burner results (i.e., 271 PPM NO_x and 2.26% LOI).

7.6 Burner Stoichiometry and Ohio Mahoning 7 Coal Fineness Effects

Figure 7-5 shows the effects of excess combustion air on NO_X and LOI when firing 70% through 200 mesh pulverized Mahoning 7 coal at 29.3 MW_t (100 million Btu/hr) for configurations with (SMSWRL) and without (SMNOZL) a coal nozzle swirler. Increasing the excess air converted more fuel-N to NO_X, and decreased the CO formation and LOI. In the absence of the coal nozzle swirler, the plug-in DRB-4Z™ burner generated 10% less NO_x and 27% lower LOI than its full-diameter [3] counterpart.

At 17% excess air and 70% through a 200-mesh screen PC fineness, NO_X emissions from firing the Mahoning 7 coal averaged 165 PPMV (0.23 lb/million Btu) without the swirler, but increased to 177 PPMV (0.24 lb/million Btu) when a multi-blade swirler was installed in the coal nozzle. Conversely, the average LOI levels dropped from 6.40% to 5.43% when the swirler was installed. These changes are attributable to better mixing between the fuel and oxidizer. Use of the swirler could be considered as an option in situations requiring very low unburned carbon levels. Burning the fine grind PC (89% through a 200-mesh screen) did not have an appreciable effect on NO_X but lowered the LOI levels by an average of about 2 percentage points relative to standard grind PC firing results. Another configuration that reduced the coal nozzle diameter by 39% with the installation of two sleeve inserts achieved 154 PPMV NO_X (0.22 lb/million Btu) and 6.27% LOI under normal operating conditions.

Further plug-in DRB-4Z™ PC burner emissions characterization tests with the reference Pittsburgh 8 coal were conducted without the coal nozzle swirler (SMNOZL configuration) to ensure that the NO_X emissions goal (86 g/GJ or 0.20 lb/million Btu) could be met at a reasonable unburned carbon level. An existing 100 million Btu/hr version of a commercial, full-diameter, DRB-XCL® low-NO_X PC burner was also installed and tested in the CEDF to obtain baseline emissions data for comparison with the plug-in DRB-4Z™ PC burner results.

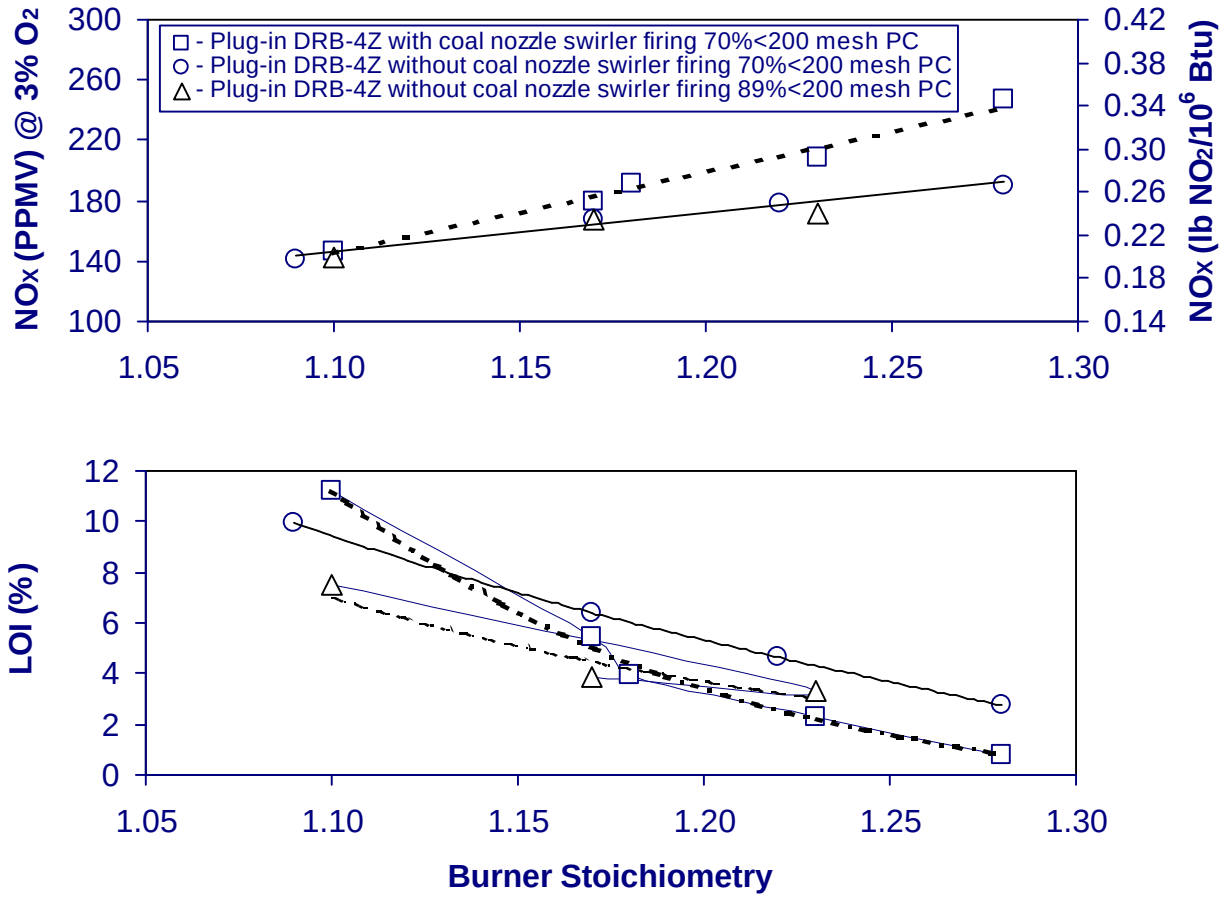

Figure 7-5. Hardware configuration, excess air, and coal fineness effects on NO_X and LOI for the ultra low-NO_X plug-in DRB-4Z PC burner firing pulverized Mahoning 7 coal at 29.3 MW_t (100 million Btu/hr)

7.7 Burner Hardware and Coal Variation Effects

Baseline performance results of the DRB-XCL® low-NO_X PC at full load operation and different stoichiometries are illustrated in Figure 7-6 and compared with corresponding results from the plug-in DRB-4Z™ tests. Here, the baseline DRB-XCL® burner was fired with the standard fineness pulverized Pittsburgh 8 coal. But the plug-in DRB-4Z™ burner (SMNOZL configuration without the coal nozzle swirler) was fired with the standard grind as well as coarse grind PC.

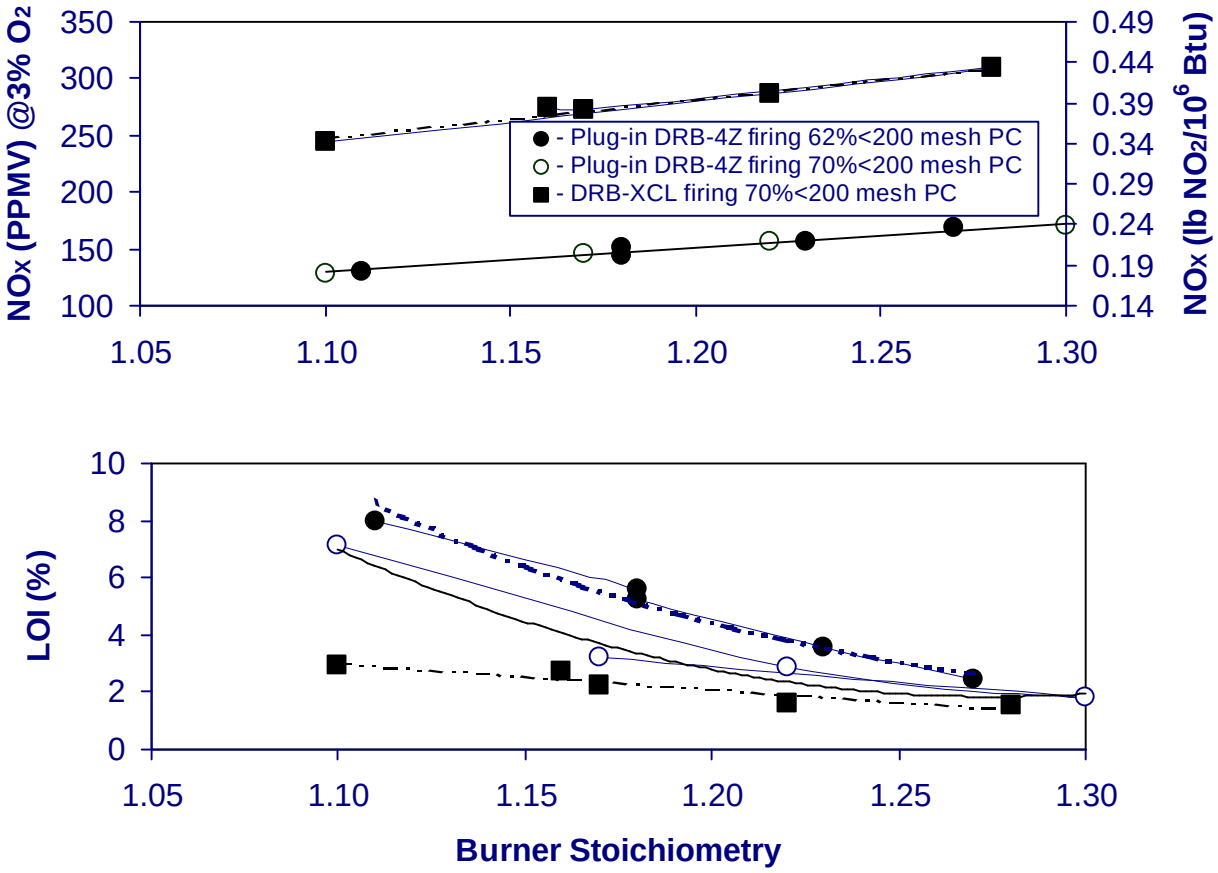

Figure 7-6. Excess air and PC fineness effects on NO_X and LOI for the plug-in DRB-4Z™ and the full-diameter DRB-XCL® low-NO_X PC burners firing pulverized Pittsburgh 8 coal at 29.3 MW_t (100 million Btu/hr)

Without staging, full load firing of the plug-in DRB-4Z™ with 70% through 200 mesh Pittsburgh 8 coal at 17% excess combustion air resulted in average NO_X, LOI, and burner ΔP values of 145 PPMV (0.20 lb NO_2/million Btu), 3.19%, and 4.7 in H_2O, respectively. These superb results represent 47% lower NO_X and only 28% higher LOI than what was achieved with the commercial prototype of the low-NO_X XCL® PC burner in the CEDF. Decreasing the coal fineness generally slowed the fuel oxidation and increased the CO and LOI levels without an appreciable change in NO_X emissions. Although the LOI levels for the plug-in DRB-4Z™ burner increased as expected with decreasing pulverized coal fineness, mill upgrades in commercial applications can be considered to improve the carbon burnout. Firing the Pittsburgh 8 coal in the plug-in DRB-4Z™ burner produced less NO_X and unburned carbon than burning Mahoning 7 coal due to its lower fixed carbon-to-volatile matter ratio and fuel-N content.

7.8 Air Staging Effects

Air staging effects on NO_X and $PM_{2.5}$ emissions were characterized at a fixed overall excess air level of 17%. Both the burner and OFA register settings were re-optimized at a nominal burner stoichiometry of 0.88. Burner stoichiometry was then varied from 0.88 to 1.00 by splitting the total secondary airflow between the burner and the OFA ports. Figure 7-7 shows the effect of burner stoichiometry on NO_X and LOI for the DRB-4Z™ burner. Raising the burner stoichiometry from 0.88 to 1.00 during staged testing increased the NO_X emissions and decreased the LOI. With the burner stoichiometry set at 0.88 and the overall combustion stoichiometry at 1.17 (17% excess air), average NO_X and LOI values were 104 PPMV (0.14 lb NO_2/million Btu) and 4.64%, respectively. Consequently, we also met our staged combustion NO_X goal of 64 g/GJ (0.15 lb NO_2/million Btu) in the test facility.

Since the burner was not re-sized with a smaller throat diameter for staging (less air flow), its aerodynamics and mixing patterns may not have been optimal for minimizing NO_X and LOI levels at all stoichiometries. And although the CEDF burner-to-overfire port residence time during staged combustion was longer than what is available in most commercial units, the 30% NO_X reduction and 45% LOI increase from unstaged operation is typical of field performance.

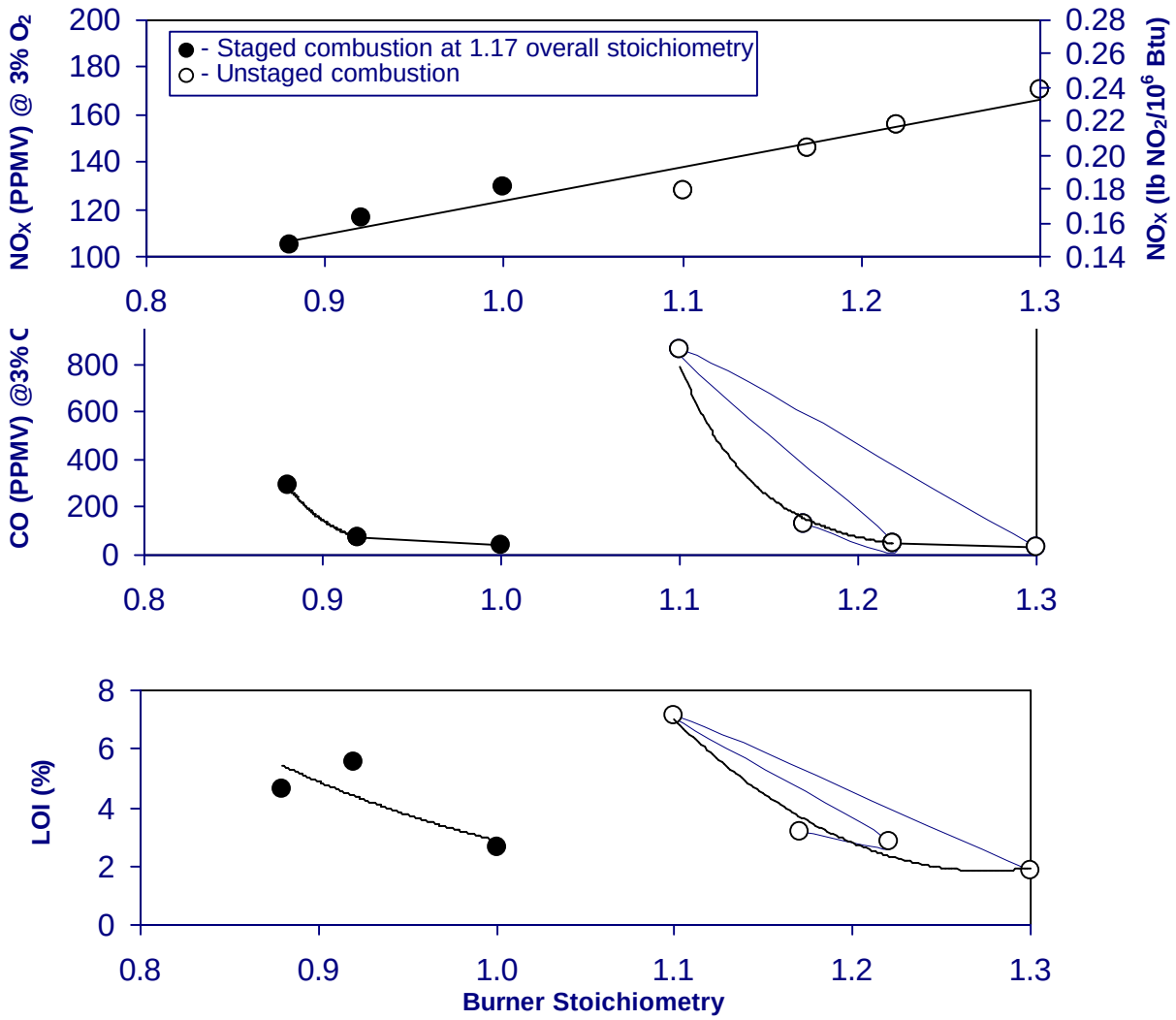

Figure 7-7. Burner stoichiometry effects on NO_X and LOI for the ultra low-NO_X DRB-4ZÔ PC burner. Nominal firing conditions: 70% through 200 mesh screen fineness Pittsburgh 8 coal at 29.3 MW_t (100 million Btu/hr)

7.9 Thermal Load Effects

Figures 7-8 and 7-9 show the thermal load effect on NO_X and LOI for the DRB-XCL® and the plug-in DRB-4Z™ burners. Part load (17.6 MW_t or ~60 million Btu/hr) and minimum load (10.3 MW_t; ~35 million Btu/hr) operations at a fixed stoichiometry resulted in little to moderate increases in LOI for both burners due to the cooler furnace environment. Lower furnace temperatures at minimum heat input also led to lower NO_X emissions for the DRB-XCL® burner. But more NO_X was generated for the plug-in DRB-4Z™ burner (without the coal nozzle swirler) at minimum load in comparison with full load data. Non-optimum (off-design) burner aerodynamics at minimum load is likely to have influenced the outcome in the latter case. Nevertheless, the flames were always attached even at minimum load.

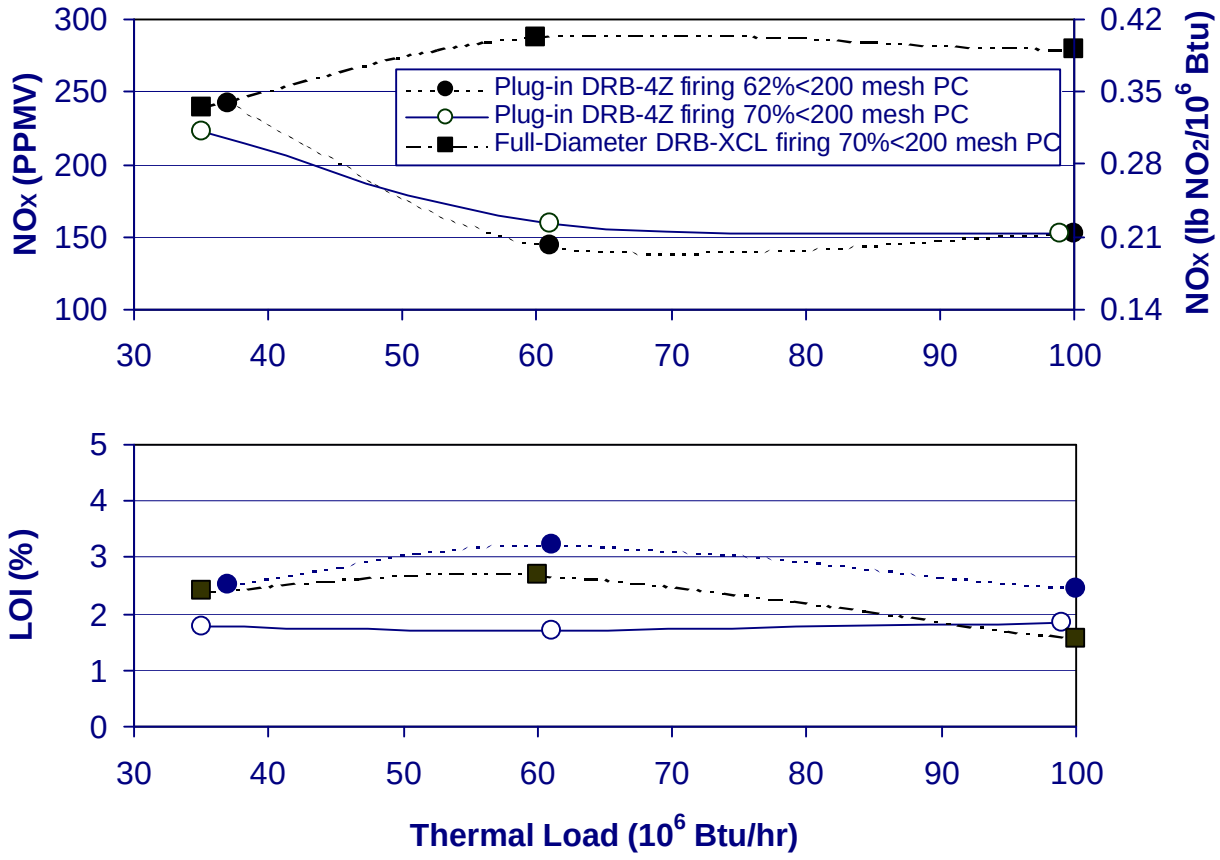

Figure 7-8. Thermal load, hardware configuration, and coal fineness effects on NO_X and LOI for the Plug-in DRB-4Z™ and the DRB-XCL® low-NO_X PC burners when firing pulverized Pittsburgh 8 coal at 29% excess air

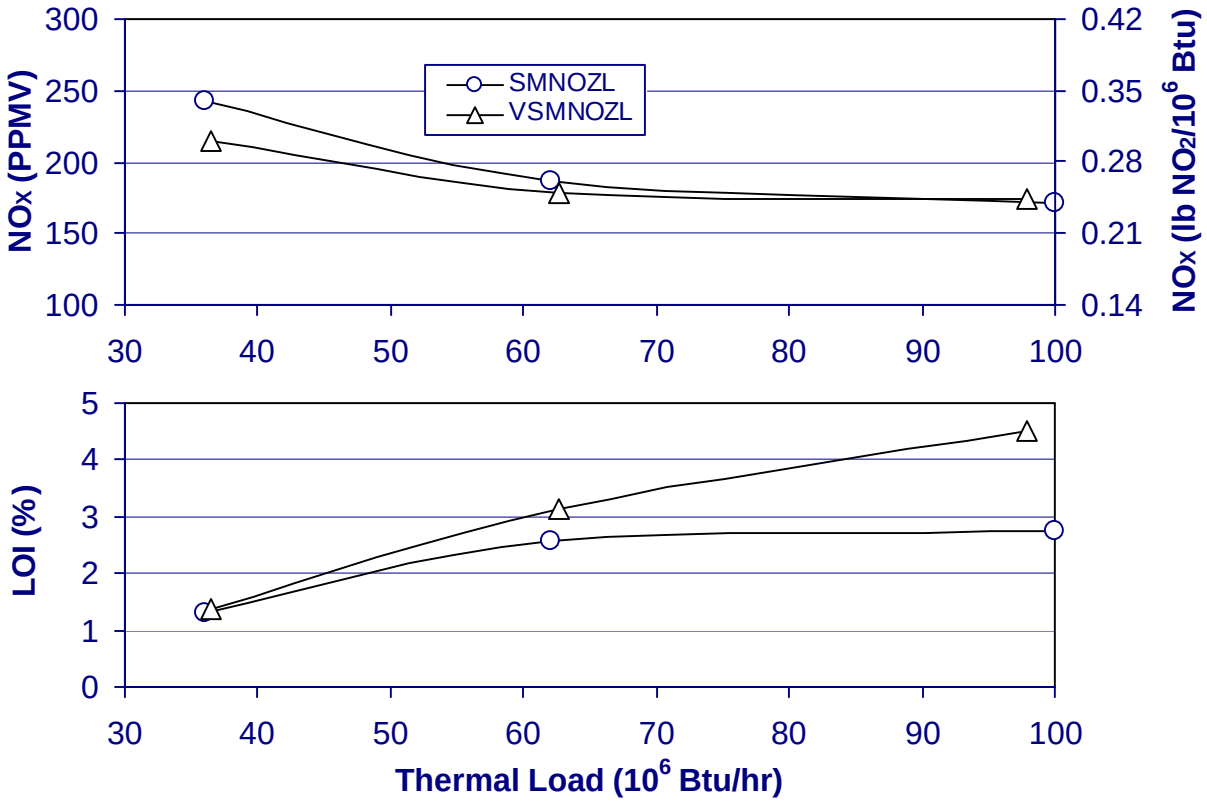

Figure 7-9. Thermal load and hardware configuration effects on NO_X and LOI for the Plug-in DRB-4Z™ PC burner when firing 70% through 200 mesh screen pulverized Mahoning 7 coal at 29% excess air

7.10 Unburned Carbon Correlation with LOI

A discrepancy between the unburned carbon (UBC) content of the ESP fly ash and the LOI value from a sample collected at the convective pass section exit (upstream of the ESP) prompted further investigation. Twenty-three convective pass exit fly ash samples from high-volatile Pittsburgh 8 coal combustion by the DRB-XCL® PC burner and the plug-in DRB-4Z™ PC burner were analyzed for unburned carbon and compared with LOI values. Figure 7-10 compares the two measurements spanning a 1 to 9% LOI range. For the plug-in DRB-4Z™ PC burner, the UBC values were always slightly less than LOI levels, regardless of the firing mode. But for the DRB-XCL® PC burner, the difference was substantial and the UBC figures were about 50% of the LOI values. In search of an answer, we setout to measure and compare the sulfur, nitrogen, hydrogen, carbon, and moisture contents of two fly ash samples, representing identical LOI levels (1.7%). One sample was from the DRB-4Z™ PC burner test set while the other came from firing the DRB-XCL® PC burner. Table 7-1 lists the measured constituents. As it turned out, the total combustibles (carbon, hydrogen, and sulfur) are very close to the LOI values on a dry basis. In other words, the discrepancy between the as-received LOI and the dry unburned carbon is mainly due to the presence of moisture and other

non-carbonaceous combustible matter in the fly ash. Since burner design can influence the physical characteristics of fly ash, it is possible that combustion-generated fly ash from the DRB-XCL® PC burner may have been more conducive to adsorption of sulfur-containing compounds and the ambient moisture than the fly ash from the DRB-4Z™ PC burner. The difference is expected to diminish at higher LOI values where UBC becomes the dominant form of unburned combustibles in the fly ash.

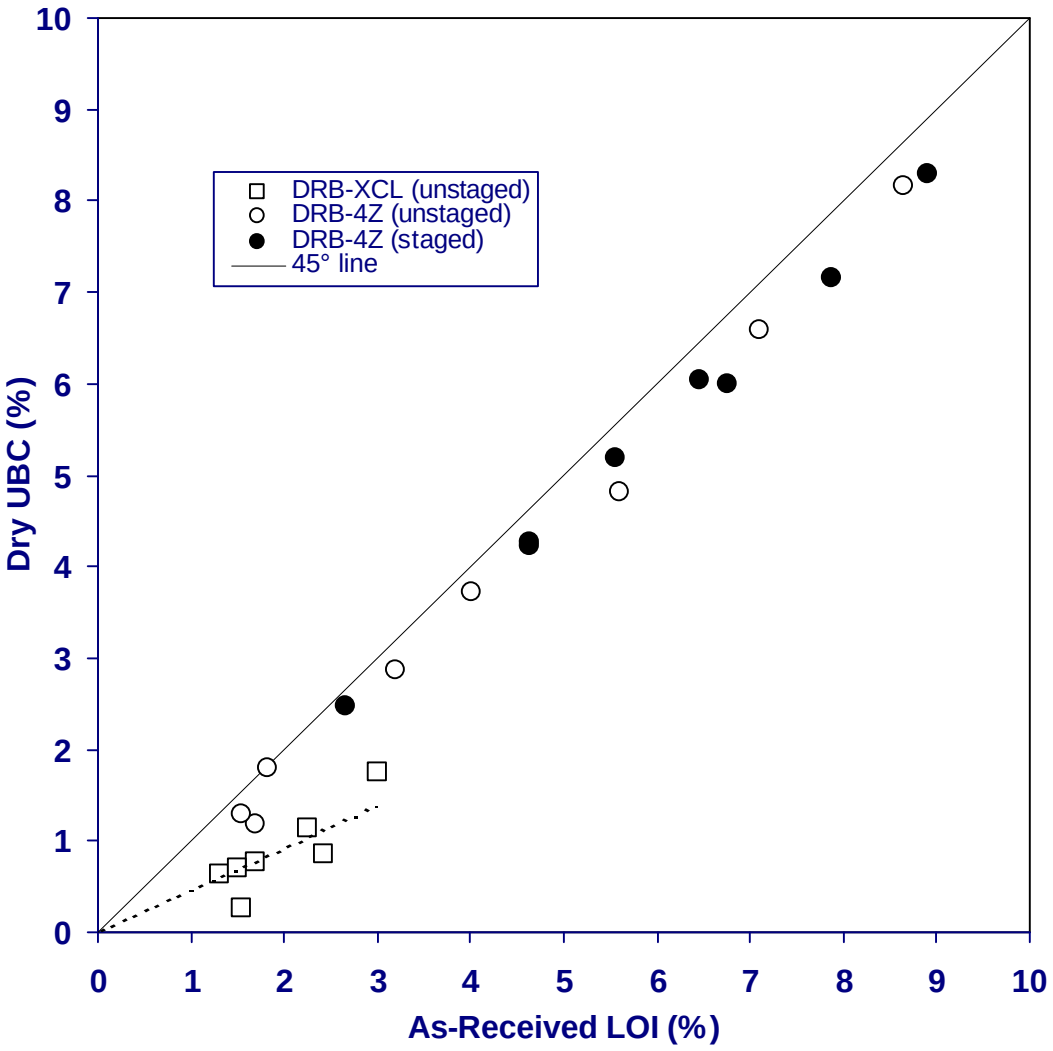

Figure 7-10. Comparison of as-received LOI and dry unburned carbon of fly ash samples representing Pittsburgh 8 coal firing in the DRB-XCL® PC and plug-in DRB-4Z™ PC burners

Table 7-1. Comparison of Pittsburgh 8 Fly Ash LOI and Total Combustibles for Two Different Burners

		Composition (% mass)							
		As-Received		Dry LOI	Dry				
Test ID	Burner	LOI	Moisture		Carbon	Hydrogen	Sulfur	Nitrogen	Σ(C+H+S)
XSPIT-05	DRB-XCL®	1.70	0.38	1.32	0.77	0.12	0.26	0.00	1.15
SMNZPT-13	DRB-4Z™	1.70	0.26	1.44	1.18	0.12	0.12	0.00	1.42

8.0 PRIMARY $PM_{2.5}$ EMISSION RESULTS

The operating conditions of the CEDF equipment and the ESP for $PM_{2.5}$ tests are presented in Table 8-1. Burner settings were established before the start of sampling, and the burner/furnace operation was maintained constant within the limitations of the equipment and the variability of the coal. The total excess oxygen for all tests was held constant at about 3.2%, which is equivalent to a combustion stoichiometry ratio (S.R.) of 1.17. In Test D secondary air to the furnace was staged, with a S.R. of 0.85 at the burner and the balance supplied to the OFA ports. In Test D and E, the excess oxygen and CO concentrations were the same, while the staged combustion provided lower NO_x concentrations. $PM_{2.5}$ sampling was not conducted during upset conditions such as soot blowing.

Table 8-1. Summary of Combustion Conditions and ESP Operation for the Low NO_x and Ultra Low-NO_x $PM_{2.5}$ Sampling

Burner	Test A DRB-XCL®	Test B DRB-XCL®	Test C DRB-XCL®	Test D DRB-4Z™	Test E DRB-4Z™
Firing Mode	Low-NO_x Unstaged	Low-NO_x Unstaged	Low-NO_x Unstaged	Ultra Low-NO_x Staged	Ultra Low-NO_x Unstaged
Oxygen (dry, %)	3.18	3.18	3.14	3.14	3.17
NO_x (ppm dry at 3% O_2)	286	276	262	105	142
CO (ppm dry at 3% O_2)	34	41	46	270	264
SO_2 (ppm dry at 3% O_2)	3460	3349	3195	3345	3194
Flue Gas Flow, kg/hr (acfm)	44,200 (33480)	43,876 (32650)	43,957 (33140)	43,751 (32782)	44,043 (33341)
ESP Inlet Temperature, °C (°F)	175 (348)	169 (335)	173 (343)	165 (329)	168 (335)
Number of ESP Fields	2	3	3	2	2
Specific Collection Area (ft^2 per 1000 acfm)	185	285	281	189	186
Field - Voltage (kV)	No. 1 - 54 No. 2 - 54 No. 3 - Off	No. 1 - 54 No. 2 - 54 No. 3 - 34	No. 1 - 54 No. 2 - 54 No. 3 - 54	No. 1 - 52 No. 2 – 52 No. 3 – Off	No. 1 – 52 No. 2 - 52 No. 3 – Off

The conventional low-NO_x burner was adjusted to represent field operation, which provided low-NO_x as well as low CO and low unburned carbon in the fly ash. The ultra low-NO_x plug-in burner was adjusted to achieve the lowest possible NO_x in order to examine the effect of minimum NO_x and higher unburned carbon levels on $PM_{2.5}$.

Likewise, the ESP was operated to determine the effect of ESP operating parameters on PM emissions (Tests A, B and C), and the effect of combustion conditions on PM emissions for constant ESP operation (Tests A, D and E). The ESP was not adjusted to achieve specific values of particulate emissions.

Size classified fly ash samples using $PM_{10}/PM_{2.5}$ cyclones and a cascade impactor were collected at both the ESP inlet and outlet. The mass of size classified fly ash at the ESP outlet was sufficient to evaluate the particle size distribution, but was of insufficient size to permit reliable chemical analysis. The size classified fly ash from the inlet of the ESP was used for detailed chemical analyses. Chemical analyses of the fly ash samples from the ESP outlet collected using the High Volume sampler were performed for comparison to the size classified results at the inlet.

8.1 Size Distribution of the Coal and Fly Ash

Samples of "as-fired" pulverized coal were collected during the combustion and PM tests. These samples are immediately sieved to ensure that the coal is not too coarse or fine, thereby affecting the combustion results. Samples were also collected during the PM sampling to ensure that the coal grind was not influencing the fly ash collected at the inlet to the ESP.

The pulverized coal samples collected during four of the five tests were also analyzed for size distribution using a Microtrac optical particle sizing instrument. The mass median diameter of these samples is given in Table 8-2. Also shown in Table 8-2 are the mass median diameters of the fly ash determined from gas sampling measurements ($PM_{10}/_{2.5}$) assuming a particle specific gravity of 2.5 at the inlet to the ESP. The mass median diameter of the fly ash from the first and second ESP fields was also measured using the Microtrac.

Table 8-2. Mass Median Diameter of the Pulverized Coal and the Fly Ash Collected at the ESP Inlet

Test	Microtrac Mass Median Diameter of Coal (microns)	Mass Median Diameter of Fly Ash at the ESP Inlet (microns)[1]	Microtrac Mass Median Diameter – ESP Field 1 (microns)	Microtrac Mass Median Diameter – ESP Field 2 (microns)
Test A	41.34	15.7	21.6	12.2
Test B	43.64	17.2	N/A	N/A
Test C	50.55	20.0	22.0	11.6
Test D	N/A	17.7	N/A	N/A
Test E	46.59	16.5	23.0	21.8

(1)Based on $PM_{10}/PM_{2.5}$ cyclone measurements with assumed specific gravity of 2.5

Table 8.2 shows that the median diameter of the pulverized coal varied slightly from test to test, ranging from about 40 to 50 microns. Interestingly, the variation in calculated mass median diameter of the fly ash collected with the $PM_{10}/PM_{2.5}$ cyclones at the ESP inlet coincides with the variation in the pulverized coal. The median diameters of the fly ash from the ESP fields are about the same as at the ESP inlet. Median diameters for Tests A and C show a larger median size for the first ESP field,

while the median size for both ESP fields is about the same for Test E. In general, the median diameters of the fly ash are about as expected based on the size of the pulverized coal.

The aerodynamic particle size distribution at the ESP inlet was estimated using the $PM_{10}/PM_{2.5}$ measurements and is shown in Figure 8-1 for the three combustion conditions. One curve represents the average distribution for Tests A, B, and C, while the other two are for staged and unstaged ultra low-NO_x combustion. The figure shows that the aerodynamic particle size is nearly the same for all three test conditions. Fly ash size distribution based on cascade impactor measurements show the same trend, but contain more scatter because of the limited sampling time associated with the measurement.

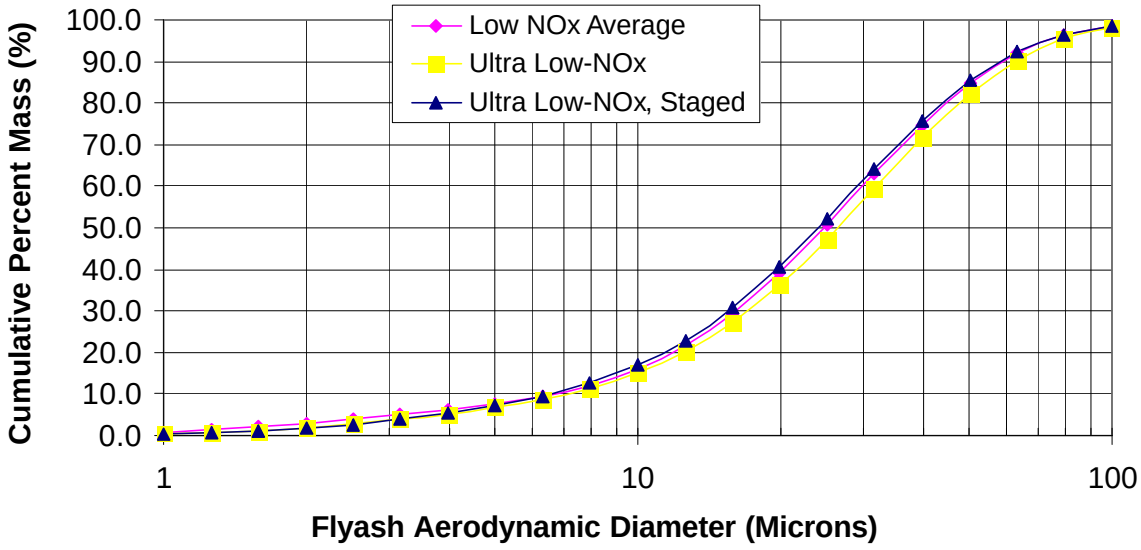

Figure 8-1. Size distribution of the fly ash at the ESP inlet based on the aerodynamic diameter for the low-NO_x and ultra low-NO_x tests

Fly ash from the $PM_{10}/PM_{2.5}$ sampling was photographed using a Scanning Electron Microscope (SEM). Figures 8-2 and 8-3 show the particle size fractions greater than 10 microns and the particle size fraction between 2.5 microns and 10 microns, respectively. The visual size of the fly ash in the photographs reflects the measurement range of the cyclones in general. Most of the fly ash are uniformly spherical.

An SEM photograph of the particulate less than 2.5 microns is shown in Figure 8-4. Individual spherical particles are visible in this picture, but resolution of the larger particulate is relatively poor because of the “fuzz” that is deposited on the filter. The composition of the fuzz was not specifically determined, but it may be a form of sulfate which existed in quite high concentrations in the sub-2.5 microns size fraction.

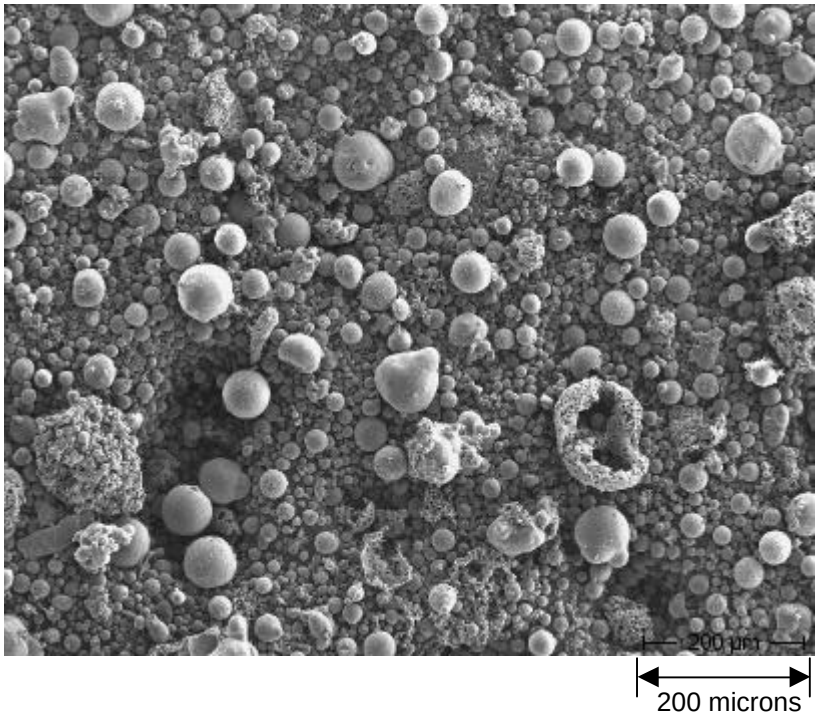

Figure 8-2. SEM particulate matter > 10 microns

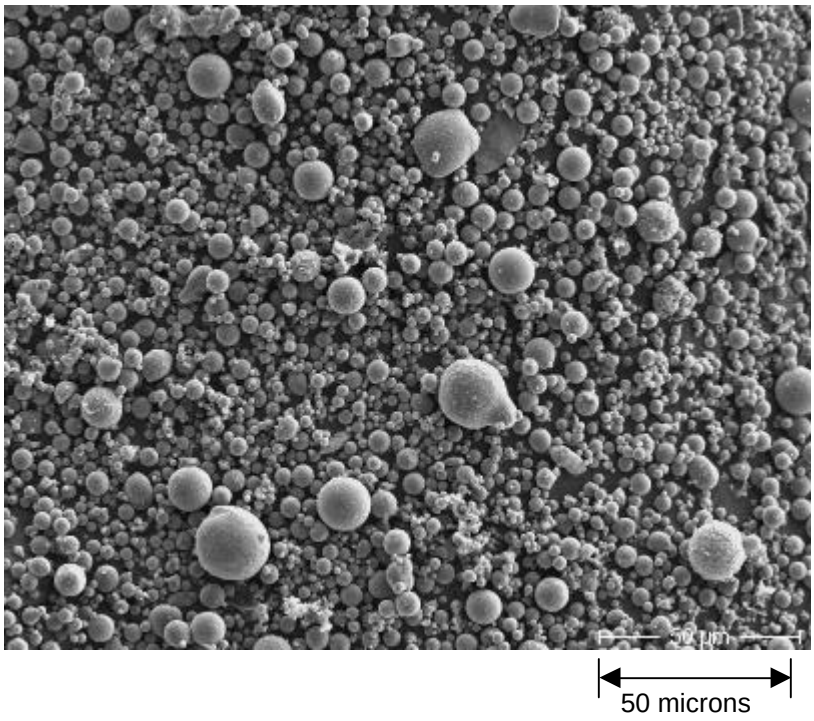

Figure 8-3. SEM of 10 microns > particulate matter > 2.5 microns

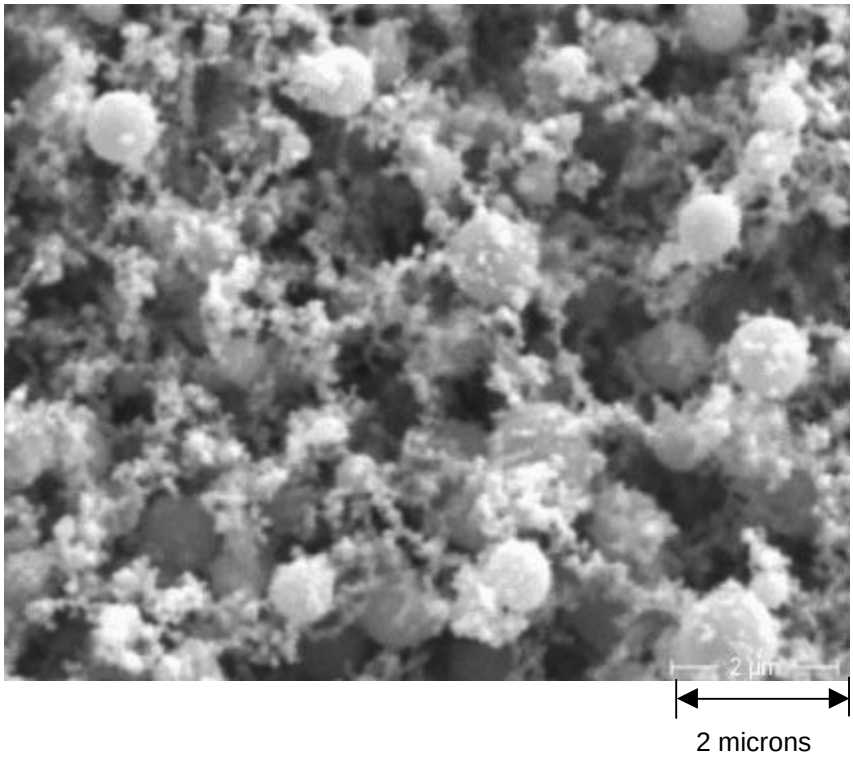

Figure 8-4. SEM of particulate matter < 2.5 microns

8.2 Mass Loading at the Inlet and Outlet of the ESP

The ash loading in the flue gas at the inlet of the ESP for the five tests is shown in Figure 8-5. Tests A, B, and C are all at the same conventional low-NO_x combustion condition, but show a gradual increase in the inlet particle loading over time. These tests were conducted on the second through fourth day of boiler operation after a clean start, and reflect the change with time of fly ash retention in the boiler and flues.

The ash loading at the ESP inlet for the ultra low-NO_x staged and unstaged tests (D and E) are greater on average than for the commercial low-NO_x tests. The ultra low-NO_x tests were conducted after several weeks of boiler operation, and probably more nearly represent steady state particle loading to the ESP. Based on the coal ultimate analysis, an ash loading of 6 gm/dscm represents a 75% carry-through of the ash in the coal. The segmented bars in Figure 8-5 represent size fractions greater and less than 10 microns. The mass fraction of particulate smaller than 10 microns is relatively constant for all tests, and averaged about 15% to 20% of the total.

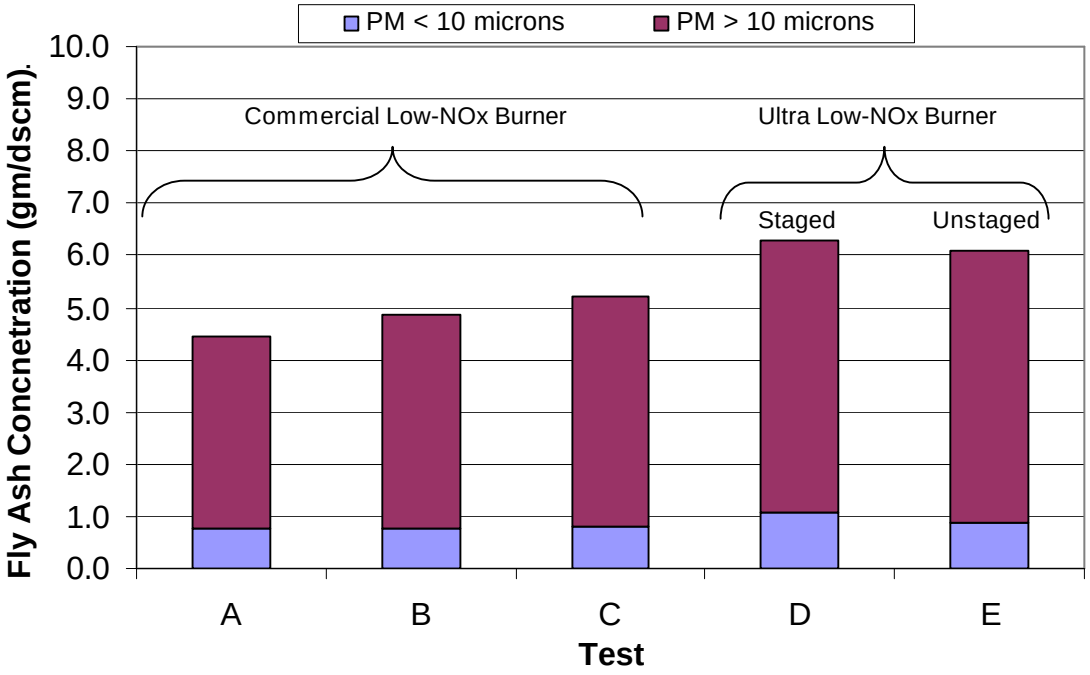

Figure 8-5. Fly ash loading at the inlet to the ESP for the low-NO_x and ultra low-NO_x tests

The particle loading at the ESP outlet for Tests A through E are presented in Figure 8-6. The particulate emissions for all of the tests are below the NSPS limit of 0.03 lb/million Btu (about 0.05 gm/dscm). The particle removal efficiency for each test is listed above the corresponding bar in the figure. For each test the removal efficiency is in excess of 99.3%.

In contrast to the particulate loading at the ESP inlet, the particle loading at the ESP outlet decreased for Tests A, B, and C. The improvement in particulate removal efficiency for these three tests coincides with an increase in the SCA and field voltages as listed in Table 8-1.

The ash loading at the ESP outlet for the ultra low-NO_x tests (D and E) are greater than for Test A, even though the number of ESP fields (2) and field voltage (52-54kV) for the three tests were nominally the same. However, the field currents for Tests D and E were significantly less than for Test A. This indicates a more resistive ash, which can contribute to the decrease in particle removal efficiency for Test D and E.

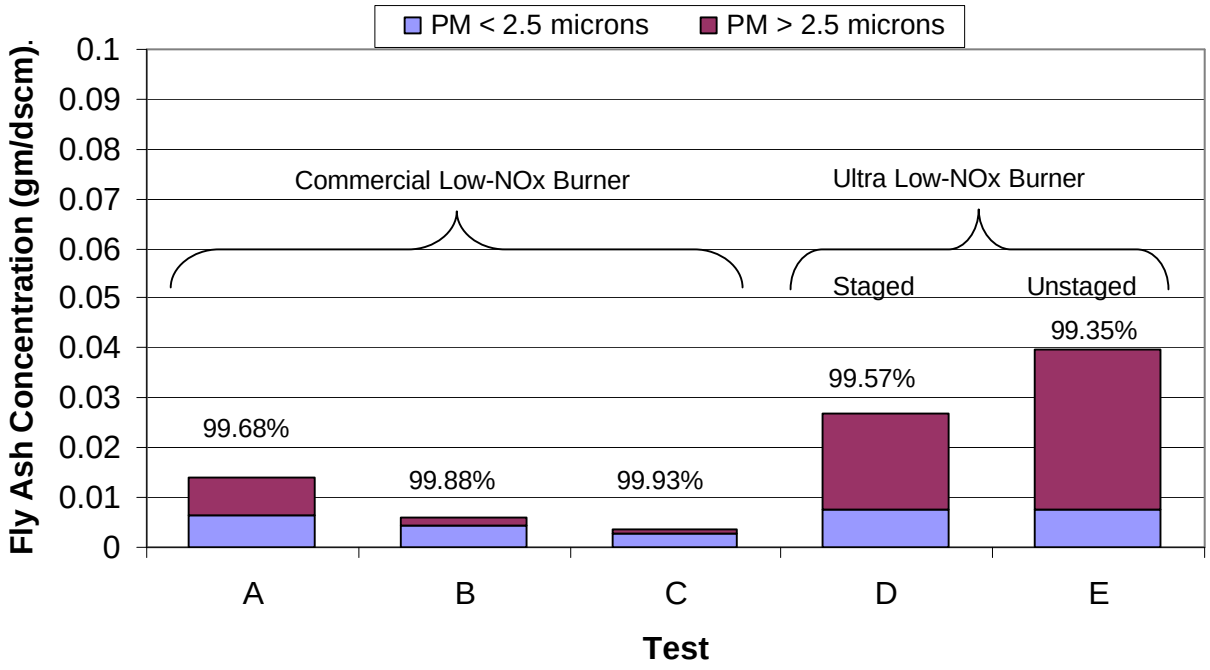

Figure 8-6. Particle loading at the ESP outlet as a function of ESP operation and combustion condition

The segmented bars in Figure 8-6 represent the mass of particulate that is less than and greater than 2.5 microns. Comparison of Test A, B, and C show that the mass concentration of both size ranges decreased as ESP voltage and SCA increased. Comparison of Test A with D and E show that the mass fraction of particulate smaller than 2.5 microns was about the same. Compared to Test A, nearly all of the increase in particulate loading for Tests D and E is a result of an increase in PM greater than 2.5 microns. An increase in the mass loading of this size fraction may be associated with re-entrainment of the particulate after rapping the collection plates.

8.3 Carbon

8.3.1 Carbon in the Ash at the ESP Inlet and Outlet

Carbon that is found in the ash at the ESP inlet can be in two forms. Char is the carbon in the coal that goes unburned through the combustion process, while soot is carbon that has condensed to a particulate. Char is typically found in particles larger than 10 microns while soot is typically less than 2.5 microns. The percent carbon in the ash at the ESP inlet is shown in Figure 8-7 as a function of particle size range and combustion condition (refer to Table 8-1 for CEDF and burner operating conditions). The measured and calculated carbon content of the ash at the ESP outlet is also shown. The calculated carbon content was determined using the size classified carbon concentration at the ESP inlet and the measured fly ash mass distribution at the ESP

outlet. The measured carbon content of the ash at the ESP outlet for low-NO_x combustion is not shown because sample size and carbon content were too small for accurate measurements. The carbon dioxide absorption (ASTM D-3178) analysis was used for all data in Figure 8-7.

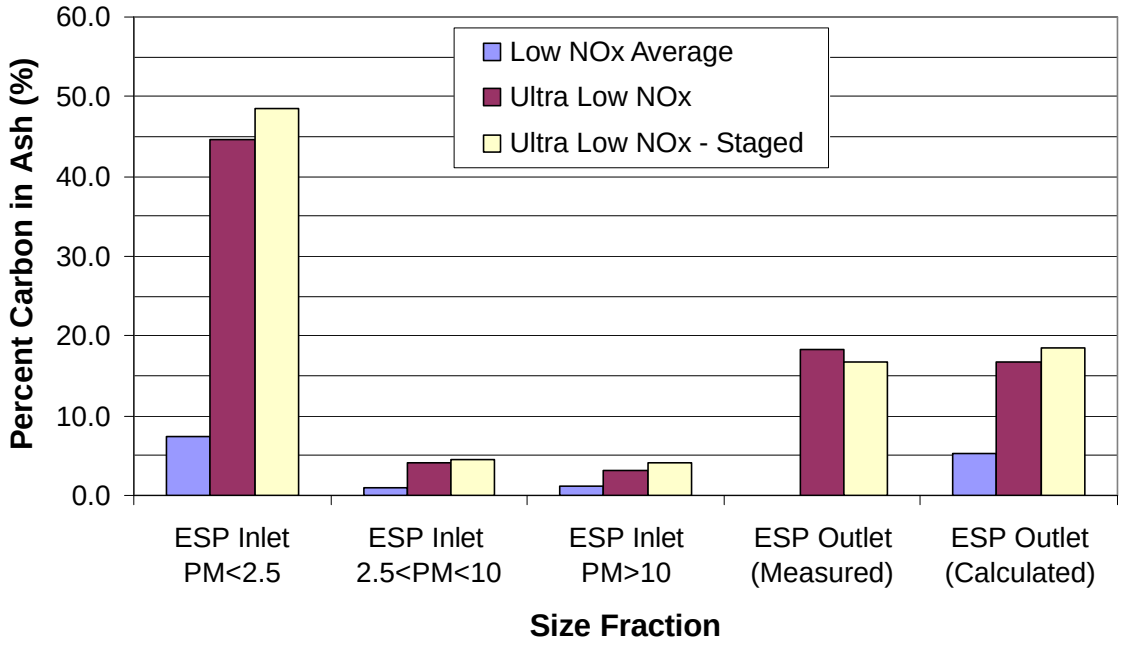

Figure 8-7 Percent carbon in the fly ash as a function of combustion condition and size fraction

The carbon content of the ash for ultra low-NO_x test conditions at the ESP inlet averages about 4.8%, and is greater than the 1.3% carbon measured for standard low-NO_x combustion conditions. Figure 8-7 also shows that the carbon content of the ash increases significantly as particle size decreases, and that this trend is more pronounced for the ultra low-NO_x combustion conditions. For example, the average carbon content of the ash for ultra low-NO_x combustion is about 3 times greater than conventional low-NO_x. However, for the PM < 2.5 microns, the carbon content for the ultra low-NO_x conditions is 6 to 7 times greater. This enrichment at small particle size also causes a high carbon content in the ash at the ESP outlet for the ultra low-NO_x tests. It should be noted that the ultra low-NO_x burner was adjusted during the test to achieve a targeted value of NO_x, while also generating an acceptably low CO concentration. Unburned carbon was not an optimized parameter for the ultra low-NO_x burner.

The calculated values of carbon in ash at the ESP outlet shown in Figure 8.7 are in good agreement with the measured values. In the absence of partitioning or phase change, the concentration of any ash constituent at the ESP outlet should be equal to the mass weighted concentration by size summed over the size distribution at the ESP outlet. Algebraically, this can be written as:

$$C_{avg} = \sum (m_i * C_i) / \sum m_I$$

where:

C_{avg} is the average concentration of a constituent in the flyash

m_i is the mass of flyash in the i^{th} size bin

C_i is the constituent concentration in the i^{th} size bin

8.3.2 Comparison of Carbon in Ash Measurement Methods

Three different measurement methods were used to evaluate the unburned carbon in fly ash at the inlet to the ESP: loss-on-ignition (LOI), thermal optical analysis (TOA), and carbon dioxide absorption as discussed in Section 6.3.4. The original test plan was to use LOI and TOA. LOI is a loss-of-weight method often used during burner development programs. TOA was also planned because it is used to determine the carbon content of ambient $PM_{2.5}$ samples. TOA is a very sensitive method that reports carbon as organic, carbonate, and elemental, as well as the total.

For the low-NO_x combustion tests, carbon in the ash was determined at the ESP inlet for total particulate and the three size fractions, PM > 10 microns, 10 microns > PM > 2.5 microns, and PM < 2.5 microns. At the ESP outlet, carbon was determined for total particulate only. Carbon content by size fractions were not obtained at the outlet because sample sizes were too small for accurate measurements.

Results of the three carbon in ash analyses presented in Table 8-3 show a large variation in the carbon content of the ash for fine particulate. The LOI results for fine particulate were surprisingly high compared with the TOA results. This is shown in the table for the ESP outlet total and ESP inlet size fraction less than 2.5 microns. Visual observation of the ash showed a light gray color that indicated low carbon in the ESP inlet and outlet ash. For this reason it was believed that the LOI values were biased high.

Table 8-3. Carbon Results for Tests A, B, and C					
Test	**Location**	**Size**	**LOI (% Carbon)**	**TOA (% Carbon)**	**Carbon Dioxide Absorption (% Carbon)**
A,B,C Average	ESP Outlet	Total	11.45	0.11	--
A,B,C Average	ESP Inlet	PM < 2.5	15.36	0.67	7.35
A,B,C Average	ESP Inlet	2.5 < PM < 10	3.11	1.03	0.93
A,B,C Average	ESP Inlet	PM >10	1.34	0.30	1.15

To confirm this assumption the ash samples were tested using a carbon dioxide absorption method (ASTM D-3178). The LOI and CO_2 absorption methods both ignite the ash at high temperature in an oxygen environment. The LOI is then the loss in weight of the sample, while the CO_2 absorption measures the mass of CO_2 absorbed by ascarite. For most fresh ash samples collected at high temperature (~400°C), the LOI is usually all carbon. For size classified ash samples collected at moderate temperature (~175°C), the loss in weight can be carbon and also condensed or adsorbed compounds that are off gassed on heating to high temperature. For example, sulfuric acid is found predominantly in the fine size fraction and is released from ash on heating. The CO_2 absorption technique is less ambiguous than LOI because the measured mass is specific to carbon.

For the larger size particulate, the three techniques are in reasonable agreement. Since the CO_2 absorption is a measure of carbon and is an established technique for coal and ash analyses, it was used as the basis of comparison for the carbon in ash results.

Thermal Optical Analyzer (TOA) Method

The TOA method is a direct measure of the carbon content of the ash using a flame ionization detector. By virtue of the method of operation associated with the TOA, portions of the total carbon are identified as organic and elemental. The organic/elemental breakdown for Tests A, B, and C are presented in Table 8-4.

For the TOA method, the ash must be analyzed on a filter. If the ash is not collected on a filter by virtue of the collection method, then it must be put onto a filter manually. The EPA draft PM10/2.5 method used in this project collects fine particulate (< 2.5 microns) on quartz filters – therefore lending itself to the TOA method. Particulate larger than 2.5 microns is caught in cyclone separators prior to the filters. To analyze the larger particulate with the TOA method it was manually put on a filter.

Table 8-4. TOA Carbon Results					
Test	**Location**	**Size**	**TOA Organic (% Carbon)**	**TOA Elemental (% Carbon)**	**TOA Total (% Carbon)**
A,B,C Average	ESP Outlet	Total	0.03	0.08	0.11
A,B,C Average	ESP Inlet	PM < 2.5	0.16	0.51	0.67
A,B,C Average	ESP Inlet	2.5 < PM < 10	0.37	0.66	1.03
A,B,C Average	ESP Inlet	PM >10	0.05	0.25	0.30

Advantages of the TOA method are that the total carbon is divided into organic and elemental components and the technique has a very low detection limit (~10 microns carbon). The disadvantage of the method is the need to deposit loose particulate onto a filter manually. It was found that keeping the ash on the filter could be difficult. Also, because the analysis requires heating the particulate by a flowing gas stream, the larger particulate may not be heated sufficiently to completely combust the carbon. These method disadvantages for the larger particulate could be addressed through method development specific to the larger size fractions.

8.4 Soluble Ions

The concentrations of soluble ions in the ash as a function of particle size range and combustion condition are shown in Figure 8-8. The measured and calculated ion concentration at the ESP outlet is also presented. The variation in ion concentration with particle size exhibits the same trend as for carbon, with increasing concentration for decreasing particle size. Combustion conditions cause very little effect on the soluble ion concentration with the exception of the $PM_{2.5}$ size range. The lower percentage ion concentration in the $PM_{2.5}$ for ultra low-NO_x combustion may be a result of a “dilution effect” of the carbon content of this ash.

Similar to the results for carbon, the concentration of soluble ions at the outlet calculated using the outlet mass distribution and the ion concentration with size measured at the inlet is in good agreement with the measured concentration.

The soluble ions included in Figure 8-8 are Na, K, Cl, NO_3 and SO_4. The relative amounts of these ions in the $PM_{2.5}$ size fraction are shown in Figure 8-9. The ion concentration spans a wide range, with approximately 90% of the total ion concentration due to sulfate. The data in this figure also show that the ion concentration for ultra low-NO_x combustion is slightly lower than for conventional low-NO_x combustion. Similar to Figure 8-8, this may simply result from the greater carbon content of the ash for ultra low-NO_x combustion.

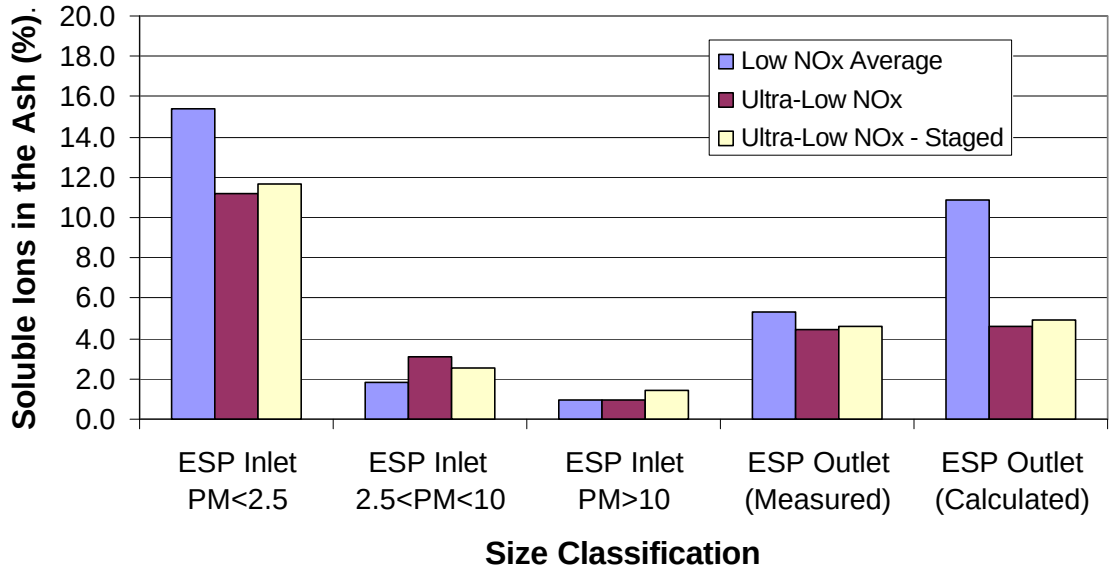

Figure 8-8. Concentration of soluble ions in the fly ash for different size ranges and combustion conditions

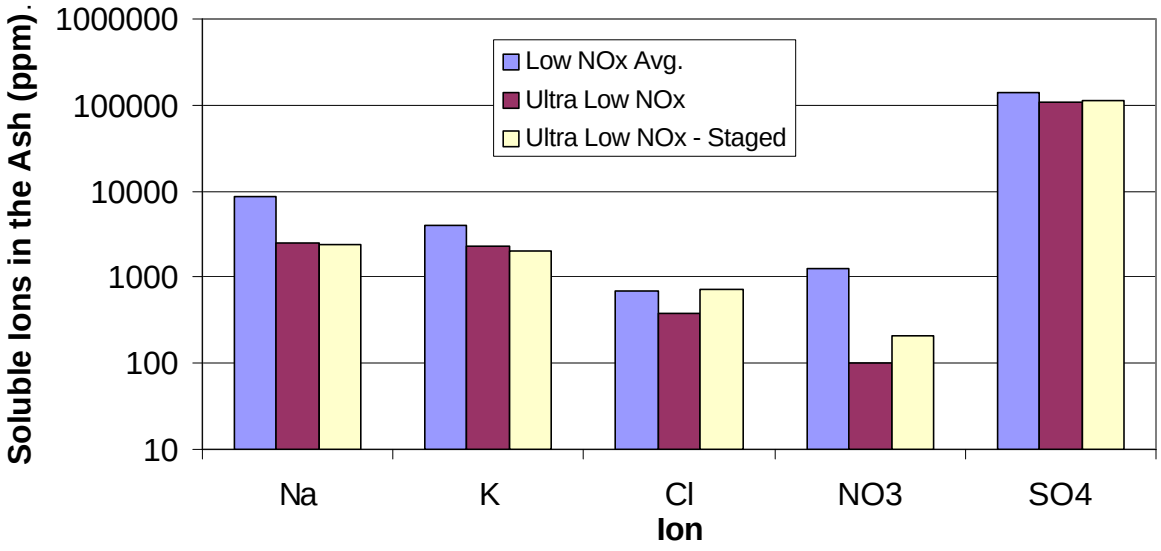

Figure 8-9. Soluble ion concentration in the $PM_{2.5}$ size fraction for different combustion conditions

8.5 Major Elements

The concentrations of major elements in the fly ash were quantitatively determined using Inductively Coupled Plasma emission spectroscopy. Samples that were analyzed included the ashed coal, the three size fractions of particulate provided by $PM_{10}/PM_{2.5}$ sampling at the ESP inlet, the particulate catch at the ESP outlet, and the ash collected in the ESP hoppers. These samples were analyzed for each of the three combustion conditions.

Table 8-5 shows the average element concentration in the particulate (μg/gm) for the ashed coal, and the PM >10 microns collected at the ESP inlet. The standard deviation shown in Table 8-5 is expressed as a percentage of the average. The elements included in this list are those with a measured concentration in excess of 500 μg/gm, and includes data for Tests A, B, D, and E.

Table 8-5. Average Concentration of Major Elements from Ashed Coal and From PM > 10 microns Collected at the ESP Inlet

Element	Average Concentration (mg/gm)	Standard Deviation (% of average)	Assumed Oxide Form	Calculated Concentration (% of total)
Al	109538.9	1.0	Al_2O_3	20.69
B	875.4	43.16	-	0.09
Ca	16648.4	3.99	CaO	2.33
Fe	202040.3	5.38	Fe_2O_3	28.86
Mg	4069.8	1.12	MgO	0.67
Na	3888.0	7.33	-	0.39
P	13056.4	0.60	-	1.31
S	5032.0	69.41	SO_4	1.51
Si	189177.5	1.39	SiO_2	40.46
St	650.2	1.36	-	0.07
Ti	5871.2	3.63	TiO_2	0.98
Mass Sum	**551000**	**N/A**		**97.36**

As indicated in the table the standard deviation in the element concentration (which includes instrument repeatability) is less than 7% for all elements except boron and sulfur. Boron is present in variable concentrations because it may form gaseous compounds in the furnace and escape the solid phase. Sulfur is present in much higher concentrations, but most is converted to gaseous sulfur dioxide. For example, the measured sulfur concentration in the ash is about 0.5%, whereas the sulfur in the coal is greater than 3%.

The sum of the individual element concentrations is listed at the bottom of Table 8-5 and amounts to 0.551 gm/gm, or about half of the mass of the fly ash. The balance of the fly ash mass is primarily oxygen which forms oxides with almost all of the elements listed and is not measured using ICP. An example of the effect of the oxide formation on the total mass is also shown in Table 8-5. The fourth column lists an assumed common oxide of the element and column five is a calculation of the mass of the oxide expressed as a percent of the total. The total mass balance of the oxides of the elements then sums to 97.4%.

The small standard deviations in Table 8-5 shows that the element concentration of the PM > 10 microns is essentially the same as the element concentration in the ashed coal, and is not dependent on combustion condition. The concentration of the elements in different size fractions normalized to the concentration in the ashed coal is shown in Figure 8-10. The four bars for each element gives the relative concentration of the PM > 10 microns, the PM between 2.5 and 10 microns, PM < 2.5 microns for low-NO_x combustion, and the PM < 2.5 microns for ultra low-NO_x combustion. The data in Figure 8-10 have been adjusted to a 0% carbon basis.

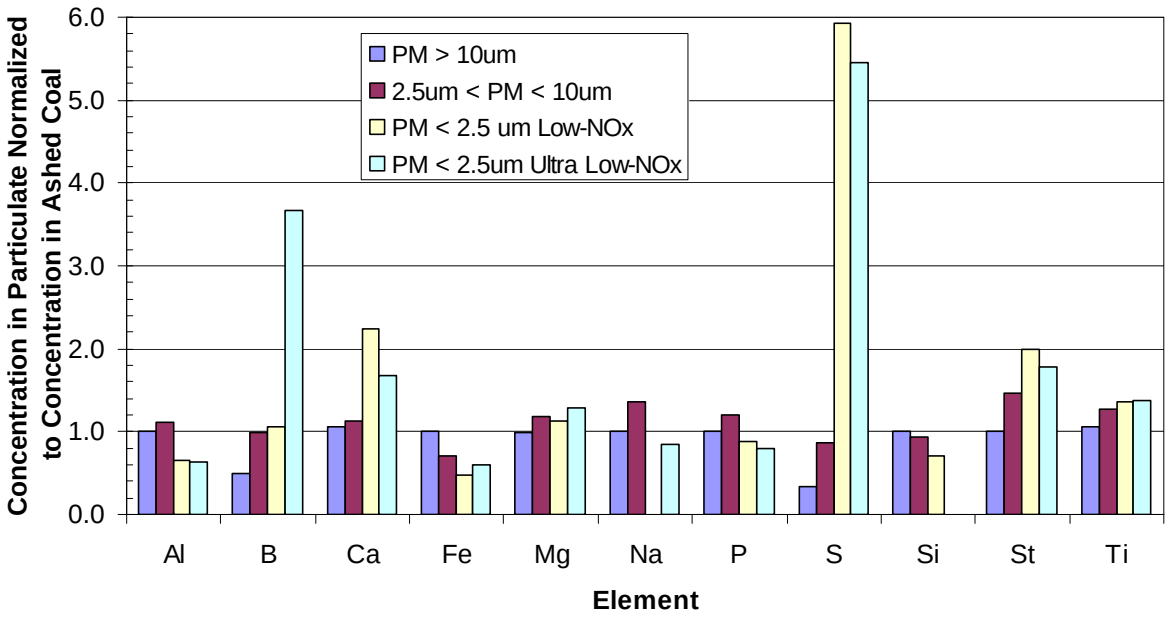

Figure 8-10. Concentration of major elements in fly ash from the ESP inlet normalized to the concentration in ashed coal

As described above and shown in Table 8-6, the concentration of the PM > 10 microns is essentially the same as that in the ashed coal (normalized concentration of 1.0) with the exception of boron and sulfur. The concentration of boron and sulfur is variable because they form gaseous species. Many of the elements show

an increase in concentration with a decrease in particle size. Examples are B, Ca, Mg, S, St, and Ti. The other elements show a trend toward decreased element concentration in the smaller particulate. Examples of these are Al, Fe, P, and Si.

Table 8-6. Measured Concentration and Minimum Detection Limit of Trace Elements in an Ashed Coal Sample

	Element	Concentration in Coal Ash (μg/gm)	Minimum Detection Limit (μg/gm)
Significant Concentration in the Coal Ash	Cr	321.7	7.5
	Ni	301.8	12.5
	Zn	196.4	2.5
	Cu	75.9	5.0
Marginal Concentration in the Coal Ash	Pb	47.5	24.0
	Co	13.0	5.0
	Be	5.7	1.3
	Sb	4.5	2.5
	Cd	1.2	0.3
Volatile Element	Se	127.9	2.5
	As	56.2	2.5
	Hg	2.1	0.05
	Total	1153.8	

It should be noted here that the element concentration in PM < 10 microns has only a small impact on a mass balance because this size fraction represents only about 15% of the fly ash. The elemental concentration in PM < 2.5 microns has a smaller impact as it accounts for only about 2.5% of the ash.

8.6 Trace Elements

The elements considered as trace elements are those that were measured using either Graphite Furnace Atomic Absorption (GFAA) or Cold Vapor Atomic Absorption (CVAA). As with the major elements, the concentration of the trace elements in the fly ash was categorized by size fraction and combustion condition.

Table 8-6 lists the trace elements, the concentration of these elements in the ashed coal, and for comparison, the minimum detection limit (MDL) of the measurement. The elements are split into several groups in the table. The first group contains those elements with significant concentration in the coal ash compared to the MDL. The second group contains those elements with a marginal concentration in the coal ash compared to the MDL. These elements have been included because the concentration is significant in certain size fractions. The third category contains those

elements that are volatile and may not in general partition to the particle phase after they are vaporized in the furnace. As indicated in the bottom row of the table the mass of these trace elements totals to about 0.1% (1000 μg/gm) of the coal ash.

The concentration of the trace elements in the first two groups are shown in Figure 8-11 as a function of fly ash size fraction for low-NO_x combustion. For comparison, the element concentration in the PM < 2.5 micron size fraction corrected to 0% carbon is also shown for the ultra low-NO_x combustion condition.

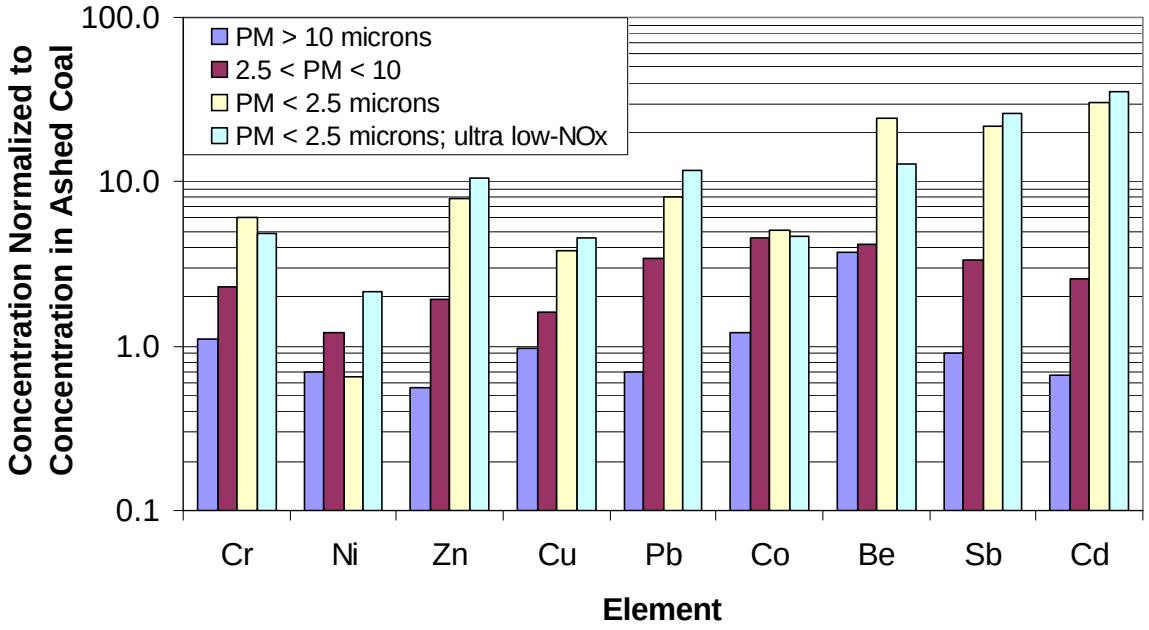

Figure 8-11. Concentration of trace elements in fly ash from the ESP inlet normalized to the concentration in ashed coal

As with the major elements shown in Figure 8-10, the normalized trace element concentration in the PM >10 microns is about 1.0. However, the range of variation with particle size range for the different elements is quite large. For all elements, the concentration increases as the size of the ash particulate decreases. The normalized element concentration in the PM < 2.5 micron size fraction is on the order of 5 to 10 for most elements. The elements with normalized concentrations greater than 10 are also those elements with large uncertainty in the coal ash concentration. In general, the enrichment in the PM < 2.5 microns size range for the trace elements is greater than for the major species (shown in Figure 8-10).

Similar to the results for soluble ions and major elements, the trace element concentration data for the size fraction less than 2.5 microns show no trend with combustion condition when the data are adjusted to a 0% carbon basis. Although not presented, the trace element concentration data for the two size fractions greater than 2.5 microns also show no effect of combustion conditions on trace element.

The normalized concentration of the volatile elements listed in Table 8-6 is shown in Figure 8-12 as a function of size range and combustion condition. Similar to the other comparisons, the element concentration in the PM < 2.5 microns for ultra low-NO_x combustion has been adjusted to 0% carbon.

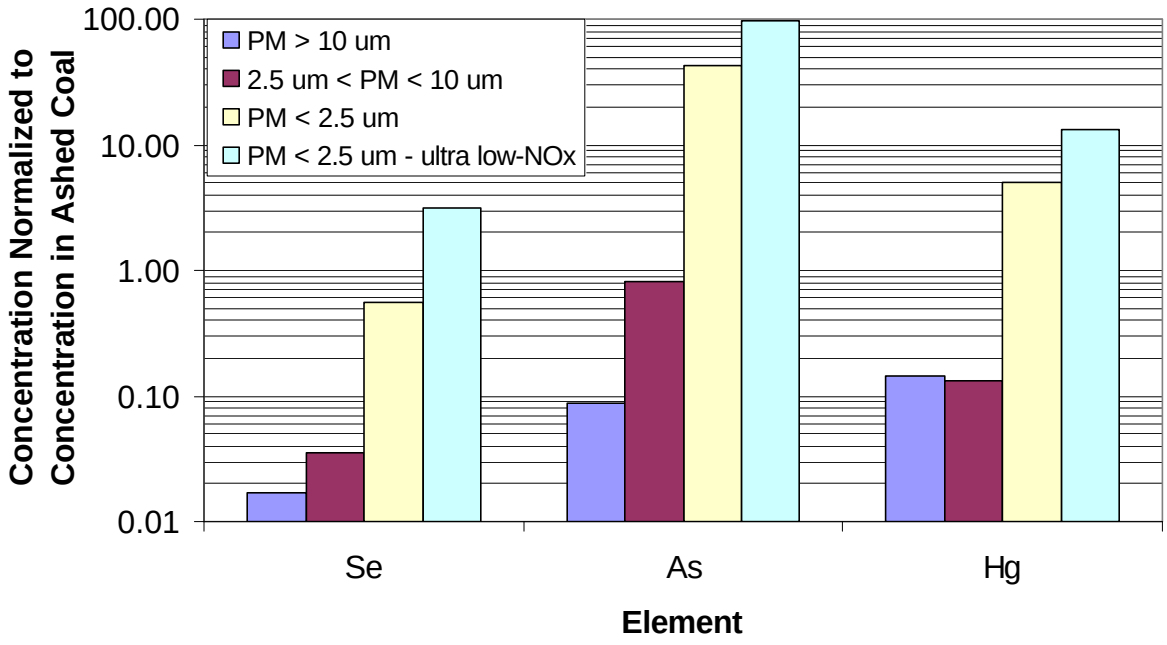

Figure 8-12. Concentration of volatile trace elements in fly ash from the ESP inlet normalized to the concentration in the coal ash

The normalized concentration of the elements in the PM > 10 micron size fraction are all significantly less than 1. These elements are sufficiently volatile that they are completely vaporized in the combustion zone, and may not form high temperature oxides. At the lower temperatures at the back end of the boiler these elements can condense or adsorb to particulate. These physical phenomena favor the smallest particles with high surface area, resulting in the highest concentrations on the smallest sizes.

Comparison of the PM < 2.5 microns element concentrations for the low-NO_x and ultra low-NO_x tests show that the element concentrations in the ultra low-NO_x ash are consistently 2 to 5 times greater than for the low-NO_x tests. This is in contrast to previous comparisons of trace elements in which the carbon adjusted concentration of the ultra low-NO_x combustion concentration data is about the same as the concentration for normal low-NO_x.

These volatile elements may have an affinity for adsorption to carbon (mercury for example), so that the high carbon content of the ultra low-NO_x PM < 2.5 microns provides an additional mechanism for collecting these elements.

9.0 CONCLUSIONS

9.1 Ultra-Low NO_X Burner

A prototype, 100 million Btu/hr, ultra low-NO_X plug-in PC burner was developed with the aid of computer modeling and successfully tested for commercial deployment in wall-fired units that are subject to considerable NO_X control requirements. The burner is a small throat version of the B&W full-diameter DRB-4Z™ ultra low-NO_X PC burner with new features for pressure drop and unburned carbon reductions. Without staging, full load firing of the plug-in DRB-4Z™ with 70% through 200-mesh, high-volatile, Pittsburgh 8 coal at 17% excess combustion air resulted in 145 PPMV NO_X (0.20 lb NO_2/million Btu), 3.19% LOI, and 4.7 in H_2O burner ΔP. Air staging the burner at 0.88 stoichiometry with all other conditions being the same lowered the NO_X levels to 104 PPMV (0.14 lb NO_2/million Btu). In summary, the unstaged and staged NO_X goals were met in the CEDF with acceptable carbon burnout and burner pressure drop.

The burner was also test fired with the high-volatile Mahoning 7 coal having a slightly higher fixed carbon-to-volatile matter ratio and fuel-nitrogen content. At 17% excess air and 70% through a 200-mesh screen PC fineness, NO_X emissions and LOI values from firing the Mahoning 7 coal averaged 165 PPMV (0.23 lb/million Btu) and 6.40%. When a multi-blade swirler was installed in the coal nozzle, NO_X increased to 177 PPMV (0.24 lb/million Btu) and LOI levels dropped to 5.43% due to better mixing between the fuel and oxidizer. Use of the swirler could be considered as an option in situations requiring very low unburned carbon levels. Increasing the coal fineness did not have an appreciable effect on NO_X but lowered the LOI levels. B&W is now offering the ultra low-NO_X plug-in DRB-4Z™ PC burner for commercial installation in utility boilers.

9.2 Primary $PM_{2.5}$ Emissions

Size classified fly ash samples representative of commercial low-NO_x and ultra low-NO_x combustion of Pittsburgh 8 coal were collected at the inlet and outlet of an ESP. For the specific combustion conditions tested, ultra low-NO_x combustion resulted in higher unburned carbon than conventional low-NO_x combustion (4.3% vs 1.3%). The greater carbon-in-ash for the ultra low-NO_x combustion was not unexpected since the burner was not optimized for unburned carbon. For all test conditions the particulate removal efficiency of the ESP exceeded 99.3% and emissions were less than the NSPS limits of ~48 mg/dscm.

With constant combustion conditions, the removal efficiency of the ESP increased as the ESP voltage and Specific Collection Area (SCA) was increased. The associated decrease in particle emissions occurred in size fractions both larger and smaller than 2.5 microns. For constant ESP voltage and SCA, the removal efficiency for the ultra low-NO_x combustion ash was less than for the low-NO_x combustion ash. The decrease in removal efficiency was accompanied by a decrease in ESP current. The emission of $PM_{2.5}$ from the ESP increased only slightly as a result of the change in combustion

conditions. Most of the increase in emissions was in the size fraction greater than 2.5 microns, indicating particle re-entrainment. These results may be specific to the coal tested in this program.

Although the increase in unburned carbon on an average basis was quite small, the increase in carbon content was strongly dependent on particle size. While the carbon content of PM greater than 10 microns increased from about 1% to 4%, the carbon content of the $PM_{2.5}$ size fraction increased from about 7% to 45%.

In general, the concentration of inorganic elements and trace species in the fly ash was dependent on the particle size fraction. The smallest particles tended to have higher concentrations of species/elements than larger particles. This trend was strongly dependent on the volatility of the element or species. The concentration of the least volatile elements tended to be depleted in the smallest particles while the concentration of the most volatile elements/species tended to be enriched.

The concentration of most elements by particle size range was independent of combustion condition when evaluated on a carbon free basis. The exceptions to this generality were Se, As, and Hg. These concentration of these elements in the $PM_{2.5}$ size fraction remained relatively constant as the carbon content increased.

The concentration of soluble ions in the fly ash showed little change with combustion condition when evaluated on a carbon free basis. For the high sulfur Pittsburgh 8 coal that was burned in these tests, the predominate ionic species in the fly ash was sulfate. As with the volatile elements, soluble ions were enriched in the $PM_{2.5}$ size fraction.

The average concentrations of carbon and ionic species at the outlet of the ESP were calculated using the size classified concentration data from the ESP inlet, and the particulate mass distribution from the ESP outlet. These calculated concentrations compared well with measured values. This approach should work well for any non-volatile species that does not change phase as it proceeds through the ESP or other particulate collection device.

10.0 COMMERCIALIZATION OF PLUG-IN ULTRA LOW-NO_X BURNER

Following the successful performance demonstration at 100 million Btu/hr, B&W has been awarded one retrofit contract at Allegheny Energy's Ft. Martin 2 power plant in West Virginia for the installation of the ultra low-NO_x Plug-in DRB-4Z™ PC burner. B&W will install forty (40) Plug-in DRB-4Z™ PC burners in this 576 MWe unit for firing an eastern bituminous coal.

11.0 REFERENCES

1. Sivy, J.L., Rodgers, L.W., Kaufman, K.C., and Koslosky, J.V. "Development of an Advanced Low-NO_x Burner in Support of B&W's Advanced Coal-Fired Low Emission Boiler System," Presented at the American Flame Research Committee Fall International Symposium, Monterey, CA, October 1995.

2. Sivy, J.L., Kaufman, K.C., and McDonald, D.K., "The Development of a Combustion System for B&W's Advanced Coal-Fired Low-Emission Boiler System," Presented at the 22nd International Technical Conference on Coal Utilization and Fuel Systems, Clearwater, FL, March 1997.

3. Sivy, J.L., Sarv, H., and Koslosky, J.V., "NO_X Subsystem Evaluation of B&W's Advanced Coal-Fired Low Emission Boiler System at 100 MBtu/hr," Proceedings of the EPRI-DOE-EPA Combined Utility Air Pollutant Control Symposium, Washington, DC, August 1997.

4. "An Improved Pulverized Coal Burner," U.S. Patent No. 5,829,369.

5. Fiveland, W.A., Cornelius, D.K., and Oberjohn, W.J., "COMO: A Numerical Model for Predicting Furnace Performance in Axisymmetric Geometries", *ASME Paper No. 84-HT-103,* 1984.

6. Fiveland, W.A., and Jessee, J.P., "Mathematical Modeling of Pulverized Coal Combustion in Axisymmetric Geometries," *Joint EPRI/ASME Power Conference*, Phoenix, AZ, October 1994.

7. Fiveland, W.A., and Jessee, J.P., "Comparison of Discrete Ordinates Formulations for Radiative Heat Transfer in Multidimensional Geometries," *Journal of Thermophysics and Heat Transfer*, Vol. 9, No. 1, pp. 47-54, 1995.

8. Rhie, C.M., and Chow, W.L., "Numerical Study of the Turbulent Flow Past an Airfoil with Trailing Edge Separation, *AIAA J.*, vol. 21, pp. 1525-1532, 1983.

9. Jones, W.P. and Launder, B.E., "The Prediction of Laminarisation with a Two Equation Turbulence Model," *Int. J. Heat Mass Transfer*, Vol. 15, p. 301, 1972.

10. Beer, J. M., and Chigier, N. A., "Combustion Aerodynamics", Robert E. Krieger Publishing Co., Malabar FL, 1983.

11. Idelchik, I.E., *Handbook of Hydraulic Resistance*, 3rd Edition, ISBN 1-56700-074-6, Begell House, Inc., New York, NY, 1996.

12. Ubhayakar, S.K., *et. al*, "Rapid Devolatilization of Pulverized Coal in Hot Combustion Gases", *Sixteenth Symposium (international) on Combustion,* pp. 427-436, The Combustion Institute, 1976.

APPENDIX A

Flue Gas Sampling and Analysis Matrix

The types of analyses used to characterize samples (listed in Table 6-7) require different filter substrates, with different particulate loading requirements. The size of the backup filter and the length of the sample time was adjusted to provide particle loadings appropriate for the chemical analyses. Table A-1 provides a listing of the gas sampling measurements at the ESP inlet, the representative particle loading on the filter, the filter size, and the sample time for each measurement. The particle catch at the ESP inlet was based on a flue gas particle loading of 4 lb/million Btu. Table A-2 provides a list of flue gas sampling measurements at the ESP outlet. The data in Table A-2 was based on a particulate loading of 0.03 lb/million Btu. The sampling matrix at the ESP inlet and ESP outlet was repeated for each of the three ESP operating conditions for Test Series I. Table A-1 and A-2 gives nominal sample flow rates, sample times, and collected particulate mass used for sampling. The same sampling matrix was used for Test Series IV with the ultra low-NO_x staged and unstaged combustion.

Table A-1. Sampling Matrix at the ESP Inlet (Particulate Load = 4 lb/million Btu)

Method	Filtering		Sample		$PM_{2.5}$		Analysis
	Size	Type	Flow (dscfm)	Time (min)	Total (mg)	Density (mg/cm^2)	
$PM_{10}/PM_{2.5}$[1]	8" X 10"	Teflon	0.35	20	130	0.25	Mass, SEM
$PM_{10}/PM_{2.5}$[1]	8" X 10"	Quartz	0.35	20	130	0.25	Mass, TOA (OC, EC)
$PM_{10}/PM_{2.5}$[1]	8" X 10"	Quartz	0.35	180	1167	2.26	Mass, LOI, Ions and Elements
$PM_{10}/PM_{2.5}$[1]	8" X 10"	Teflon	0.35	180	1167	2.26	Mass
M-201A	62 mm	Quartz	0.5	20	185		Particle Size Distribution.

[1] $PM_{10}/PM_{2.5}$ refers to "Draft Method for Determination of $PM_{10}/PM_{2.5}$ Emissions (Constant Sampling Rate Procedure), EPA Method PRE 4.

Table A-2. Sampling Matrix at the ESP Outlet (Particulate Load = 0.03 lb/million Btu)

Method	Back-up Filter		Sample		$PM_{2.5}$		Analysis
	Size	Type	Flow (dscfm)	Time (min)	Total (mg)	Density (mg/cm^2)	
$PM_{10}/PM_{2.5}$[1]	8" X 10"	Teflon	0.35	120	58	0.11	Mass, SEM
$PM_{10}/PM_{2.5}$[1] & M-202	100 mm	Quartz	0.35	60	29	0.37	Mass, TOA (OC, EC)
M-201A & M-202	62 mm	Quartz	0.5	60	42	(-)	Particle Size Distribution
Controlled Condensation	---	---	---	---	---	---	Sulfuric Acid
High Vol.	8" X 10"	Teflon	8	120	1334	2.59	Mass
High Vol.	8" X 10"	Quartz	8	120	1334	2.59	Mass, LOI, Ions and Elements

[1] $PM_{10}/PM_{2.5}$ refers to "Draft Method for Determination of $PM_{10}/PM_{2.5}$ Emissions (Constant Sampling Rate Procedure), EPA Method PRE 4.

In addition to the particle collection listed in Table A-1 and A-2, the standard gas species were measured and recorded during the test. These species include CO, CO_2, O_2, NO_x, and SO_2.

Table A-3 shows the chemical analyses that were performed on the collected samples from the three ESP operating conditions in Test Series I (Tests A, B, and C). Similar matrices were followed for Test Series IV (Tests D and E). This table provides a summary of the sampling and analyses that were conducted in this test program. The samples identified in the table represent the following:

- The three size fractions associated with the draft EPA $PM_{10}/PM_{2.5}$ sampling at the inlet and outlet of the ESP,
- The eight size fractions provided by cascade impactor sampling at the ESP inlet and outlet,
- Condensable organic and inorganic fractions at the ESP outlet
- Fly ash samples from the hoppers of the three operating fields of the ESP, an
- Composite pulverized coal sample.

As indicated in the tables, the $PM_{2.5}$ samples at the inlet and outlet of the ESP are the focus of the chemical analyses. Additionally, the larger size fractions of the particulate at the ESP inlet and the particulate from the ESP hoppers were characterized. Analyses were not conducted for PM > 2.5 microns at the ESP outlet. The mass of the collected particulate at this location was very small, and of insufficient quantity for detailed analyses. Instead, analyses of this size fraction were made on particulate collected at the ESP inlet.

Table A-3. Sample Analysis Matrix for Tests IA, IB, and IC

Sample	Mass	Carbon		Elements	Ions	Ultimate/ Proximate	Size Distribution
	Loading	TOA	LOI	ICP/AA	IC/FES/ ISE		Microtrac
Coal (Test A Composite)				IA		IA	IA
ESP_{in} PM <2.5 microns	IA,IB,IC	IA,IB,IC	IA,IB,IC	IA,IB,IC	IA,IB,IC		
ESP_{in} 10 microns > PM >2.5 microns	IA,IB,IC	IA,IB,IC	IA,IB,IC	IA,IC	IA,IB,IC		
ESP_{in} PM >10 microns	IA,IB,IC	IA,IB,IC	IA,IB,IC	IA,IC	IA,IB,IC		
ESP_{in} Cascade Impactor	IA,IB,IC						
ESP_{out} PM <2.5 microns	IA,IB,IC	IA,IB,IC	IA,IB,IC	IA,IB,IC	IA,IB,IC		
ESP_{out} 10 micron > PM >2.5 microns	IA,IB,IC						
ESP_{out} PM >10 microns	IA,IB,IC						
ESP_{out} Cascade Impactor	IA,IB,IC						
ESP_{out} Condensable Organic	IA,IB,IC						
ESP_{out} Condensable Inorganic	IA,IB,IC				IA,IB,IC		
ESP_{out} Controlled Condensation					IA[1],IB[1],IC[1]		
ESP Field 1 Ash			IA,IC	IA	IA		IA,IC
ESP Field 2 Ash			IA,IC	IA	IA		IA,IC
ESP Field 3 Ash			IA,IC	IA	IA		IA,IC

[1]Sulfuric Acid

APPENDIX B

Limits of Detection for Ions and Elements, and Detailed Sample Preparation and Analysis Procedures

Table B-1 contains the limits of detection for elements measured using ICP and GFAA/CVAA. The limits of detection are based on a 40 mg particulate sample digested in 100 ml of acid (dilution of 2500:1). Elements of relatively high concentration were measured with ICP. Trace elements were measured with GFAA. Mercury was measured with CVAA.

Table B-2 contains the detection limits for ions using ICP, FES and ISE. The limits of detection are based on an extraction of 40 mg of particulate sample with 40 ml of de-ionized water.

Table B-3 and B-4 provide a list of the analyses on collected particulate and pulverized coal respectively, and the reference to the sample preparation and analysis procedures. The sample preparation and analysis procedures are based on ASME, ASTM and EPA procedures.

Table B-1. Estimated Detection Limits for the Elements in the Particulate Based on a 40 mg Particulate Sample and a 100 ml Acid Digestion

Element	Element Detection Limit in the Particulate (ppm)	
	ICP	GFAA or CVAA
Al	152.5	
Ca	257.5	
Fe	85	
K	512.5	
Mg	60	
Na	157.5	
P	260	
Si	430	
Ti	7.5	
Ba	7.5	
Sr	2.5	
Mn	10	
B	75	
Zn		2.5
Zr	20	
Pb	80	25
V	17.5	
Cr	30	7.5
Li	7.5	
Ni	35	12.5
Cu		5
As		2.5
Co		5
Mo	22.5	
Be		1.25
Sb		2.5
Se		2.5
Cd		0.25
Hg		0.25

Table B-2. Estimated Detection Limits For Soluble Ions in the Particulate Based on a 40 mg Particulate Sample and a 40 ml De-ionized Water Extraction

Ions	Measurement Technique	Detection Limit in the Solution (ppb)	Detection Limit in the Solid (ppm)
Chlorides, Fluorides, Sulfates, Nitrates, Phosphates	IC	1	1
Sodium, Potassium	FES	1	1
Ammonia	ISE	10	10

Table B-3. Method References for Preparation and Analysis of Particulate Samples

Analyte	Sample Analysis		Sample Preparation	
	Method	Reference	Method	Reference
Carbon	Loss of Ignition (LOI)	ASME 4.07, modified	None	
	Thermal Optical Analyzer (TOA)	NIOSH 5040		
Elements	Inductively Coupled Plasma (ICP-AES)	EPA 6010B	Microwave Direction	EPA 3052
	Graphite Furnace Atomic Absorption (GFAA)	EPA 7000A		
As	Hydride Generation Atomic Absorption (HGAA)	EPA 7061A		
Se	Hydride Generation Atomic Absorption (HGAA)	EPA 7741A		
Hg	Cold Vapor Atomic Absorption (CVAA)	EPA 7471A		
Chloride, Fluoride, Sulfate, Nitrate, Phosphate	Ion Chromotography (IC)	ASTM D4327, modified	Hot Water Extraction	
Sodium, Potassium	Flame Emission (FES)	ASTM D1428		
Ammonia	Ion Selective Electrode (ISE)	ASTM D1426		

Table B-4. Method References for Preparation and Analysis of Pulverized Coal Samples

Analyte	Sample Analysis		Sample Preparation	
	Method	Reference	Method	Reference
Elements	Inductively Coupled Plasma (ICP-AES)	EPA 6010B	Ashing/ Microwave Digestion	ASTM 3683-94/ EPA 3052
	Graphite Furnace Atomic Absorption (GFAA)	EPA 7000A		
As	Hydride Generation Atomic Absorption (HGAA)	EPA 7061A		
Se	Hydride Generation Atomic Absorption (HGAA)	EPA 7741A		
Hg	Cold Vapor Atomic Absorption (CVAA)	ASTM D3684-94	Oxygen Bomb	ASTM D3684-94
Chloride	Ion Selective Electrode (ISE)	ASTM D4208-93	Oxygen Bomb	ASTM D4208-93
Fluoride	Ion Selective Electrode (ISE)	ASTM D3761-96	Oxygen Bomb	ASTM D3761-96
Heating Value	Calorimetry	ASTM D2015-19	None	
Moisture, Ash Volatile Matter, Fixed Carbon	Proximate Analysis	ASTM 3172-89	None	
Carbon, Hydrogen Sulfur, Nitrogen Ash, Oxygen	Ultimate Analysis	ASTM 3176	None	